

MICAELA MARGARIDA FERREIRA DE SOUSA

**A STUDY ON HISTORICAL DYES USED IN
TEXTILES: DRAGON'S BLOOD, INDIGO AND MAUVE**

Dissertação apresentada para obtenção do Grau
de Doutor em Conservação e Restauro, especialidade
Ciências da Conservação, pela Universidade Nova de
Lisboa, Faculdade de Ciências e Tecnologia.

LISBOA
2008

Acknowledgments

I would like to thank my supervisors Prof. Maria João Melo (Faculdade de Ciências e Tecnologia – Universidade Nova de Lisboa: FCT-UNL) and Prof. Joaquim Marçalo (Instituto Tecnológico e Nuclear: ITN) for giving me the opportunity to participate in the project: “*The Molecules of Colour in Art: a photochemical study*” as well as the general supervision of my PhD project. I’m also grateful to Prof. Sérgio Seixas de Melo (Universidade de Coimbra: UC), the project coordinator.

I would also like to thank all the people involved in this PhD project: Prof. Jorge Parola (FCT-UNL) for the RMN analysis, supervision of indigo work in homogeneous media and supervision of mauve counter ions analysis; Prof. Fernando Pina (FCT-UNL) for the supervision on the dragon’s blood flavylum characterization; Prof. Conceição Oliveira (Instituto Superior Técnico: IST) for her help in the MS measurements; researcher Catarina Miguel (FCT-UNL) for validating and obtaining some indigo photodegradation results on homogeneous media; master student Isa Rodrigues (FCT-UNL) for the HPLC-DAD analysis on the Andean Paracas textiles; Prof. Fernando Catarino (Faculty of Sciences – University of Lisbon: FC-UL) for the dragon’s blood resins botanical details and Prof. João Lopes (University of Porto: UP) for the dragon’s blood PCA analysis.

Moreover I’m grateful to all the people and institutions that sent samples of the different organic dyes analysis: a) *Dragon’s blood samples*: the botanical garden of Lisbon, the botanical garden of Ajuda, to Roberto Jardim, director of the botanical garden of Madeira, to the Natural Park of Madeira for the *Dracaena draco* samples and Prof. J. Pavlis for the *Dracaena cinnabari* samples. I also would like to thank Dr. Anita Quye for the dragon’s blood samples and Ms H. Chantre for the Cape Verde species. I am grateful to Frances Cook (Royal Botanic Gardens: RBG, Kew) who helped in the sampling of dragon’s blood EBC, collection and also for her valuable comments. B) *Mauve dye samples*: Perth Museum (Scotland), Museum of Science and Industry in Manchester, Columbia University, New York City, and the Science Museum, London, for the samples. I also would like to thank to P.J. Morris (Science Museum) responsible for sending all the mauve samples and for his valuable comments. Also I’m grateful to Prof. Anthony Travis (Sidney M. Edelstein Center for the History and Philosophy of Science) and Prof. Henry Rzepa (Imperial College) who were very helpful in the discussion of the mauve dye results.

I also would like to thank to my PhD colleagues who have been my partners on this journey with exchange of ideas, knowledge and discussions. I am also grateful to the DCR “staff” as Ana Maria and Márcia Vilarigues for all the support.

Finally I’m grateful to POCI (POCI/QUI/55672/2004 and PTDC/EAT/65445/2006), FCT and FEDER for further funding.

Resumo

Nesta tese de doutoramento foram estudados três corantes históricos a nível molecular nomeadamente o **índigo**, um corante milenar utilizado desde a altura dos egípcios e dos romanos; o **sangue de dragão**, uma resina vermelha utilizada por diversas culturas com variados fins artísticos e medicinais e o corante sintético **malva** que revolucionou toda a história da química e indústria da cor. Com este estudo pretende-se obter uma melhor conservação e valorização do património cultural, nomeadamente de têxteis.

Flavílios naturais foram redescobertos como cromóforos responsáveis pela cor vermelha das resinas sangue de dragão. O cloreto de 7,4'-dihidroxi-5-metilflavílio (dracoflavílio) foi pela primeira vez identificado e caracterizado por HPLC-DAD-MS e RMN em resinas provenientes de dragoeiros *Dracaena draco*, enquanto que o cloreto de 7,4'-dihidroxi-5-metilflavílio foi identificado pela primeira vez em resinas dos dragoeiros *Dracaena cinnabari*. Mais de 50 resinas sangue de dragão de proveniência conhecida e identificada por especialistas foram analisadas por HPLC-DAD seleccionando-se o 7,6-dihidroxi-5-metilflavílio (dracorodin), o cloreto de 7,4'-dihidroxi-5-metilflavílio (dracoflavílio) e o cloreto de 7,4'-dihidroxi-5-metilflavílio como marcadores de espécie para resinas obtidas a partir do *Daemonorops spp.*, *Dracaena draco* e *Dracaena cinnabari*, respectivamente. Este método foi aplicado com sucesso na identificação de resinas colhidas no século XIX pertencente ao Royal Botanic Garden, Kew (uma colaboração com o Royal Botanic Garden, Kew).

A caracterização da rede complexa de reacções químicas em solução aquosa destes flavílios, para condições ácidas ou ligeiramente ácidas revelaram que a principal espécie em equilíbrio a pH 4-6, para o dracoflavílio e a dracordina, é a base vermelha quinoidal (**A**).

A fotodegradação do **índigo** e um derivado do índigo solúvel em água (índigo carmin) foi realizada em meio líquido e no estado sólido. Foram obtidos os rendimentos de fotodegradação com irradiação cromática a 335nm e 610 nm. A isatina foi o principal produto de degradação identificado por HPLC-DAD-MS para o índigo, enquanto que o índigo carmin revelou a presença de isatina sulfonada. Os resultados obtidos foram confirmados com a análise dos corantes azuis de têxteis milenários da cultura Pré-Colombiana de Paracas (uma colaboração com o Museu of Fine Arts, Boston).

A caracterização da **malva** por HPLC-DAD-MS e por RMN revelou que contrariamente ao descrito na literatura, a malva é uma mistura complexa constituída por cerca de 13 cromóforos roxos. Da análise de amostras históricas de malva, foi possível verificar que a malva original feita nos primeiros anos de 1856-57 por Perkin, existe apenas em têxteis históricos. Os sais históricos, incluindo a amostra exposta no Museu Científico de Londres como "a malva original realizada por William Perkin em 1856" foram sintetizados depois de 1862 (uma colaboração com o Science Museum, Londres).

Abstract

A characterization at the molecular level of three important historic dyes was undertaken: the most popular **blue** in the history of humankind, indigo, one the most ancient **red** resins, dragon's blood, and the first synthetic dye with high commercial value, **mauve**. The molecular studies evolved along two axes: the characterization of relevant chromophores for mauve and dragon's blood resins and the study of indigo photochemistry.

Natural flavylum compounds were rediscovered as the chromophores responsible for the red colour in dragon's blood resins. 7,4'-dihydroxy-5-methoxyflavylum (dracoflavylum) was for the first time identified in samples of the resin *dragon's blood*, extracted from the tree *Dracaena draco*. Also, 7,4'-dihydroxyflavylum was identified for the first time as the red natural flavylum in *Dracaena cinnabari* species. Following these results, the use of flavylum compounds as markers to identify the species source of dragon's blood resins is proposed. This method was built-up on the analyses of more than 50 resin samples from different trees, and further successfully tested on 19th century Kew Gardens collection (*in a collaboration with Kew Gardens, Kew*). Moreover, the complex network of reversible chemical reactions, at acidic or slightly basic conditions, that dracoflavylum undergoes in aqueous solution is described, and it is concluded that the red colour of these resins is due to the stable quinoid base, which is the major species in the pH range 4-6.

The photodegradation of **indigo** and its water-soluble derivative indigo carmine was carried out in liquid and organized media. Photodegradation quantum yields were obtained for monochromatic irradiation at 335 nm and 610 nm; the main photodegradation product was identified by HPLC-DAD-MS as being isatin for indigo. The stability of indigo and the mechanisms of degradation are discussed and compared to what was observed in millenary Paracas textiles (*in a collaboration with Museum of Fine Arts, Boston*).

The characterization of **mauve** revealed that, contrarily to what is reported in the literature, the dye is a complex mixture of at least 13 chromophores with the 7-amino-5-phenyl-3-(phenylamino)phenazin-5-ium core. From the analysis of historic mauve samples it was possible to verify that the "original mauve", made in the early years of 1856-7 by Perkin, exists in historic textile samples. The historic salt samples analysed, including the one displayed in the Science Museum of London as the "original mauve performed by William Perkin in 1856", were found to be later than 1862 (*in a collaboration with Science Museum, London*).

Symbols and Notations

A	Quinoid base species
A ⁻	Quinoid base ionized species
AH ⁺	Flavylium cation species
B	Hemiacetal species
C ₀	Summation of the concentration of all flavylium species at the equilibrium
C _c	Cis-chalcone species
C _c ⁻	Cis-chalcone ionized species
C _t	Trans-chalcone species
C _t ⁻	Trans-chalcone ionized species
K _{a1}	Equilibrium constant of flavylium deprotonation leading to the quinoid base (A) species
K _{a2}	Equilibrium constant of quinoid base deprotonation leading to the ionized quinoid base (A ⁻) species
K _h	Equilibrium constant of flavylium hydration leading to the hemiacetal (B) species
K _i	Equilibrium constant of cis-trans isomerisation to form the chalcone species
K _t	Equilibrium constant of tautomerisation reaction to form the chalcone species(C _c)
ε	Molar absorptivity coefficient
HPLC-DAD	High performance liquid chromatography – diode array detector
rt	Retention time
λ _{max}	Maximum wavelength absorption in the ultraviolet-visible spectra
hν	Light
I ₀	intensity of the incident light
I _{abs}	total light absorbed
IC-AEC	Ion chromatography – anion exchange chromatography
ICP-AES	Inductively coupled plasma – atomic emission spectrometry
k _{ic}	Rate constant of internal conversion deactivation
k _{isc}	Rate constant of intersystem crossing deactivation
k _f	Rate constant of fluorescence deactivation
k _p	Rate constant of phosphorescence deactivation

MS	Mass spectrometry
FD-MS	Field-desorption mass spectra
HRMS	High-resolution mass spectra
LC-MS	Liquid chromatography –Mass spectrometry
NMR	Nuclear Magnetic resonance
¹ H NMR	Proton Nuclear Magnetic resonance
¹³ C NMR	Carbon 13 Nuclear Magnetic resonance
COSY	Correlation spectroscopy
HMBC	Heteronuclear Multiple Bond Correlation
HMQC	Heteronuclear Multiple Quantum Coherence
HSQC	Heteronuclear Single Quantum Coherence
NOESY	Nuclear Overhauser effect spectroscopy
δ	Chemical shift
PCA	Principal component analysis
Φ_R	Quantum yield of reaction
S ₀	Singlet state
S ₁	Excited ground state
sp.	One species
spp.	More than one species
TIC	Total ion chromatogram (MS)
UV-Vis	Ultraviolet-visible spectroscopy
V _{sol}	Solution volume

Index of contents

General Introduction - <i>Molecular and photochemical studies on historical dyes: dragon's blood, indigo and mauve</i>	1
<hr/>	
1. Preamble	1
2. Chromophores characterization	1
3. Photophysical characterization	2
4. Photochemical characterization	4
Chapter 1 - Dragon's Blood	5
<hr/>	
1.1 Overview	5
1.1.1 <i>Dracaenaceae</i>	6
1.1.2 <i>Palmae</i>	8
1.1.3 <i>Euphorbiaceae</i>	9
1.1.4 <i>Others</i>	9
1.2 Chemical composition – The red colourants beyond	10
1.3 Results	13
1.3.1 <i>Dragon's blood resins data library</i>	13
1.3.2 <i>Flavylium markers identification</i>	14
1.3.2.1 <i>Dracaena draco: 7,4'-dihydroxy-5-methoxyflavylium</i>	16
1.3.2.2 <i>Dracaena cinnabari: 7,4'-dihydroxyflavylium</i>	16
1.3.2.3 <i>Daemonorops draco: 7-hydroxy-5-methoxy-6-methylflavylium</i>	17
1.3.3 <i>The Economic Botany Collections at the Royal Botanic Gardens (EBC, RBG) – Kew</i>	17
1.3.3.1 <i>Daemonorops draco (synonym, Daemonorops propinqua) and Daemonorops sp.</i>	18
1.3.3.2 <i>Dracaena cinnabari, Dracaena ombet (synonym D. schizantha) and Dracaena sp.</i>	20
1.3.3.3 <i>Dracaena draco</i>	24
1.3.4 <i>Flavylium markers characterization</i>	27
1.3.4.1 <i>Flavylium chemical reactions network – the dragon's blood red colour</i>	27
1.3.4.1.1 <i>Dracoflavylium</i>	28
1.3.4.1.2 <i>Dracorhodin and 7,4'-dihydroxyflavylium</i>	29
1.4 Conclusions	30

Chapter 2 - Indigo Dye	32
<hr/>	
2.1 Overview	32
2.2 Chemical composition – revealing the blue colour	32
2.3. Indigo photodegradation	33
2.4 Results	35
2.4.1 <i>Monochromatic irradiation in homogeneous media</i>	36
2.4.1.1 <i>Indigo in DMF</i>	36
2.4.1.2 <i>Indigo carmine in DMF and water</i>	38
2.4.2 <i>Monochromatic irradiation in heterogeneous media</i>	39
2.4.3 <i>Polychromatic irradiation in heterogeneous media</i>	41
2.4.4 <i>Characterization of the degradation products in Andean millenary textiles</i>	42
2.5 Conclusions	44
Chapter 3 - Mauve Dye	45
<hr/>	
3.1 Overview	45
3.2. Chemical composition – pursuing a perfect colour	47
3.3 Results	50
3.3.1 <i>Syntheses</i>	50
3.3.2 <i>Original samples</i>	53
3.3.2.1 <i>Original mauve textile samples</i>	53
3.3.2.1.1 <i>Group I - Perth, Science Museum F5 and F6</i>	55
3.3.2.1.2 <i>Group II - ScMF1, F2, F3 and F4</i>	56
3.3.2.2 <i>Original mauve salt samples</i>	57
3.3.2.2.1 <i>Science Museum 1, Chandler Museum and Science Museum 3</i>	58
3.3.2.2.2 <i>Museum SI Manchester 1, Science Museum 4 and Science Museum 2</i>	59
3.3.2.2.3 <i>Museum SI Manchester 2 and JCE 1926</i>	60
3.3.3. <i>Accelerated aging study</i>	61
3.3.3.1 <i>Mauve dyed textile reconstruction</i>	61
3.3.3.2 <i>Mauve dyed historic textiles</i>	62
3.4 Conclusions	62
General Conclusion	64
<hr/>	
References and notes	66
<hr/>	

Appendix I – Experimental section	74
<hr/>	
I.1 General	74
I.2 Instrumentation	74
<i>I.2.1 HPLC-DAD</i>	74
<i>I.2.2 LC-MS</i>	76
<i>I.2.3 MS</i>	77
<i>I.2.4 NMR spectroscopy</i>	77
<i>I.2.5 IC-AEC</i>	77
<i>I.2.6 ICP-AES</i>	78
<i>I.2.7 Optical Microscopic</i>	78
<i>I.2.8 Monochromatic irradiation</i>	78
<i>I.2.9 Solar Box Camera</i>	78
<i>I.2.10 UV/Vis spectra</i>	78
I.2.11 Colorimeter	78
I.3 Methods	79
<i>I.3.1 Dragon’s Blood</i>	79
<i>I.3.1.1 Resin samples</i>	79
<i>I.3.1.2 Collection/sampling of resin samples</i>	87
<i>I.3.1.3 Extraction of the dragon’s blood dye chromophores, purification and characterization of the natural flavylum markers</i>	88
<i>I.3.1.4 PCA analysis</i>	89
<i>I.3.1.5 Characterization of the flavylum compounds network chemical reactions</i>	89
<i>I.3.2 Indigo</i>	89
1.3.2.1 Actinometry	89
<i>I.3.2.2 Homogeneous media –monochromatic irradiation</i>	91
<i>I.3.2.2.1 Quantum yield</i>	91
<i>I.3.2.3 Heterogeneous media –monochromatic irradiation</i>	92
<i>I.3.2.3.1 Quantum yield</i>	92
<i>I.3.2.4. Heterogeneous media - polychromatic irradiation</i>	93
<i>I.3.2.5 Indigo photodegradation HPLC-DAD calibration curves</i>	93
<i>I.3.2.6 Andean indigo dyed fibres extraction</i>	93
<i>I.3.3 Mauve dye</i>	94
<i>I.3.3.1 Synthesis</i>	94
<i>I. 3.3.2 Mauve dye sources</i>	94
<i>I.3.3.3 Extraction and characterization of the mauve dye</i>	98
<i>I.3.3.4 Mordant analysis</i>	100
<i>I.3.3.5 Polychromatic irradiation</i>	101

I.4 References	101
Appendix II – Dragon’s blood data	102
<hr/>	
II.1 NMR and MS characterization	102
<i>II.1.1 Dracoflavylum</i>	102
<i>II.1.2 Dracorhodin</i>	103
<i>II.1.3 7,4'-dihydroxyflavylum</i>	104
II.2 PCA analysis	105
II.3 Network of Chemical reactions	107
<i>II.3.1 Dracoflavylum</i>	107
<i>II.3.1 A⁻ concentration in the equilibrium</i>	108
<i>II.3.2 Dracorhodin and 7,4'-dihydroxyflavylum</i>	109
II.4 References	109
Appendix III – Indigo dye data	110
<hr/>	
III.1 <i>I₀</i> and photodegradation quantum yields	110
III.2 Indigo photodegradation calibration curves HPLC-DAD	111
III.3 HPLC-DAD characterization	112
<i>III.3.1 Indigo dye</i>	112
<i>III.3.2 Indigo carmine</i>	112
III.4 Solar Box exposure	113
III.5 Indigo Andean Textiles	113
III.6 References	114
Appendix IV – Mauve dye data	115
<hr/>	
IV.1 Synthesis – Stoichiometries of the mauveine chromophores	115
<i>IV.1.1 Formation of Mauveine A</i>	115
<i>IV.1.2 Formation of Mauveine B</i>	116
<i>IV.1.3 Formation of Pseudo-mauveine</i>	117
IV.2 Mauve dye summarized characterization	119
IV.3 HPLC-DAD/LC-MS characterization	120
<i>IV.3.1 Mauve dyed textiles</i>	120
<i>IV.3.2 Mauve salts</i>	124
<i>IV.3.3 Mauve from other sources: mauve-dyed textiles</i>	125
IV.4 NMR characterization (structure elucidation)	126
<i>IV.4.1 Mauveine B2</i>	126
<i>IV.4.2 Mauveine C</i>	127
<i>IV.4.3 Pseudo-mauveine</i>	128

<i>IV.4.4 Mauveine C_{25a}</i>	129
<i>IV.4.5 Mauveine C_{25b}</i>	130
IV.5 ICP-AES characterization of the mordents from mauve dyed textiles	131
IV.6 Anion exchange chromatography of counter ions from mauve salts	131
IV.7 Heterogeneous media - polychromatic irradiation	133
IV.8 References	133

Index of figures

Chapter 1

Figure 1.1- Possible de-excitation pathways of excited molecules	2
Figure 1.2 - Adapted Jablonski scheme	3
Figure 1.3– a) Resin from <i>Dracaena draco</i> tree; b) Resin from <i>Daemonorops micrantha</i> (Griff.) Becc palm	6
Figure 1.4 – <i>Dracaena cinnabari</i> Balf, Socotra	6
Figure 1.5 – <i>Dracaena serrulata</i> Baker	6
Figure 1.6 – <i>Dracaena ombet</i> Kotschy & Peyr	7
Figure 1.7 – <i>Dracaena draco</i> L., Lisbon	7
Figure 1.8 – <i>Dracaena draco</i> L., Icod	8
Figure 1.9 – <i>Daemonorops draco</i> sp.	9
Figure 1.10 – <i>Croton lechleri</i>	9
Figure 1.11- <i>Pterocarpus officinallis</i>	10
Figure 1.12- <i>Dracaena cochinchinensis</i> (Lour.)	10
Figure 1.13 – Chemical structure of anthocyanins	11
Figure 1.14 – Network of chemical reactions for 7,4'-dihydroxy-5-methoxyflavylium	12
Figure 1.15 – PCA analysis of <i>Dracaena draco</i> , <i>Dracaena cinnabari</i> and <i>Daemonorops draco</i> HPLC data library chromatograms	16
Figure 1.16 – PCA analysis of <i>Dracaena draco</i> , <i>Dracaena cinnabari</i> and <i>Daemonorops draco</i> HPLC data library and EBC, Kew chromatograms	18
Figure 1.17 – HPLC profile of <i>Dracaena cinnabari</i> and <i>Dracaena schizantha</i> samples from EBC, K collection	23
Figure 1.18 – HPLC profiles of two resin samples labelled as <i>Dracaena draco</i> from the “Great Dragon Tree” of Tenerife - EBC, K collection	25
Figure 1.19 - UV-Vis absorption spectra variations of dracoflavylium with pH jumps	28
Figure 1.20 - Mole fractions distribution with pH for dracoflavylium at the equilibrium	28
Figure 1.21 - UV-Vis absorption spectra variations of dracorhodin with pH jumps	29

Chapter 2

Figure 2.1 – Production of indigotin and indirubin from plant leaves	33
Figure 2.2 - Indigo carmine	34
Figure 2.3 – Indigo reduction mechanism in non acidic media	35
Figure 2.4 – UV-vis spectra of indigo and isatin in DMF	36
Figure 2.5 – Monitorization by HPLC-DAD of indigo irradiation at 335 nm in homogeneous media	38
Figure 2.6 – Photodegradation of indigo carmine in bacteriological gelatine	41

Figure 2.7 - Monitorization by HPLC-DAD of indigo photodegradation in the solid state	42
---	----

Chapter 3

Figure 3.1 – Structure of the N-phenylphenazidium salt discovered by O. Fischer and E. Hepp in 1893 and R. Nietzki in 1896	49
Figure 3.2 – Mauveine structures discovered by Otto Meth-Cohn and Mandy Smith in 1994	49
Figure 3.3 - Fully characterised products isolated from modern mauve synthesis and mauve historical salt samples	52
Figure 3.4 – Mauve dyed textile samples from museum collections	54
Figure 3.5 –Mauve dyed shawl, ScMF6 sample	55
Figure 3.6 –Historical salt mauve samples.	58
Figure 3.7 – Mauve dyed textile reconstruction before and after 48h of irradiation	61

Appendix I – Experimental section

Figure I.1 – a) Resin collected from the branch; b) Resin collected from the stem; c) Extraction of the resin with acidified MeOH (AH ⁺) and MeOH (A)	87
Figure I.2 – <i>Dracaena</i> and <i>Daemonorops</i> samples	88
Figure I.3 – Gelatine indigo carmine gel before a) and after b) 335nm irradiation	93
Figure I.4 – Indigo glass slides irradiated in the solar box.	93
Figure I.5 – Perth Museum sample before and after extraction with MeOH / HCOOH	99

Appendix II – Dragon’s blood data

Figure II.1 - 7,4'-dihydroxy-5-methoxyflavylium hydrogen sulphate	102
Figure II.2 - 7-hydroxy-5-methoxy-6-methylflavylium	103
Figure II.3 - 7,4'-dihydroxyflavylium.	105
Figure II.4 - PCA analysis of <i>Daemonorops spp.</i> samples	106
Figure II.5 - PCA analysis of <i>Dracaena spp.</i> samples	106
Figure II.6 - pH jump of the compound 7,4'-dihydroxy-5-methoxyflavylium, from 1 to 8.8	108

Appendix III – Indigo data

Figure III.1 – HPLC-DAD chromatogram of indigo dye	112
Figure III.2– HPLC-DAD chromatogram of indigo carmine	113
Figure III.3 - HPLC-DAD chromatogram of an indigo Andean textile sample	114

Appendix IV-Mauve dye data

Figure IV.1 – Formation of mauveine A	115
Figure IV.2 –Formation of mauveine B	116

Figure IV.3 –Formation of pseudo-mauveine	117
Figure IV.4 – Mauve dyed textiles HPLC-DAD chromatograms	120
Figure IV.5 - HPLC-MS total ion chromatogram (TIC) Science Museum 1 salt sample	121
Figure IV.6 - HPLC-MS total ion chromatogram (TIC) of Science Museum F6	122
Figure IV.7 - HPLC-MS TIC of Museum SI Manchester 2 salt sample	123
Figure IV.8 - Mauve salts HPLC-DAD chromatograms	124
Figure IV.9 - Mauve-dyed textiles HPLC-DAD chromatograms from other sources	125
Figure IV.10 - Mauveine B2	126
Figure IV.11 - Mauveine C	127
Figure IV.12- Pseudo-mauveine	128
Figure IV.13 – Mauveine C _{25a}	129
Figure IV.14 – Mauveine C _{25b}	130
Figure IV.15 - Mauve salts IC-AEC chromatograms	132

Index of Tables

Chapter 1

Table 1.1 - Chemical structures responsible for the red colour in dragon's blood resins	11
Table 1.2 – HPLC data for <i>Daemonorops draco</i> , <i>Dracaena draco</i> , <i>Dracaena cinnabari</i> resins and respective flavylum markers.	15
Table 1.3 – <i>Daemonorops</i> samples from EBC, K analysed by HPLC-DAD	19
Table 1.4 - <i>Dracaena cinnabari</i> samples from EBC, K analysed by HPLC-DAD	21
Table 1.5 – <i>Dracaena draco</i> samples from EBC, K analysed by HPLC-DAD	24

Chapter 2

Table 2.1 - Absorption maxima and extinction coefficients of indigo, isatin and indigo carmine in DMF at T=293 K	36
Table 2.2 - Quantum yields of reaction, Φ_R , for indigo in DMF at T=293 K	37
Table 2.3 – Compounds identified by HPLC-DAD with the photodegradation of indigo carmine in water and DMF with 335nm irradiation	39
Table 2.4 - Quantum yields of reaction, Φ_R , for indigo carmine in aqueous gels and water at T=293 K	40
Table 2.5 – Relative concentration of the principal chromophores and main products identified in Andean Textiles by HPLC-DAD	43

Chapter 3

Table 3.1 – Syntheses of mauve dye with different ratios of aniline and toluidine	50
Table 3.2 – Relative percentages of the mauveine chromophores in the synthesized mauve dye	53
Table 3.3 - Relative percentages of the main chromophores of the mauve dyed textile sample	54
Table 3.4 - Relative percentages of the main chromophores of the mauveine salt samples and respective counter-ions	57

Appendix I – Experimental section

Table I.1 – Elution gradients used for mauve dye analysis	75
Table I.2 - Library samples analysed by HPLC-DAD	80
Table I.3 – Historical mauve samples	95
Table I.4 –Extraction methods tested in mauve dyed silk textile	99
Table I.5 – Mauveine chromophores distribution in mauve dyed textile	100
Table I.6 - Ion standards and respective retention times in water	100

Appendix II – Dragon’s blood data

Table II.1 – ^1H and ^{13}C -NMR data for 7,4'-dihydroxy-5-methoxyflavylium	103
Table II.2 – ^1H and ^{13}C -NMR data for 7-hydroxy-5-methoxy-6-methylflavylium	104
Table II.3 – ^1H and ^{13}C NMR data for 7,4'-dihydroxyflavylium	105

Appendix III – Indigo data

Table III.1 – I_0 and parameters for the 335 nm and 610 nm irradiations	110
Table III.2 – Indigo ϕ_R and parameters for the 335 nm and 610 nm irradiations	110
Table III.3 – Indigo carmine ϕ_R and parameters for the 335 nm and 610 nm irradiations	111
Table III.4 – HPLC-DAD calibration curves of indigo and isatin	111

Appendix IV-Mauve dye data

Table IV.1 – Concentration of the starting materials used in the 4 mauve dye syntheses	118
Table IV.2 – Concentrations of $\text{K}_2\text{Cr}_2\text{O}_7$ and H_2SO_4 necessary for mauve synthesis	118
Table IV.3 - Structures and summarized spectral data for mauveine compounds	119
Table IV.4 - ^1H - and ^{13}C -NMR data for the isolated mauveine B2	126
Table IV.5 - ^1H - and ^{13}C -NMR data for the isolated mauveine C	127
Table IV.6 - ^1H - and ^{13}C -NMR data for the isolated pseudo-mauveine	128
Table IV.7 - ^1H - and ^{13}C -NMR data for the isolated mauveine C_{25a}	129
Table IV.8 - ^1H - and ^{13}C -NMR data for the isolated mauveine C_{25b}	130
Table IV.9 - Mordant analysis of three mauve-dyed textile samples	131
Table IV.10 - Counter-ions of the mauve salt samples	133

General Introduction - *Molecular and photochemical studies on historical dyes: dragon's blood, indigo and mauve*

1. Preamble

Before the discovery of mauve dye and later thousands of synthetic dyes that resemble a colourful rainbow [1] in the nineteenth century, the colours used to dye a textile since pre-historic times were obtained from natural sources – vegetable or animal [2,3]. For the blue and purple colours, indigo derivatives were mainly used. For red dyed textiles, anthraquinone based dyes could be found and the yellows were obtained from an enormous variety of local plant species, mostly from the flavonoid family [2,3]. From these organic dyes, dragon's blood and indigo were chosen for the red and blue colour study, respectively. The synthetic mauve dye, a landmark in the history of chemistry and dye industry, was also studied.

A characterization at the molecular level of dragon's blood, indigo and mauve dye is the main aim of this thesis. A more in-depth understanding will in turn enable a better conservation and access to our cultural heritage, namely to ancient textiles. This PhD thesis was carried out in the framework of the project *Molecules of Colour in Art: a Photochemical Study*, where the molecular studies evolved along three main axes with: i) structural characterization of the most relevant chromophores in each dye; ii) photophysical characterization and iii) photochemical characterization. In this thesis, the structural characterization of dragon's blood, indigo and mauve dye, as well as the photodegradation of indigo will be presented.

In each chapter an introduction to each organic dye is presented, followed by its molecular characterization and photodegradation for the indigo dye. A brief summary of the principal conclusions is also presented.

2. Chromophores' characterization

Organic dyes are usually a complex mixture of different chromophores that bring colour to the textile. In natural dyes, such as dragon's blood, the presence of several chromophores with different relative proportions according to the dyeing source, the local, date and season of the sampling amongst others [4,6], can give a kind of fingerprint very useful in the identification of dyes in works of art, such as textiles [2,7]. With this information amongst others factors, it will be possible, for example, to establish conception dates, assign production centres, identify textile trade routes, etc [8]. Moreover, successful photophysical and photodegradation characterization is only possible when the molecules

involved are well characterized structurally. In synthetic dyes, like the mauve dye, a complex pattern of chromophores can also be found, when the synthetic procedure gives several coloured products. Nevertheless, a simpler pattern can be found in natural and synthetic dyes as the case of the indigo dye where usually only the indigotin chromophore is retained on the fibres during the dyeing bath [2]. For this reason the photodegradation of indigo in homogeneous and heterogeneous media was carried out.

3. Photophysical characterization

Organic dyes being coloured molecules will absorb in the UV-Vis region and therefore photochemical reactions that will dictate the stability of the molecule can occur. When these molecules absorb radiation, the resulting extra energy produces an excited state molecule, which can be considered an entire new molecule since several properties as its polarity, acidity, oxidation and reduction properties, just to name a few, are entirely different from the ground state molecule [9-12]. The lifetime of an excited molecule is usually very small, in the order of nanoseconds or even less. It can return to the ground state with emission of fluorescence (i.e. emission of photons), internal conversion (i.e. direct return to the ground state without emission of fluorescence), intersystem crossing (possibly followed by emission of phosphorescence), intramolecular charge transfer; proton transfer; photochemical reactions, amongst others (see figure 1.1), which compete with each other while the molecule is in the excited state.

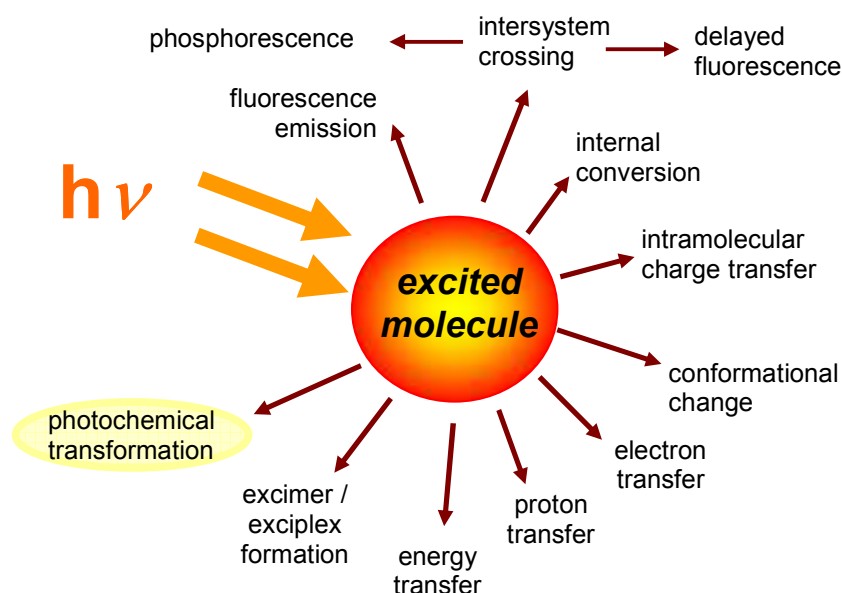


Figure 1.1- Possible de-excitation pathways of excited molecules, adapted from [9].

When the excited molecule loses energy through chemical reactions we are in the photochemistry field but when the excited molecule is converted to the ground state, with the excess of energy being released as radiative or non radiative energy we are in the photophysics domain [11,12]. In the excited state, bonds can be broken and new ones formed; if the processes involving bond breaking and formation are reversible, they will be considered as non radiative photophysical deactivations (figure 1.2). If they are irreversible, they will be studied as a photochemical reaction and an important parameter for its characterization is defined as the quantum yield of reaction (see below).

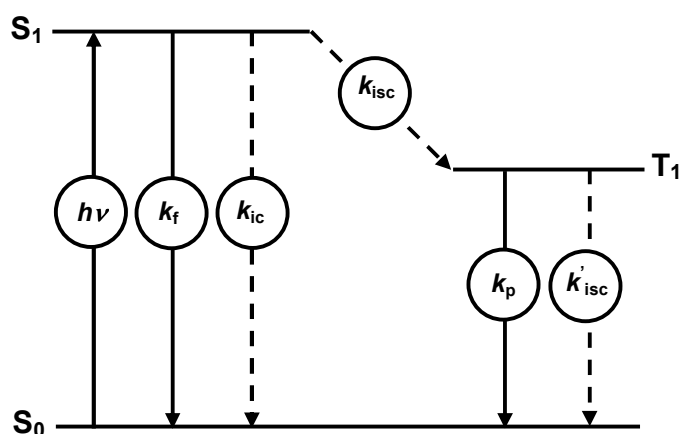


Figure 1.2: Adapted Jablonski scheme [9], where the k_f (fluorescence deactivation) and k_p (phosphorescence deactivation) are the rate constants for the radiative processes and the k'_{isc} (intersystem crossing deactivation), k_{ic} (internal conversion deactivation) and k_{isc} (intersystem crossing deactivation) are the non-radiative processes. The S_0 and S_1 are the singlet and excited ground state respectively and T_1 is the first triplet state.

For a full photophysical characterization, absorption, fluorescence and phosphorescence spectra can be obtained; triplet-triplet absorption analysis is also performed. Moreover, fluorescence lifetimes and quantum yields can be determined and the rate constants responsible for the excited state deactivation can be calculated.

The photophysical characterization will enable a better understanding of the photochemistry as well as more precise lifetime of the molecule. The study of the influence of oxygen in the photochemistry and reactivity of these dyes will, in turn, enable a better understanding of which are the photophysical parameters that play a relevant role in the photodegradation mechanism. Furthermore, it will enable the prediction of the colour changes over time.

4. Photochemical characterization

One important parameter, as mentioned before, in the characterization of photochemical reactions is the photodegradation quantum yield of a reaction that can be defined as:

$$\Phi = \frac{\text{Amount of reactant consumed or product formed}}{\text{Amount of photon absorbed}} \quad \text{per unit of time}$$

The quantum yield obtained should take into account the role of oxygen in the photodegradation reaction as photooxidation can contribute for the global mechanism of fading. Therefore, the photodegradation quantum yield in the presence and absence of oxygen should be calculated.

Moreover, the main photoproducts should also be identified as well as the intermediates formed after monochromatic irradiation, in order to obtain the principal degradation mechanisms occurred during the light induced fading.

A systematic approach to the study of the photophysics and photochemistry of these colourants cannot be found in the literature. Particular importance has been given to the molecular characterization of the cited molecules rather than on a full understanding of the photodegradation mechanisms. It is important to remember that the most known organic dyes had to overcome the barrier of light and washing fading during hundreds of years. Therefore, their degradation is somehow a slow process and for that reason the photophysical and photochemical characterization of these organic dyes is a complex and time-consuming task. Nevertheless, it is important to know their molecular mechanisms of degradation, in order to be able to plan strategies to prevent their fading and improve their durability.

With the results presented in this thesis, new knowledge into historic dyes at their molecular level is provided and, from now on, it will be easier to perform a detailed photophysical and photochemical study of these organic dyes as well as applying the results obtained in the research and conservation of textiles.

Chapter 1 - Dragon's Blood

1.1 *Dragon's blood overview*

Dragon's blood is a natural resin [13] with a rich deep red colour obtained essentially from three different families of plants, namely *Dracaenaceae*, *Palmae* and *Euphorbiaceae* [14-17]. It may sound like an exotic ingredient of a witch's brew or a magic potion. Indeed, legends refer that dragon's blood was the result of a fight between a dragon and an elephant until death, where a dragon tree sprung up from the congealed blood dropped by both animals, giving "magical" properties to the red resin [14-17]. In the Greek mythology it was mentioned that Hercules killed Geriones (the three headed monster) from the Eriteya Island, and from his blood a tree was also born with red fruits which produced the dragon's blood resin [18]. Curiously, the red resin has been applied for centuries in traditional medicine with different clinical and ethnomedical uses where pharmacological assays have frequently corroborated its medical applications (and therefore the "magical" properties of dragon's blood) against cancer, ulcers and wounds, amongst others [19-28]. Apart from this, dragon's blood has also been used in the past with several artistic purposes [14-17,29].

Attempts to unveil the trade history of dragon's blood resins, the use of its sources and even its chemical composition have been difficult due to botanical misunderstanding and the diversity of dragon trees [14-17,30-32]. It is believed that in the past, one of the principal sources of dragon's blood was *Dracaena cinnabari* Balf. (*Dracaenaceae*) from Socotra Island [14-16]. Today the main dragon's blood resin commercially available is obtained from the species *Daemonorops draco* (Willd.) Blume (synonym *Daemonorops propinqua* Becc.) from Thailand, Sumatra and Borneo [14-16,30,33]. However, a great diversity of dragon's blood resins has been used since ancient times until today, due to the different dyeing sources of the resin available in each geographic area [14-16,27-28].

The resin can be collected from natural exudates that occur in injured areas in the stem and branches of the tree (*Dracaenaceae* and *Euphorbiaceae* families, figure 1.3a) or can be obtained from the fruits which are covered with small scales through where the resin exudes forming a brittle red resinous layer outside the fruits (*Palmae* family, figure 1.3b) [14-16,34-37].



Figure 1.3– a) Resin from *Dracaena draco* tree; b) Resin from *Daemonorops micrantha* (Griff.) Becc. [13].

1.1.1 *Dracaenaceae* (mostly larger Mediterranean)

In the *Dracaenaceae* family, which comprises between 60 and 100 species, only 5 species have the growth habit of a tree with an umbrella type crown producing dragon's blood resin [34,35,38-41]. These trees are the *Dracaena cinnabari* Balf. (figure 1.4) which is endemic of Socotra Island [38]; *Dracaena serrulata* Baker (figure 1.5) from the south-western Arabia [34,35]; the *Dracaena ombet* Kotschy & Peyr (synonym *Dracaena schizantha* Baker, figure 1.6) from North-East tropical Africa and western Arabian peninsula [40]; *Dracaena draco* L. (figure 1.7) from the Macaronesian Islands as Madeira, Azores, Cape Verde and Canarias [34,35] or from Morocco being reported there as *Dracaena draco* L. subsp. *Ajgal* Benabid et Cuzin [41], and finally the recently identified *Dracaena tamaranea* A. Marrero & al. (similar to *Dracaena draco* L.) from the Gran Canaria (Canary Islands)[39].



Figure 1.4 – *Dracaena cinnabari* Balf, Socotra [42].

Figure 1.5 – *Dracaena serrulata* Baker [43].



Figure 1.6 – *Dracaena ombet* Kotschy & Peyr [44].

Figure 1.7 – *Dracaena draco* L., Lisbon.

It is believed that these dragon trees with a bizarre prehistoric appearance share a common origin due to the similar morphological features and the existence of comparable fossils (*Dracaenites brongniartii* Saporta, *Dracaenites narbonensis* Saporta and *Dracaenites sepultus* Saporta) from Tertiary deposits (65 million to 1.8 million years ago) in Southern Europe [38,39]. During the Tertiary period, the drastic climate changes at the end of the Oligocene brought about the almost extinction of the subtropical vegetation throughout the South of Europe and North Africa, from the Atlantic to the Indian Oceans and lead to a biogeographic dissociation between the living dragon's tree of East and West Africa. Only a few specimens of the ancient flora survived on both sides of the African continent where the environmental conditions were more stable due to the tempering effect of the sea [39]. Far from one another, these remaining colonies continued to develop independently, giving rise to the actual five species of dragon's tree of the *Dracaena* genus. As long isolation exists, each species will tend to become slightly different from others [37,39]. Nevertheless, similarities can be drawn between the five species mentioned.

Important colonies of this ancient relic flora are the *Dracaena cinnabari* dragon's tree of Socotra Island with an age between 200 and 300 years old [38]. However, studies point out that this *Dracaena cinnabari* woodland will reach the stage of intensive disintegration within 30-77 years due to climate changes [38,45]. Other very famous exemplar was the Great Dragon Tree of Orotova (Tenerife) believed to have an estimated age of 6000 years old. The dragon tree fell in 1817 due to a hurricane. Today, the oldest *Dracaena draco* tree in Icod (Tenerife) has an estimated age of 700 years old [13-16] (figure 1.8). Being monocots, its age is very difficult to estimate due to the lack of annual growth rings.

Nevertheless, the dragon's tree age can be estimated with different indirect methods being the most usual the number's determination of the sausage-shaped section that normally display between 11 and 16 years for *Dracaena draco* and 14-30 years for *Dracaena cinnabari* [38].



Figure 1.8 – *Dracaena draco* L., Icod [46]

1.1.2 *Palmae* (mostly South East Asia)

In the *Palmae* family, the species that produce dragon's blood resin belong to genus rattan *Daemonorops* which comprises about 115 species [36,37,47]. The *Daemonorops* genus is divided into two sections, the *Cymbospatha* and the *Piptospatha* being the most important product of the last one, the dragon's blood powder. The dragon's blood species are confined to Malaysia, Thailand and West Indonesia, where the red resin is an item of trade between Borneo, Sumatra, the Malay Peninsula and even China [16]. As in the *Dracaenaceae* family, they are a natural unit taxa where some species have slightly diverged because of isolation or adaptation [37-39]. As mentioned before, the most commonly used *Daemonorops sp.* dragon's blood species is *Daemonorops draco* (Willd.) Blume (synonym *Daemonorops propinqua* Becc. Species, figure 1.9), but up to 10 species are known, namely the *Daemonorops brachystachys* Furtado from Peninsula Malaysia to North Sumatra, *Daemonorops didymophylla* Becc. Ex JD Hooker from Peninsula Thailand to West Malesia, Sumatra, *Daemonorops dracuncula* Ridl. from Sumatra (Kep. Mentawai), *Daemonorops dransfieldii* Rustiami from Sumatra, *Daemonorops maculate* J. Dransf. from Borneo, *Daemonorops micrantha* (Griff.) Becc. from Peninsula Malaysia and Borneo, *Daemonorops rubra* (Reinw. ex Mart.) Blume from Jawa, *Daemonorops sabut* Becc. from Peninsula Thailand to West Malesia [36,37], and the recently discovered *Daemonorops acehensis* Rustiami from Sumatra as well the *Daemonorops siberutensis* Rustiami from Sumatra (Kep. Mentawai) [47].



Figure 1.9 – *Daemonorops draco* sp. [48].

1.1.3 *Euphorbiaceae* (mostly Latin America)

In the *Euphorbiaceae* family the production of dragon's blood belongs to genus *Croton* (figure 1.10) widespread in tropical regions of the Old and New World with circa 1300 species [27-28].



Figure 1.10 – *Croton lechleri*, [49].

Several species of *Croton*, namely *Croton lechleri* from South American (Ecuador, Peru, Colombia and Bolivia), *Croton palanostigma* Klotzsch from South American tropics (Peru), *Croton draco* Cham & Schtdl. from Mexico and Central America, *Croton urucurana* Baill from Brazil and Paraguai, *Croton erythrorchilus* Müll.-Arg. from Peru, *Croton perspicuosus* Croizat, *Croton aromaticus* L. from Sri Lanka, and *Croton rimbachii* Croizat have been used in the production of the red resin [27, 28].

1.1.4 Others

Other known sources of dragon's blood are the *Pterocarpus officinalis* Jacq. (synonymous of *Pterocarpus draco* L., *Leguminosae* family, figure 1.11) from West Indian, Caribbean, coastal areas of Central and northern South America [15,16,50] and the shrub *Dracaena cochinchinensis* (Lour.) S. C. Chen (*Dracaenaceae* family, figure 1.12) from China, S.W. Guangxi to S. Yunnan, to Indochina believed by some authors to be the original source of the dragon's blood used for thousands of years in traditional Chinese medicine [25,51].



Figure 1.11-*Pterocarpus officinallis* [52]

Figure 1.12-Shrub *Dracaena cochinchinensis* (Lour.) [53]

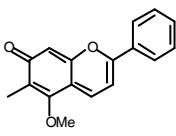
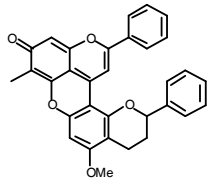
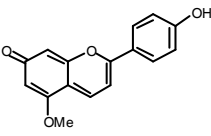
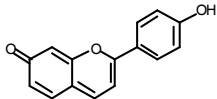
However, it is known that for Chinese herbal medicine *Daemonorops* was also imported into China from South-East Asia, and others sources as ***Dracaena angustifolia* (Medik.) Roxb** (tropical and subtropical Asia to North Australia including Taiwan, Guangdong and Yunnan) and ***Dracaena cambodiana* Pierre ex Gagnep.** (South Hainan to Indochina) [52] were also used.

1.2 Chemical composition – The red colourants unveiled

The dragon's blood resins are a complex mixture of several compounds. Recent phytochemical studies on the genera *Dracaena* and *Daemonorops* identified several compounds as saponins [19-21,55], chalcones [23], flavonoids [23,56-58], sterols [59], and flavans [58,59], amongst others. These compounds are colourless or display a yellowish colour. However, for the *Daemonorops sp.* resins, besides the presence of chalcones, flavans and flavonoids, red flavylum pigments as dracorhodin and dracorubin were also identified [60,62-69]. It was in 1936 that Brockmann and Haase published the first attempt to identify the red colourants of a powdered commercial dragon's blood resin probably from a *Daemonorops sp.* source in which they isolated one of the red compounds and named it as dracorubin [62]. A second colourant, dracorhodin, was identified in 1943 by Brockmann and Junge that have also synthesized the molecule and concluded it was a natural 2-phenyl-1-benzopyrylium (a flavylum salt) from the anthocyanins family [64]. A more straightforward synthesis, and consequent confirmation of the structure, was published by Robertson and Whalley, in 1950 [65]. The structure of dracorubin was proposed by Robertson and Whalley in 1950 [65] and the molecule was only synthesized

in 1975, by Whalley [66]. In the meantime, two other natural red flavylium colorants from dragon's blood were characterized and named as nordracorhodin and nordracorubin [60,67] (table 1.1).

Table 1.1 - Chemical structures responsible for the red colour in dragon's blood resins. The structures correspond to the quinoid bases (**A**).

Dracorhodin	Dracorubin	Dracoflavylum	7, 4'- dihydroxy-flavylium
			
1943 [64], 1950 [65]	1936 [62], 1937 [63], 1950 [68], 1976 [66]	2006 [69]	2008 [70]

The presence of natural flavylium compounds in dragon's blood resin from *Daemonorops* sp. has been mislaid during the last decades [19-22,26,30-32]. However, those natural flavylium compounds contribute significantly to the final deep red colour of dragon's blood resin.

Synthetic flavylium salts, natural flavylium and anthocyanins have in common the 2-phenyl-1-benzopyrylium chromophore unit. In terms of molecular structure, flavylium salts were the first to be discovered, Bülow [71] 1901, followed by the natural anthocyanins, Willstätter [72], and finally by natural flavylium compounds [73].

Anthocyanins are characterized by the existence of an O-glucoside in position 3 (monoglucoside). A sugar can also be present in position 5 (diglucosides) or less frequently in position 7 [74], figure 1.13. On the other hand, in anthocyanidins hydroxyl groups take the positions of the glucosides, leading to unstable structures in solution. On the contrary, the so-called desoxyanthocyanidins, that corresponds to "anthocyanidins" lacking the hydroxyl in position 3 (but bearing a hydroxyl in position 5), are quite stable in solution.

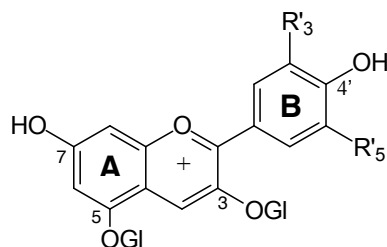


Figure 1.13 – In the basic chemical structure of anthocyanins, an hydroxyl group is present in positions 4' and 7, and a sugar in position 3 (monoglucosides) or 3 and 5 (diglucosides).

In the seventies of the last century, it was firmly established by Dubois and Brouillard (anthocyanins) [75] and McClelland (synthetic flavylium salts) [76] that both families of compounds undergo multiple structural alterations in aqueous solution, following the same basic mechanism [77] (see figure 1.14).

The flavylium cation (**AH⁺**) is the dominant species in very acidic solutions, but with increasing of pH a series of more or less reversible reactions occur: 1) deprotonation leading to the quinoid base (**A**), 2) hydration of the flavilyum cation giving rise to the colourless hemiacetal (**B**), 3) tautomerisation reaction, responsible for ring opening, to give the pale-yellow Z-chalcone form (**Cc**), and finally, 4) cis-trans isomerisation to form the pale-yellow chalcone (**Ct**). Furthermore, at higher pH, and depending on the number of hydroxyl groups, further deprotonated species are found, such as **Ctⁿ⁻** and **Aⁿ⁻**. The relevant contribution for the colour is given by **AH⁺** and the quinoid bases.

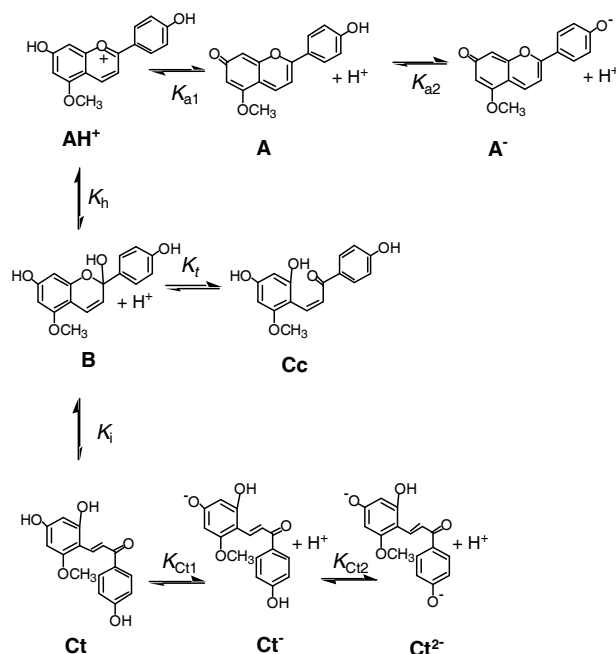


Figure 1.14 – Network of chemical reactions for 7,4'-dihydroxy-5-methoxyflavylium in solution [69] (see section 1.3.4.1).

In this work, the discovery of natural flavylium compounds in resins [69,70], namely the compounds 7,4'-dihydroxy-5-methoxyflavylium and 7,4'-dihydroxyflavylium from *Dracaena draco* and from *Dracaena cinnabari*, respectively, is reported for the first time. A fingerprint study of these red chromophores in dragon's blood resins from *Dracaena* and

Daemonorops trees was performed using high performance liquid chromatography with diode array detector (HPLC-DAD) and principal component analysis (PCA).

These natural flavylum markers do not fit the commonly accepted definition of anthocyanidin or 3-deoxyanthocyanidin [78] as some authors recently have proposed for analogous structures from *Arrabidaea chica* [79], as a methoxy group was found in position 5. Their structure and chemical behaviour are closer to the so-called synthetic flavylum salts, as will be described below.

1.3 Results

Due to the great diversity of dragon's blood resins and botanical misunderstandings amongst others in the literature, previously to the resin red compounds characterization, an HPLC-DAD data base was built (see appendix I - experimental section, section I.3 p.79). Moreover, a method based on flavylum markers was developed for the resins identification and applied to the XIX century dragon's blood collection of the Economic Botany Collections at the Royal Botanic Gardens, Kew (EBC, K). Afterwards the dragon's blood flavylum characterization was performed.

1.3.1 Dragon's blood resins data library

From the circa 30 species referred in the section 1.1, only three species (*Dracaena draco*, *Dracaena cinnabari* and *Daemonorops draco*), which were probably the most important species used in Europe, were selected for the construction of the dragon's blood HPLC-DAD library (see appendix I - experimental section, table I.2, p. 80, for library HPLC-DAD dragon's blood samples). The aim of the HPLC library was the distinction of dragon's blood species and subsequent identification of unknown resins. An initial HPLC-DAD screening revealed the presence of different flavylum compounds responsible for the red colour of the resins. The use of the flavylum compounds as potential species markers for dragon's blood resins was for the first time investigated.

Circa 50 samples from *Dracaena draco*, *Dracaena cinnabari* and *Daemonorops draco* (mostly collected in botanical gardens) were analyzed by HPLC-DAD. The results obtained were subsequently applied to 37 samples of dragon's blood from EBC, K (labelled as *Daemonorops draco*, *Daemonorops sp.*, *Dracaena cinnabari*, *Dracaena draco*, *Dracaena schizantha* and *Dracaena sp.*). The EBC, K contains perhaps the largest and most reliably identified assemblage of dragon's blood resins dating from the 19th century which were donated by Sir Isaac Bailey Balfour or the Pharmaceutical Society of Great Britain, amongst others [14,16].

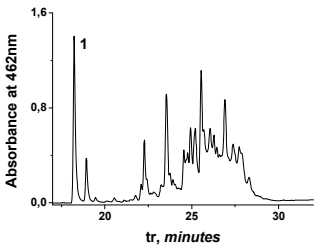
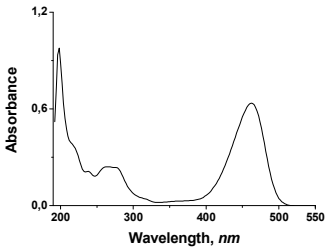
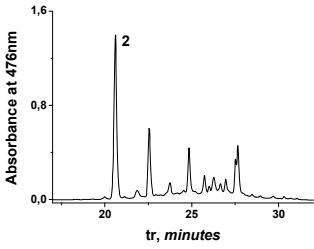
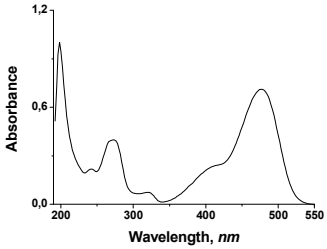
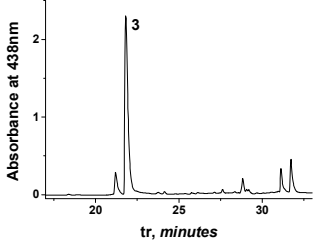
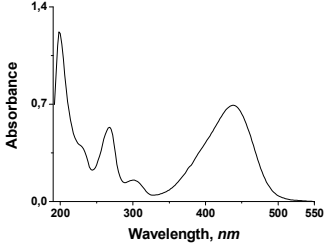
1.3.2 Flavylium markers identification

Samples from known provenance, with the species correctly identified by experts, were used to build-up the HPLC-DAD database (i.e. for the *Dracaenaceae*, 33 samples of *Dracaena draco* and 9 samples of *Dracaena cinnabari*). It was also possible to characterize roughly the tree age (for more details see appendix I – experimental section, table I.2, p. 80). The situation was different for the *Daemonorops draco* resin, where only 2 commercial samples were acquired. However, this limitation was overcome with the analysis of the dragon's blood EBC, K collection (see section 1.3.3.1).

In all the samples analysed, the red colour resulted from the contribution of single flavylium chromophores, as for instance, dracorhodin, and condensed flavylium molecules, such as dracorubin [23,24,62-69] (see table 1.1). More importantly, it was observed (table 1.2) that *Dracaena draco*, *Dracaena cinnabari* and *Daemonorops draco* presented each one a characteristic flavylium: 7,4'-dihydroxy-5-methoxyflavylium (dracoflavylium), 7,4'-dihydroxyflavylium and 7-hydroxy-5-methoxy-6-methylflavylium (dracorhodin), respectively. As can be observed in table 1.1, these compounds have the 2-phenyl-1-benzopyrylium core in common, but a different substitution pattern, consequently each exhibit characteristic UV-Vis spectra and retention times (table 1.2). This, in turn, enables a straightforward identification of these flavylium chromophores by HPLC-DAD, which leads to the identification of the dragon's blood source (table 1.2). Besides these markers, the chromatograms acquired at the wavelengths for red detection (462 nm) for each resin type are also characteristic for these species and, after PCA, could also be used as a fingerprint (see table 1.2 and figure 1.15).

The PCA principal components represented in Figure 1.15 can be analysed according to the corresponding loadings (each sample PCA score is the inner product between the sample chromatogram and the loading corresponding to a given principal component). It was observed that the loading for the first score, PC#1, contains strong positive peaks at 20.5, 27.4 and 27.9 min and strong negative peaks at 18.0, 18.7 and 23.3 min. The former correspond to *Dracaena draco* elution peaks while the latter correspond to *Dracaena cinnabari* peaks. Therefore, the first PCA component, PC#1, is able to discriminate between these two *Dracaena* species (positive scores for *Dracaena draco* and negative scores for *Dracaena cinnabari* in the first component axis). The third score, PC#3, exhibits two strong positive peaks at 21.1 and 21.7 min. These peaks correspond to peaks observed in *Daemonorops draco* chromatograms (see table 1.2). No other relevant peaks were observed in the third loading which means that this component captures only the *Daemonorops draco* samples information (strong positive scores in the third score).

Table 1.2 – HPLC chromatogram profiles, retention times and absorption maxima for *Daemonorops draco*, *Dracaena draco*, *Dracaena cinnabari* resins and respective flavylum markers.

Species	Chromatogram	Flavylum marker	Spectrum' Flavylum marker
<i>Dracaena cinnabari</i> Balf. f. (Source: Firmihin and Hamadero in Socotra Island; mean age circa 250 years old)		(1) 7,4'-dihydroxyflavylum $t_r = 18.03 \pm 0.15$ min $\lambda_{\max} = 462$ nm	
<i>Dracaena draco</i> L. (source: Natural Park of Madeira; age: circa 200 years old)		(2) Dracoflavylum 7,4'-dihydroxy-5-methoxyflavylum $t_r = 20.51 \pm 0.12$ min $\lambda_{\max} = 476$ nm	
<i>Daemonorops draco</i> (Wild.) Blume (source: Zecchi; age unknown)		(3) Dracorhodin 7,6-dihydroxy-5-methoxyflavylum $t_r = 21.76 \pm 0.07$ min $\lambda_{\max} = 438$ nm	

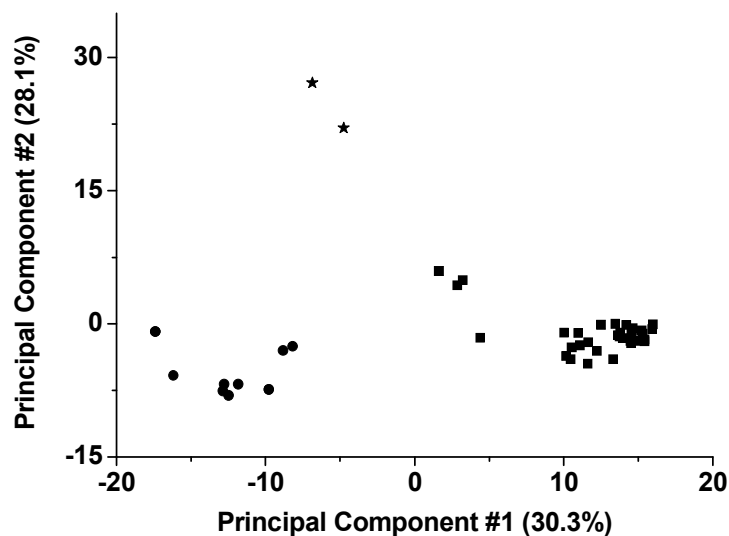


Figure 1.15 – PCA analysis of *Dracaena draco* (squares), *Dracaena cinnabari* (circles) and *Daemonorops draco* (stars) with HPLC data library chromatograms acquired at 462 nm..

1.3.2.1 *Dracaena draco*: 7,4'-dihydroxy-5-methoxyflavylium

The HPLC-DAD library for *Dracaena draco* was created with resins freshly gathered from Madeira, Lisbon and Cape Verde. In all the samples analysed the 7,4'-dihydroxy-5-methoxyflavylium (dracoflavylium) was always present. Samples enclosed by the dotted line are centenary trees c. 200 years old, where dracoflavylium content was the major red compound (c. 32%) (figure 1.15). In the other samples this flavylium was present as a minor product of the total amount of the red colourants of resin, ranging from 1-10% (relative area). Although relative concentration of dracoflavylium is variable, this flavylium was only found in *Dracaena draco* resins.

1.3.2.2 *Dracaena cinnabari*: 7,4'-dihydroxyflavylium

In the chromatograms used to build-up the HPLC-DAD library for *Dracaena cinnabari*, the quantity of 7,4'-dihydroxyflavylium varied from 5% to 15% of the relative area for the total amount of the red colourants of resin. The colour of this resin is due to a complex mixture of red compounds (table 1.2), with 7,4'-dihydroxyflavylium being one of the major chromophores.

1.3.2.3 *Daemonorops draco*: 7-hydroxy-5-methoxy-6-methylflavylium

In the *Daemonorops draco* resins, 7-hydroxy-5-methoxy-6-methylflavylium (dracorhodin) was the major red compound. The occurrence of dracorhodin in *Daemonorops sp.* resins has been described already in the literature [23,24,62-65].

1.3.3 The Economic Botany Collections at the Royal Botanic Gardens – Kew

After obtaining the results described above, identification of dragon's blood resin sources based on flavylium markers was applied to the largely 19th century collection of dragon's blood at EBC, K. These items comprise not only resins from the already described *Daemonorops draco*, *Dracaena draco* and *Dracaena cinnabari*, but also unnamed *Daemonorops* and *Dracaena sp.* resins and one resin from Zanzibar tentatively labelled *Dracaena schizantha* (a synonym of *Dracaena ombet*). The EBC, K collection is very heterogeneous with very different grades of resin purity. Just over 50% of the resin collection labelled as *Daemonorops draco* (or its synonym *Daemonorops propinqua*), *Dracaena cinnabari* and *Dracaena draco* species were examined.

The results obtained were analyzed and compared with the HPLC-DAD data library, using the flavylium markers and the PCA of the full chromatograms acquired at 462 nm. Both approaches gave identical results and successfully discriminated *Daemonorops draco*, *Dracaena cinnabari* and *Dracaena draco* (see figure 1.16). On the other hand, it was not possible to distinguish unambiguously the EBC, K sample labelled *Dracaena schizantha* (a synonym of *Dracaena ombet*) from the circa 30 *Dracaena cinnabari* samples analysed (HPLC-DAD library and EBC, K collection). All the samples, had the same flavylium marker; however, due to the small number of samples labelled *Dracaena schizantha*, 1 from EBC, K and 1 from the living collections (Horticulture & Public Education, Kew - HPE, K) a more conclusive result using PCA could not be drawn.

PCA shows that all the EBC, K samples are in accordance with the built-up data library (figure 1.16), therefore, being possible to establish and verify the species source. Only two samples lay outside the three established areas: the samples EBC, K 36653 (labelled *Dracaena draco*), which is probably a mixture of resins, and EBC, K 36825 (labelled *Dracaena draco*), which is not actually based on flavylium compounds. In the next sections the results obtained will be described in more detail and, whenever possible, they will be compared to previous analyses of the EBC, K red resins by Raman [30-32].

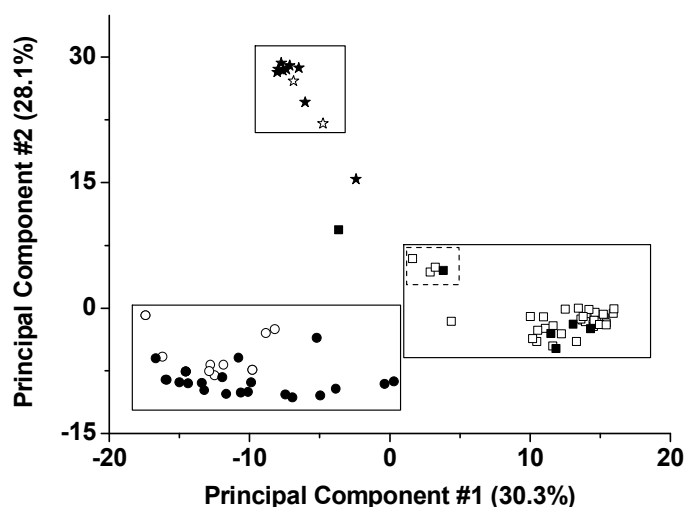


Figure 1.16 - PCA analysis of *Dracaena draco* (squares), *Dracaena cinnabari* (circles) and *Daemonorops draco* (stars); HPLC chromatograms acquired at 462 nm for data library samples (open symbols) and EBC, K samples (solid symbols). The areas assigned represent three major distinct zones enabling the species identification of the samples analyzed.

1.3.3.1 *Daemonorops draco* (synonym, *Daemonorops propinqua*) and *Daemonorops sp.*

In the EBC, K samples labelled as *Daemonorops draco* or *D. propinqua*, 7-hydroxy-5-methoxy-6-methylflavylium (dracorhodin) was identified as the major compound. This observation is in line with the recent publication which announced the two taxa as synonyms [37], *Daemonorops draco* being the accepted name [33]. Furthermore, the chromatograms obtained for these samples are very similar, as confirmed by PCA analysis (see appendix II – Dragon’s blood data, section II.2, p. 105, for PCA graphics).

The HPLC-DAD data showed that of the 9 analyzed samples labelled *Daemonorops draco*, *Daemonorops propinqua* or *Daemonorops sp.*, only 6 samples had a correct attribution (see table 1.3). In 4 samples (35489, 35495, 35500, 35526), the relative percentage of 7,6-dihydroxy-5-methoxyflavylium (dracorhodin) was circa 65% of the total area of red chromophores as found in the commercial *Daemonorops sp.* resins. In samples that were processed (35490 and 35505), the relative percentage of 7-hydroxy-5-methoxy-6-methylflavylium decreased to 55% of the total red chromophores.

Table 1.3 – Specimens of *Daemonorops* samples from EBC, K analysed by HPLC-DAD and percentage of the flavylum markers identified.

ID	EBC, K classification	Date of donation	Provenance, donor	Observations	Species % flavylum marker*
35487	<i>Daemonorops draco</i>	?	India, India Museum	Mixture of resin, bark and powder.	<i>Dracaena cinnabari</i> Circa 6% 7,4'- dihydroxyflavylum
35489	<i>Daemonorops draco</i>	1851	Singapore A.S. Hill & Son	Mostly resin. Labelled as " <i>Calamus draco</i> , in lumps, colour of powder, brick red. Contains about 12 per cent of insoluble matter". Paler and duller than other samples.	<i>Daemonorops draco</i> Circa 65% dracorhodin
35490	<i>Daemonorops draco</i>	1851	India, Calcutta, Royal Commonwealth Exhibition	Mostly resin. Labelled as "Reed dragon's blood"	<i>Daemonorops draco</i> Circa 55% dracorhodin
35495	<i>Daemonorops draco</i>	?	?, British Museum (Natural History)	Mixture of resin and powder. The sample appears to be small pieces from a reed resin.	<i>Daemonorops draco</i> Circa 65% dracorhodin
35499	<i>Daemonorops draco</i>	?	Sumatra, ?	Resin attached to fruit scales.	<i>Daemonorops sp. (?)</i> Circa 65% unknown compound ($t_r=21.03$ min, $\lambda_{max}=453$ nm)
35500	<i>Daemonorops propinqua</i>	1896	Sumatra, ?	Resin attached to fruit scales.	<i>Daemonorops draco</i> Circa 65% dracorhodin
35526	<i>Daemonorops propinqua</i>	1890	?, A Hill & Son	Mixture of resin, powder and contaminants. It looks paler and much less resinous than some other samples of lump dragon's blood.	<i>Daemonorops draco</i> Circa 65% dracorhodin
35527	<i>Daemonorops propinqua</i>	?	?, Savory & Co	Mixture of resin and powder. Lump dragon's blood.	<i>Dracaena cinnabari</i> Circa 16% 7,4'- dihydroxyflavylum
35505	<i>Daemonorops sp.</i>	1851	Sumatra, Royal Commonwealth Exhibition	Mostly resin. Similar to lump dragon's blood.	<i>Daemonorops draco</i> Circa 55% dracorhodin

*The relative peak areas were calculated with the chromatographic program ChromQuest 4.1 at the maximum wavelength absorption for each flavylum marker selected: 438 nm for dracorhodin (*Daemonorops sp.*), 462 nm for 7,4'-dihydroxyflavylum (*Dracaena cinnabari* and *Dracaena schizantha*) and 476 nm for 7,4'-dihydroxy-5-methoxyflavylum (*Dracaena draco*).

In two further samples, 35487 and 35527, labelled *Daemonorops draco* and *Daemonorops propinqua* respectively, the presence of 7,4'-dihydroxyflavylium and absence of dracorhodin prompt the conclusion that these resins were from *Dracaena cinnabari*. Both these samples appeared more glossy or resinous than other lump resins classed with this genus. Also, at least one of these 2 samples was sourced in India (see table 1.3). Finally, sample 35499 (labelled as *Daemonorops draco*) revealed the presence of an unknown red chromophore in its composition (see table 1.3) and therefore no conclusion concerning its provenance could be drawn. It seems that the names of samples of lump dragon's blood resins currently housed under the name *Daemonorops* in the EBC, K may not be accurate, and analysis of further samples using these techniques would be profitable. Some of the naming errors may have arisen due to past curation of the samples where Latin names have been assumed from the vernacular. These errors are more likely to occur from samples sourced in India as both *Daemonorops draco* and *Dracaena cinnabari* were traded there [16].

1.3.3.2 *Dracaena cinnabari*, *Dracaena ombet* (synonym *D. schizantha*) and *Dracaena sp.*

All 15 EBC, K *Dracaena cinnabari* samples showed the presence of 7,4'-dihydroxyflavylium (5-20%), in agreement with the species attribution; these samples were acquired most directly from Socotra, where the species is endemic and some from market imports (see table 1.4 for more details).

Table 1.4 - *Dracaena cinnabari* samples from EBC, K analysed by HPLC-DAD.

ID	EBC, RBC classification	Date of donation	Provenance, donor	Observations	Species % flavylum marker*
36489	<i>Dracaena cinnabari</i>	?	?, labelled Socotra dragon's blood from Allen & Co.	Mixture of resin, bark and powder	<i>Dracaena cinnabari</i> Circa 7% 7,4'-dihydroxyflavylum
36542	<i>Dracaena cinnabari</i>	07-1881	?, donated by Prof IB Balfour	Mixture of resin, bark and powder. Labelled as "Socotra Dragon's blood".	<i>Dracaena cinnabari</i> Circa 8% 7,4'-dihydroxyflavylum
36543	<i>Dracaena cinnabari</i>	1875	?, donated by Dr Vaughan	Resin. Labelled as "Socotra Dragon's blood".	<i>Dracaena cinnabari</i> Circa 5% 7,4'-dihydroxyflavylum
36545	<i>Dracaena cinnabari</i>	10-1899	?, purchased by Mather at Ripley Roberts Drug sale, 3 Mincing lane	Resin. Labelled as "Extra fine Zanzibar leas".	<i>Dracaena cinnabari</i> Circa 5% 7,4'-dihydroxyflavylum
36557	<i>Dracaena cinnabari</i>	10-1899	Zanzibar, purchased by Mather	Heterogeneous resin. Labelled as "Socotra Dragon's blood".	<i>Dracaena cinnabari</i> Circa 15% 7,4'-dihydroxyflavylum
36563	<i>Dracaena cinnabari</i>	?	?	Powder. Labelled as "Socotra Dragon's blood".	<i>Dracaena cinnabari</i> Circa 15% 7,4'-dihydroxyflavylum
36580	<i>Dracaena cinnabari</i>	10-1899	?, Kurachi, purchased by Mather	Resin. Labelled as "Fine marbles of dragon's blood"	<i>Dracaena cinnabari</i> Circa 5% 7,4'-dihydroxyflavylum
36599	<i>Dracaena cinnabari</i>	1881	Socotra, ?	Mixture of pigment and resin. Labelled as "dam el akhuwen"	<i>Dracaena cinnabari</i> Circa 17% 7,4'-dihydroxyflavylum
36611	<i>Dracaena cinnabari</i>	01-1880	?, presented by Dr JB Balfour	Tears of resin. Labelled as "Socotra Dragon's blood".	<i>Dracaena cinnabari</i> Circa 15% 7,4'-dihydroxyflavylum
36622	<i>Dracaena cinnabari</i>	?	?	Tears of resin. Labelled as "Socotra Dragon's blood".	<i>Dracaena cinnabari</i> Circa 5% 7,4'-dihydroxyflavylum
36773	<i>Dracaena cinnabari</i>	1880	Socotra, donated by Prof IB Balfour	Tears of resin. Labelled as "Edah Amsellah"	<i>Dracaena cinnabari</i> Circa 22% 7,4'-dihydroxyflavylum
36808	<i>Dracaena cinnabari</i>	?	Socotra, donated by Prof IB Balfour	Resin wrapped in bark.	<i>Dracaena cinnabari</i> Circa 20% 7,4'-dihydroxyflavylum
36809	<i>Dracaena cinnabari</i>	1880	Socotra. donated by Prof IB Balfour	Mixture of resin, pigment and bark. Labelled as "Edah-Muck-Dehar" "prepared from the boiled dust"	<i>Dracaena cinnabari</i> Circa 19% 7,4'-dihydroxyflavylum
36823	<i>Dracaena cinnabari</i>	07-1881	Socotra. donated by Prof IB Balfour	Powder. Labelled as "Edah Dukkah" "consisting of small fragments broken tears of Dragons blood"	<i>Dracaena cinnabari</i> Circa 20% 7,4'-dihydroxyflavylum

79745	<i>Dracaena cinnabari</i>	?	Socotra, ?	Tears of resin.	<i>Dracaena cinnabari</i> Circa 5% 7,4'-dihydroxyflavylium
36816	<i>Dracaena schizantha</i>	23-04-1871	Zanzibar; ?	Resin.	<i>Dracaena cinnabari?</i> Circa 15% 7,4'-dihydroxyflavylium
-	<i>Dracaena schizantha</i>	2007	Kew gardens, Palm House	Resin wrapped in bark	<i>Dracaena schizantha</i> (<i>D. ombet</i>) Circa 2% 7,4'-dihydroxyflavylium
36819	<i>Dracaena sp</i>	?	Socotra, ?	Mixture of resin, pigment and bark.	<i>Dracaena cinnabari</i> Circa 5% 7,4'-dihydroxyflavylium
36820	<i>Dracaena sp</i>	?	?	Mixture of resin, pigment and bark.	<i>Dracaena cinnabari</i> Circa 12% 7,4'-dihydroxyflavylium
36821	<i>Dracaena sp</i>	1906	Zanzibar, London Drug market	Mixture of resin, pigment and bark.	<i>Dracaena cinnabari</i> Circa 13% 7,4'-dihydroxyflavylium
36822	<i>Dracaena sp</i>	?	?, donated by East India Company	Mixture of resin, pigment and bark.	<i>Dracaena cinnabari</i> Circa 5% 7,4'-dihydroxyflavylium
75793	<i>Dracaena sp</i>	?	Socotra,	Mixture of resin, pigment and bark.	<i>Dracaena cinnabari</i> Circa 15% 7,4'-dihydroxyflavylium

*The relative peak areas were calculated as described for table 1.3

The 36816 EBC, K sample, tentatively labelled as *Dracaena schizantha* from Zanzibar and donated in 1871, also revealed the presence of 7,4'-dihydroxyflavylium, in 15% of the total of the red chromophores, and a similar chromatographic elution profile to *Dracaena cinnabari* resins (see figure 1.17A and 1.17B). Moreover, when the 36816 sample was compared with resin from a living *Dracaena ombet* (synonym *Dracaena schizantha*) tree, from Ethiopia [80], HPE, K collected in 2007, there was no match between the two (see figure 1.17B and 1.17C). In the living *Dracaena ombet* tree, the relative percentage area of 7,4'-dihydroxyflavylium (circa 2%) was less than the second flavylum eluted (circa 6%), contrary to the 36816 EBC, K sample and all the *Dracaena cinnabari* samples analyzed. Furthermore, the compounds eluted between 22 and 28 minutes in the sample from the living *Dracaena ombet* had different concentrations compared to sample EBC, K 36816 (see figure 1.17B and 1.17C). This is reflected in the PCA analysis that clearly shows that the sample collected from the living *Dracaena ombet* is different from the *Dracaena cinnabari* samples, whilst sample 36816 EBC, K *Dracaena schizantha* is similar to the EBC, K *Dracaena cinnabari* samples (see appendix II – Dragon's blood data, section II.2,

p. 105 for PCA graphics). It seems that the original label for specimen 36816 only referred to dragon's blood and not to the botanical name *Dracaena schizantha* which was tentatively, but wrongly attributed some time in the history of its curation. As the analysis shows, this specimen should have been labelled *Dracaena cinnabari* which also makes sense historically as, at this time, there was an established trade route between Socotra and Zanzibar [16]. Then, *D. cinnabari* was the most popularly traded dragon's blood. There is another sample of *D. cinnabari* from Zanzibar (EBC, K 36557) to support its presence in trade there. As no species of *Dracaena* grow naturally in Zanzibar, the only other likely source is *D. ombet* from N.E. African mainland but evidence suggests this species was very little traded [81].

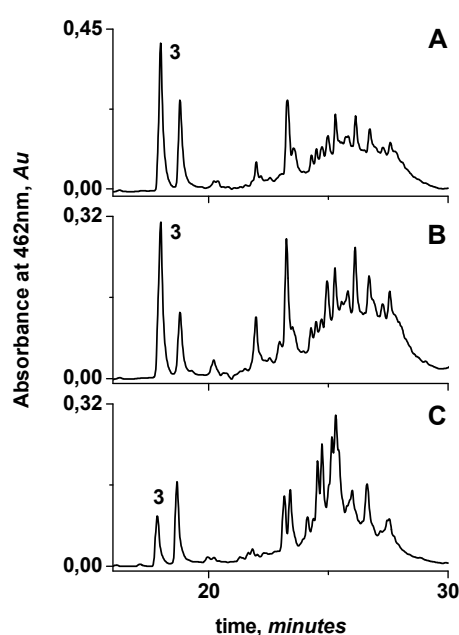


Figure 1.17 – HPLC profile of *Dracaena cinnabari* and *Dracaena schizantha* samples from EBC, K collection. A) HPLC chromatogram profile of 36809 EBC, K *Dracaena cinnabari* sample (1880); B) HPLC chromatogram profile of sample of 36816 EBC, K labelled *Dracaena schizantha* (1871); C) HPLC chromatogram profile of a resin sample collected in 2007 from a living 28 year old *Dracaena ombet* (synonym *D. schizantha*) tree from RBG, Kew. The two first chromatograms are also similar to *Dracaena cinnabari* resins collected in 2007, see table 1.2, p. 15.

In all the unknown *Dracaena* sp. samples (36819, 36820, 36821, 36822, 75793) the 7,4'-dihydroxyflavylium was detected and a similar chromatographic elution profile to *Dracaena cinnabari* resins, confirmed by PCA, was found; this points to *Dracaena cinnabari* as the source (see appendix II – Dragon's blood data, section II.2, p. 105, for PCA graphics). In the case of 36822, a sample labelled *Dracaena* sp. from the East India Company, previously suggested to belong to *Daemonorops* sp. or a degraded *Croton* sp. [32], 7,4'-

dihydroxyflavylum was detected in its composition. Moreover, its HPLC profile was also analogous to those of *Dracaena cinnabari*, strongly suggesting this species to be the source of the resin. Pearson [16] discussed that frequently in the past resins traded out of Bombay were assumed to be sourced from *Daemonorops draco*, but the East India Company also had connections with Socotra and East Africa and so both species are represented in dragon's blood sourced from India.

1.3.3.3 *Dracaena draco*

Based on the dracoflavylum marker, of the 7 samples labelled as *Dracaena draco* from the EBC, K, only four were in fact from *Dracaena draco* trees, namely, those that came from botanical gardens (26387, 26421, 36824 and 78811, table 1.5).

Table 1.5 – Specimens of *Dracaena draco* samples from EBC, K analysed by HPLC-DAD and percentage of the flavylum markers identified.

ID	EBC, RBC classification	Date of donation	Provenance, donor	Observations	Species* % flavylum marker
26397	<i>Dracaena draco</i>	1867	Kew gardens, Palm House	Red resin fragments.	<i>Dracaena draco</i> Circa 2% dracoflavylum
26421	<i>Dracaena draco</i> .	1871	Tenerife, Canary Is, ?	Red wood. Labelled as "Celebrated Dragon tree of Tenerife".	<i>Dracaena draco</i> Circa 33% dracoflavylum
36516	<i>Dracaena draco</i>	?	"Socotra?", ?	Mostly red resin. Labelled as "Resin wrapped in leaves".	<i>Daemonorops sp.</i> Circa 42% dracohodin
36653	<i>Dracaena draco</i>	?	Madeira, ?	Red resin.	<i>Dracaena draco</i> + <i>Dracaena ombet/cinnabari</i> Circa 9% dracoflavylum and 2% of 7,4'- dihydroxyflavylum
36824	<i>Dracaena draco</i>	?	Lisbon, Botanic Garden	Mostly red resin. Labelled as "Resin wrapped in leaves"	<i>Dracaena draco</i> Circa 5% dracoflavylum
36825	<i>Dracaena draco</i>	?	Tenerife, Canary Is, ?	Brown resin. Labelled as "Gum-resin exuded from the great Dragon tree of Tenerife".	<i>Pterocarpus</i> or <i>Croton sp</i> (?) Circa 37 % ellagic acid
78811	<i>Dracaena draco</i>	06-09-2004	?, Adelaide, Botanic Garden	Red resin.	<i>Dracaena draco</i> Circa 3% dracoflavylum

*The relative peak areas were calculated as described for table 1.3.

In the samples from the Botanical Garden of Lisbon (36824) and Adelaide, Botanic Garden (78811), dracoflavylum accounted for 3% and 5%, respectively, of the total amount of the

red colourants. The wood sample 26421, from the famous “Great Dragon Tree” of Tenerife, had dracoflavylium in high concentration (33%, see figure 1.18A) as was also observed in three of the samples from old trees (circa 200 years old) from Madeira Island in the data library (section 1.3.2, figure 1.15, p.16). On the other hand, the sample 36825 labelled as being from the same dragon tree, presented a brown colour instead of the usual red colour and was composed of possible hydrolyzable tannins (see figure 1.18B), where ellagic acid was identified. The occurrence of “tannins” in this specimen of dragon’s blood resin has been already reported in 1895 by H. Trimble, who concluded that the specimen was very similar to *Pterocarpus draco* L. or *Croton draco* Schltl. [82]. Indeed, in all resins from our *Dracaena draco* HPLC-DAD chromatogram library, “tannins” were not found. Probably, this sample was not obtained from a *Dracaena draco* resin. Edwards *et. al* [31] also noticed this sample was very different from other *Dracaena draco* samples, but they could not disclose the family and chemical composition of the sample.

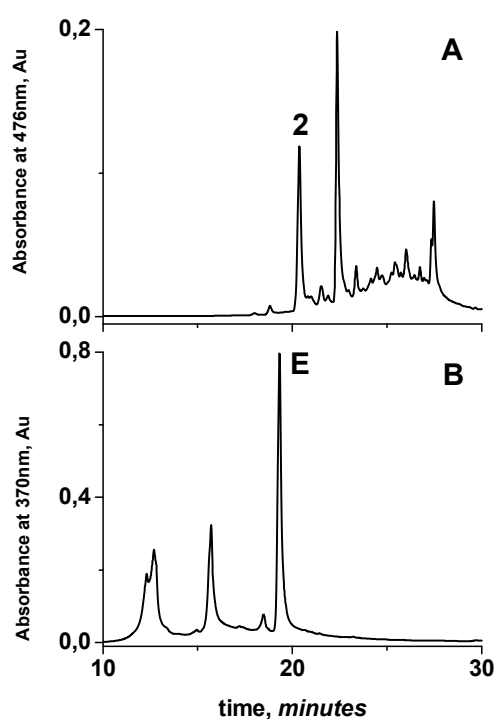


Figure 1.18 – HPLC profiles of two resin samples labelled as *Dracaena draco* from the “Great Dragon Tree” of Tenerife - EBC, K collection. A) 26421 *Dracaena draco* resin sample with dracoflavylium (2) identified, B) 36825 sample labelled as *Dracaena draco* resin, with ellagic acid (E) identified. The chromatogram B suggests this sample is not from *Dracaena draco* resin; see text for further details.

Sample 36516 is not from *Dracaena draco* resin but *Daemonorops sp.* resin, since the major compound observed was dracorhodin (42%), and no dracoflavylium was detected.

Edwards *et al.* [31] also suggested this sample could be from *Daemonorops sp.* However, due to the weak features of the Raman spectra obtained, they were not able to confirm this. The appearance of this sample, as sticks of resin wrapped in leaves, also suggests this conclusion and, interestingly, although the original label is no longer with the sample in the EBC, K, the database records "?Socotra" as the origin, suggesting illegibility in the label; Sumatra (the major origin of *Daemonorops*) is not unlike Socotra if written illegibly. Finally, sample 36653 from Madeira is possibly a mixture of different resins. Both 7,4'-dihydroxy-5-methoxyflavylium (dracoflavylium) (9% of the relative area of the total red compounds) and 7,4'-dihydroxyflavylium (2% of relative area of the total red compounds) were detected, pointing to a mixture of *Dracaena draco* and *Dracaena ombet* or *Dracaena cinnabari* resins. Edwards *et al.* detected some differences between this and a *Dracaena draco* sample from the Botanical Garden of Lisbon; however, a full identification of the resin composition could not be obtained [31].

With these results, it was possible to conclude that the flavylium chromophores that contribute to the red colour of dragon's blood resins can be used as species markers, enabling an easy and rapid discrimination between *Daemonorops* and *Dracaena*. Additionally, *Dracaena draco* and *Dracaena cinnabari* can be discriminated but *Dracaena cinnabari* and *Dracaena ombet* share the same marker, although in different concentrations. The use of the full chromatogram signal for PCA processing did not provide any further discrimination, but the results were in full agreement with the conclusions obtained using a single molecule marker. Therefore, the use of flavylium compounds as species markers was clearly validated.

It was also possible to confirm in the EBC, K collection the inventoried sources of 25 samples of resins, identify species origins for 5 samples where previously only genus was known (36819, 36820, 36821, 36822 and 75793) or where species was only tentatively assigned (36816), and clarify or discuss incorrect attributions: 4 samples with incorrect genus (35487, 35527, 36516, 36825), 1 sample correct to genus but incorrect to species (35499) and 1 mixed collection (36653). These results suggest that other samples in the EBC, K may benefit from re-examination using these techniques, especially items labelled lump dragon's blood arising out of India.

1.3.4 Flavylium markers characterization

After these positive results, a detailed characterization of the three flavylium compounds identified in dragon's blood resins is presented in order to understand the resins red colour. The 7,4'-dihydroxyflavylium data is already published in the literature [83], and only relevant aspects necessary to understand the final red colour of dragon's blood resin are presented.

1.3.4.1 Flavylium chemical reactions network – the dragon's blood red colour

Dragon's blood flavylium compounds, as reported in the literature, are involved in a complex network of chemical reactions (figure 1.14, section 1.2) in which the different forms can be reversibly interconverted by changing the pH. In acidic water, five species for each dragon's blood flavylium could be identified: **1)** the flavylium cation (AH^+) with a yellow colour for the three compounds studied, where dracoflavylium and 7,4'-dihydroxyflavylium present a maximum of absorbance more shifted to the reds (λ_{max} circa 460 nm) due to the presence of a higher number of hydroxyl groups than in dracorhodin ($\lambda_{\text{max}}=432$ nm); **2)** the quinoid neutral base reached by deprotonation of AH^+ , in which dracoflavylium and 7,4'-dihydroxyflavylium present an orange-red base **A** with a maximum at circa 495 nm and dracorhodin an orange base **A** with a maximum at 479 nm; **3)** the hemiketal (**B**) obtained by hydration of AH^+ ; **4)** the *cis*-chalcone (**Cc**) resulting from tautomerization of **B**; and **5)** the pale yellow *trans*-chalcone (**Ct**), with a maximum at circa 370 nm, formed from the isomerization of **Cc**. **B** and **Cc** are short-lived transient species whose absorption spectra have not been determined experimentally for these three flavylium compounds. In basic water, for dracoflavylium and 7,4'-dihydroxyflavylium it is possible to obtain the pink ionized quinoidal base (A^-); in the three dragon's blood flavylium compounds, the ionized *trans*-chalcones (Ct^- and Ct^{2-}), formed through the deprotonation of the hydroxyl groups, were also found in equilibrium or as transient species (see appendix II – Dragon's blood data, section II.3, p. 107 for flavylium network of chemical reactions).

In dragon's blood resin, moderately acidic pH values were found (5-6) and therefore only the acidic media and slightly basic media will be considered. More details about higher basic pH can be found in specific literature [69].

1.3.4.1.1 *Dracoflavylum*

The spectral variations of the compound 7,4'-dihydroxy-5-methoxyflavylium occurring after ca. 1 minute upon a pH jump from the stock solutions at pH=1 are shown in figure 1.19.

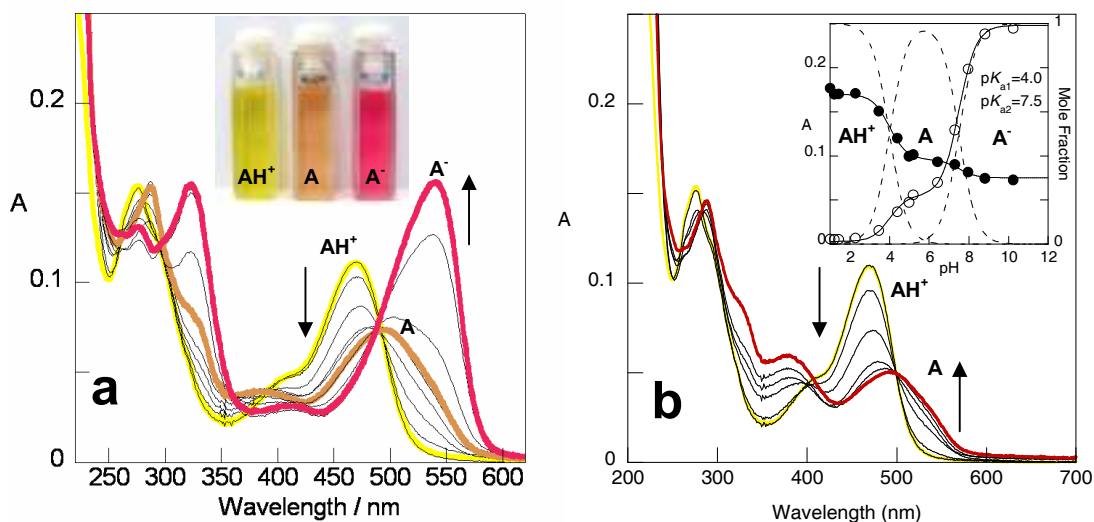


Figure 1.19. - Spectral variations occurring immediately (ca. 1 minute) upon a pH jump from equilibrated solutions of the dracoflavylum (4×10^{-6} M) at pH=1.0 to higher pH values pH=2.1; pH=3.8; pH=5.0; pH=5.7; pH=7; pH=7.5 and pH= 9.9). a) Immediately after the pH jump; b) after thermal equilibration. The calculated pK_a s immediately upon a pH jump (figure a) are 4.0 and 7.5 and are presented in the inset of figure b.

At very acidic pH values, the absorption band of the yellow flavylium cation is the dominant species ($\lambda_{\max}=476$ nm); by increasing the pH, a new band centred at 493 nm is obtained, due to the red quinoidal base **A** formation, $pK_{a1}=4.0$; further increase of the pH leads to an absorption band characteristic of the ionized base **A**⁻, $pK_{a2}=7.5$. The spectra reported in figure 1.19A are different from those of the equilibrium, presented in figure 1.19B. In the equilibrium, at acidic pH values, the flavylium cation is once more the dominant species, but at higher pH values, the equilibrium is established between the base **A** (63%) and the *trans*-chalcone **Ct** (37%), see figure 1.20.

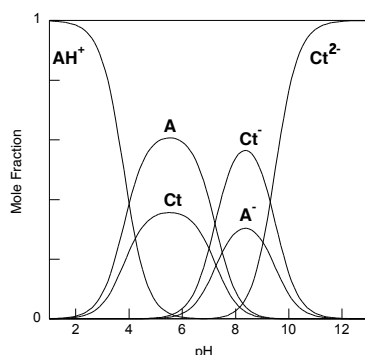


Figure 1.20 - Mole fractions distribution with pH for dracoflavylium at the equilibrium (for more details, (see appendix II – Dragon’s blood data, section II.3, p.107).

1.3.4.1.2 Dracorhodin and 7,4'-dihydroxyflavylium

The spectral variations of both dracorhodin and 7,4'-dihydroxyflavylium are similar to those reported above for dracoflavylium. The intensity of the AH^+ band ($\lambda_{\text{max}}=432$ nm for dracorhodin and $\lambda_{\text{max}}=456$ nm for 7,4'-dihydroxyflavylium) decreases with increasing pH and two bands with maxima near 370 nm and near 490 nm appear (A: $\lambda_{\text{max}}=479$ nm for dracorhodin and $\lambda_{\text{max}}=493$ nm for 7,4'-dihydroxyflavylium, assigned to *trans*-chalcone and quinoidal base respectively (see figure 1.21).

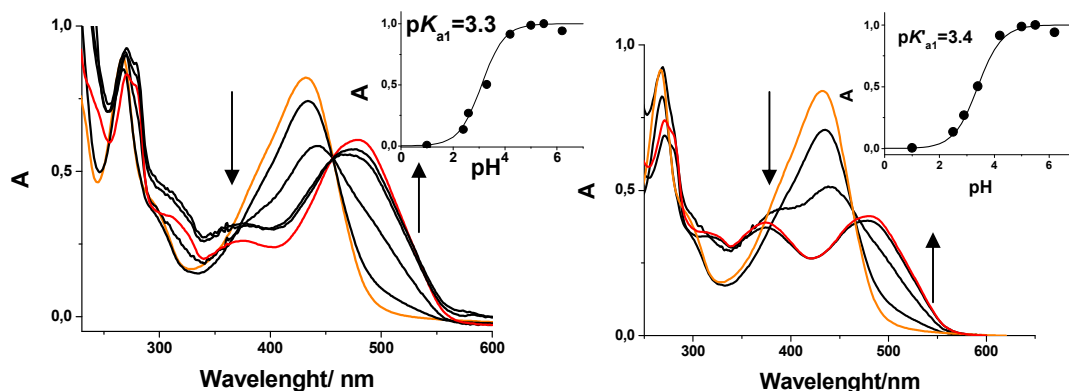


Figure 1.21 - UV/Vis absorption spectra of dracorhodin (5×10^{-6} M) at pH=1.0 to higher pH values: pH=2.5; pH=3.4; pH=5; pH=5.5; pH=6.2. a) immediately after the pH jump; b) after thermal equilibration. Insets: calculated $\text{p}K_{\text{a}1}$.

In dracorhodin, at moderately acidic pH values such as those measured for the resin, the concentration of the red base is also very high with circa 63%, (see appendix II – Dragon’s blood data, section II.3, p.109), which is similar to what was found for dracoflavylium. However, for the 7,4'-dihydroxyflavylium at pH around 5-6, the quinoidal base has a

concentration of only 10%, being the major compound the pale yellow *trans*-chalcone with 90%. Therefore, for 7,4'-dihydroxyflavylium the *cis-trans* isomerization ($k_i = 1 \times 10^3 \text{ s}^{-1}$) is faster than the deprotonation ($k_{a1} = 1 \times 10^{-4} \text{ s}^{-1}$), the tautomerization and the hydration ($k_h = 1.4 \times 10^{-6} \text{ s}^{-1}$) processes, leading to a high amount of **Ct** in moderately acidic media [83]. Both dracoflavylium and dracorhodin are the first natural flavylium compounds for which the base is the major species at biological pH (more than 60%). For the most common anthocyanins and 3-deoxyanthocyanidins in moderately acid to neutral pH, colourless **B** is the major species, together with **Ct**. The final colours, especially the blue colour present in flowers, are obtained through complex supramolecular structures [84,85]. The high content of red quinoid base in the equilibrium at moderately acidic pH for these two flavylium compounds can be related to the substituent groups and their position in the flavylium ring. It is interesting to note that both flavylium compounds with a higher content of red quinoid base have a methoxy group in the 5 position of the flavylium ring and a hydroxyl group in the 4' position. In order to evaluate the influence of the substituent groups in the formation of the red quinoid base **A**, other flavylium compounds should also be characterized, for instance a flavylium with the same substituent groups in different positions (e. g. 7,5-dihydroxy-4'-methoxyflavylium) as well as apigenidin (7,5,4'-trihydroxyflavylium). Apigenidin is a 3-deoxyanthocyanidin, the chemical ancestor of anthocyanins, with a molecular structure which can be considered between anthocyanins and synthetic flavylium salts.

1.4. Conclusions

With the characterization of dragon's blood resins it was possible to conclude that the red colour of the resins is due to the presence of several natural flavylium compounds which are characteristic of the family resin source. It was demonstrated for the first time that these natural flavylium compounds can be used as species markers, enabling an easy and rapid discrimination between *Daemonorops* and *Dracaena* dragon's blood resins.

The high percentage of the red quinoid base found in the equilibrium for the natural flavylium with an OMe group in position 5 of the 2-phenyl-1-benzopyrylium core reveals that Nature found a new strategy with this structure to stabilize the red colour in plants, besides the usual anthocyanins and deoxyanthocyanidins. In the deoxyanthocyanidins, the 2-phenyl-1-benzopyrylium structure has a hydroxyl group in position 5 and as a result stable yellow and red molecules are obtained. However, in this case, the percentage of the red basic form in the equilibrium [86] is not as high as in the natural flavylium with an OMe group also in position 5. These results suggest that the substitution of the OH group in

position 5 by the OMe is related with a natural evolution of the 2-phenyl-1-benzopyrylium compound to obtain more intense red colours. In order to confirm these results the characterization of apigenidin will be fundamental.

Nevertheless, with these approaches, natural flavylium compounds and deoxyanthocyanidins, only the yellow and red colours are obtained. In order to obtain the blue colours, the hydroxylation in position 3 is a fundamental step (anthocyanidins). However, this substituent in this position gives also instability to the molecule. The problem was solved by incorporating glycosides in that position, leading to more stable species as anthocyanins. Yet, at moderately acidic pH values, the blue colour is reminiscent at the equilibrium. The final known solution found by Nature was the construction of supramolecular structures [84,85].

Chapter 2-Indigo Dye

2.1 *Indigo dye overview*

Indigo blue is one of the oldest organic dyes used on textiles and has been known since Egyptian and Roman civilizations [2,3]. It is considered a very stable organic dye which can explain its wide application not only in textiles but also in paints and inks, and longevity [2,3,86-88]. Indeed, synthetic indigo is still used today in the production of blue jeans and even the production of indigo with microorganisms according to green chemistry principles has been recently investigated [89].

It was in 1897 that the Badische Anilin und Soda Fabrik (BASF) introduced the synthetic indigo to the market [90]. Before that, indigo was obtained from hundreds of different plants belonging to the *Leguminosae*, *Papilionoidae*, *Cruciferae* and *Polygonaceae* families, among others [2,3,88]. In Europe the main source of indigo was *Isatis Tinctoria* L. while in Asia it was obtained mostly from *Indigofera tinctoria* L. [2,3,88]. In the XVII century, the *Indigofera tinctoria* L. replaced the *Isatis tinctoria* L. in Europe once it produced a higher content of indigo dye [90]. However, in the present state-of-the-art it is not possible to distinguish the vegetable dyeing source in indigo dyed textiles, since only indigotin and indirubin (a structural isomer of indigotin) is retained in the fibre and no other markers have been identified until now [2,3,91-93]. Moreover, it is still to be learned how the dyeing process changes the relative amounts of indigotin and indirubin in the final dyed textile, because both chromophores come from the same initial precursors [94].

2.2 *Chemical composition – revealing the blue colour*

The indigo dye is composed mainly by indigotin, a $C_{16}H_{10}N_2O_2$ compound synthesised for the first time by Adolf von Baeyer and Emmerling in 1870 using isatin as starting material [90]. Its correct structural formula was discovered circa ten years later by Bayer, in 1883 [90].

The precursors of indigotin in the plant leaves are the glycosides of indoxil, namely indican and isatan B. During the fermentation process, the indoxyl glycosides are converted by enzymatic hydrolysis to indoxyl which is then converted to leuco-indigo and finally oxidised by exposure to air to indigotin. Simultaneously, the indoxyl can also be converted to indirubin [87,94,95] (for more details see figure 2.1).

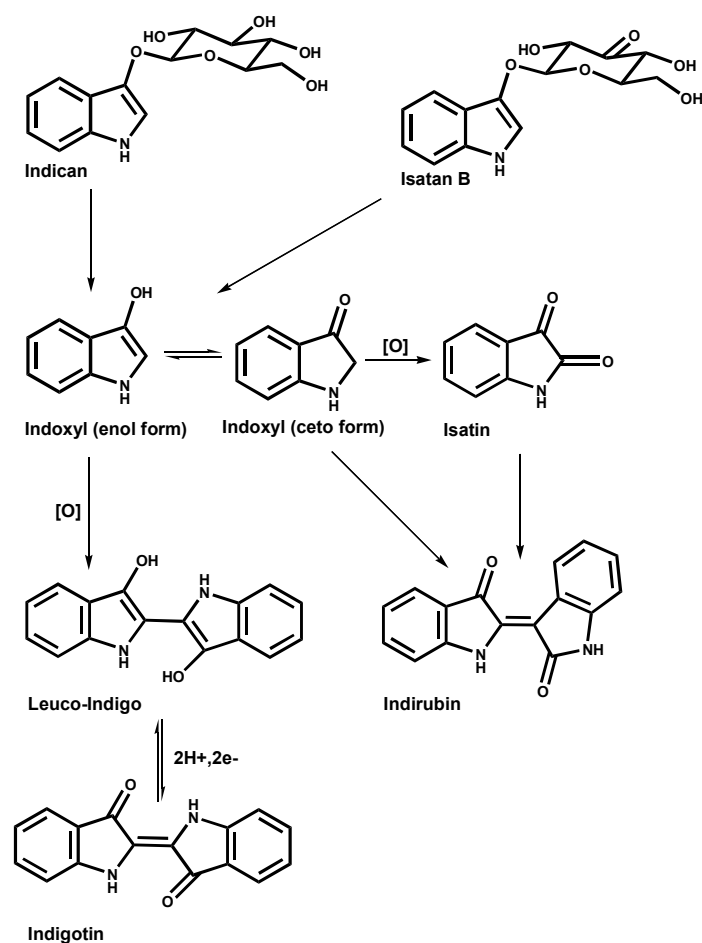


Figure 2.1 – Production of indigotin and indirubin from plant leaves [94].

The indigo dye belongs to the dye family known as vat dyes which are composed by derivatives of indigotin as the famous and expensive Tyrian Purple obtained from Mediterranean shellfish [2,3]. These vat dyes, either from plants or animals, when initially extracted, are present as colourless precursors. Only through exposure to air they reveal their final colour, due to the oxidation of the *leuco* form to the *keto* species. In this state, the vat dyes are insoluble in water and precipitate in the textile fibres [2,3].

2.3 Indigo photodegradation

Photodegradation studies of indigo date back to the 1980s, when it was found that irradiations at $\lambda > 390$ nm of indigo dissolved in different organic solvents such as chloroform, methanol or acetone, produced isatin [96,97] (see figure 2.1). A self-sensitized photooxidation for the photodegradation mechanism of indigo was proposed based only in two observations: i) indigo in a solution of 2,5-dimethyl furan and methanol leads to the formation of 2-hydroperoxy-5-methoxy-2,5-dimethyldihydro furan; ii) in the presence of

nickel dimethyldithiocarbamate (a singlet oxygen quencher) the photodegradation of indigo in chloroform is decreased. A more recent work [98] showed that a polychromatic irradiation of indigo dissolved in dichloromethane promoted the formation of isatin, isatoic anhydride and anthranilic acid.

In both works, no photodegradation quantum yields were obtained. The only published photodegradation quantum yields refers to a 254 nm irradiation of indigo carmine [99], the water soluble derivative of indigo (figure 2.2).

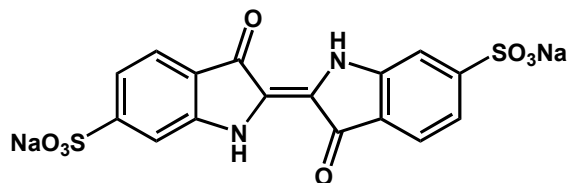


Figure 2.2 - Indigo carmine.

This dye is being studied as a probe for ozone production in antimicrobial and inflammatory actions of neutrophil cells [100,101] and as a contaminant in wastewaters that should be removed [99,102]. The advanced oxidation processes (AOPs) used for its destruction in contaminated water were carried out with ultraviolet irradiation in the presence of hydrogen peroxide or the heterogeneous catalyst TiO₂ [99]. It was observed that the mechanism and main products resulting from UV ($I_{irr} = 254 \text{ nm}$) and UV/H₂O₂ photodegradation were different from those obtained with UV/TiO₂. In the first case, the process evolved in two steps, where in the first step isatin sulfonate was the main product and in the second step isatin was converted into aliphatic acids. For the heterogeneous UV/TiO₂ systems it was concluded that indigo carmine molecules were oxidized to biodegradable breakdown products such as formic, acetic and oxalic acids [99].

Recently, other studies presented quantum yields for the possible generation of ¹O₂ by indigo and indigo carmine [103], suggesting that intersystem crossing competes with internal conversion, contrarily to previous photophysical studies of the *keto* and *leuco* forms of indigo and its derivatives [104-106]. From the photophysical characterization of indigo, it was possible to conclude that in the case of the *keto* form the major deactivation pathway involved a very efficient internal conversion from the lowest singlet excited state to the ground-state, whereas in the case of the *leuco* form competition occurred between the internal conversion, triplet formation and fluorescence deactivation processes. These differences between the two forms reveal that the *leuco* form is less photostable than the *keto* indigo species.

Therefore, in order to understand the reactivity of the molecule, electrochemical characterization of the transformation of the indigo *keto* form in its *leuco* form (figure 2.3), namely the mechanisms involved in the disruption of the central double bond, should be considered.

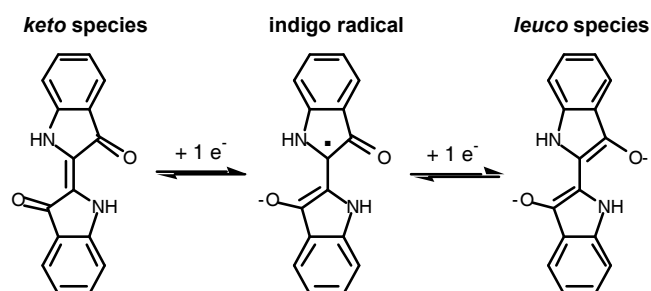


Figure 2.3 – Indigo reduction mechanism in non acidic media, adapted from [107].

A stopped flow study on indigo carmine reduction by dithionite ($S_2O_4^{2-}$) concluded that the mechanism was a two-step reduction (figure 2.3) and that the reduction potential was pH dependent. Further studies on the electrochemical reduction of indigo dissolved in organic solvents (DMSO, DMF) [107] confirmed the general reduction mechanism. More recently, an indigo radical anion was identified by EPR in the electrochemical reduction [108].

2.4 Results

In this work, significant effects of solvent purity on quantum yields of reaction for indigo and its water soluble derivative indigo carmine were observed. Quantum yields of reaction were obtained at 335 nm and 610 nm irradiation wavelengths in homogenous organic and aqueous solutions, as well as in transparent gels (proteinaceous and cellulosic). This design aimed to reproduce the dye environment in textiles, such as silk, wool and cotton, and monochromatic irradiation wavelengths were used in order to determine effectively the quantum yields of reaction. The reactions kinetics were monitored by UV-visible absorption and the resulting photoproducts were characterized by HPLC-DAD. The influence of oxygen on the reaction mechanisms is presented. Indigo in the solid state was irradiated with a Xenon polychromatic source, with a spectral distribution close to the solar spectrum. The main products and mechanisms are compared to those obtained with monochromatic irradiation. Finally, the blues of millenary Andean textiles are characterized and the degradation products found herein are compared to the experimental simulation.

2.4.1 Monochromatic irradiation in homogeneous media

2.4.1.1 Indigo in DMF

Indigo was irradiated at 335 and 610 nm in *N,N*-dimethylformamide (DMF). Its UV-vis spectrum is presented in figure 2.4, together with isatin. The wavelength maxima and molar absorption coefficients (table 2.1) show that, with both irradiation wavelengths, indigo is the main absorbing species. Irradiations at lower wavelengths as 254 nm [99] were purposely avoided, since this type of irradiation is rarely, if ever, encountered under glass indoors and can give rise to different reactions than those induced by the near ultraviolet and visible [109].

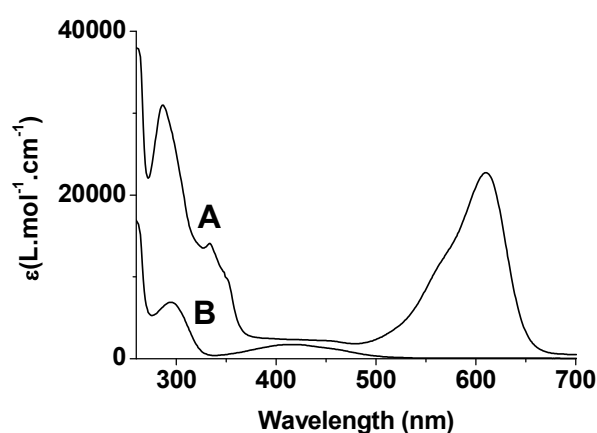


Figure 2.4 – UV-vis spectra of indigo (A) and isatin (B) in DMF.

Table 2.1 - Absorption maxima and extinction coefficients of indigo, isatin and indigo carmine in DMF at T=293 K. □ are also presented for 335 nm.

	$\lambda_{\max} /$ nm	$\epsilon_{\max} / \text{L mol}^{-1}$ cm^{-1}	$\epsilon_{335} / \text{L mol}^{-1}$ cm^{-1}
Indigo	610	22 900	11500
Isatin	418	1500*	440*
Indigo carmine	618	17 800	10000
Indigo carmine / H ₂ O	610	19 400	10100

* estimated error 25%; for all other values estimated error $\leq 10\%$.

The DMF solvent was chosen as indigo does not dissolve in water and DMF is one of the few solvents where the complete dissolution of indigo is achieved, enabling the preparation of concentrated solutions that will absorb all the incident photons of the light source. Moreover, the DMF is currently used in the extraction of indigotin from indigo dyed textiles.

It is important to stress here that only freshly distilled or freshly opened DMF was used to obtain the reaction quantum yields. In indigo solutions prepared with aged DMF it was observed that isatin was produced in the dark. For instance, the blank solution kept in the dark was reacting almost at the same rate as the indigo solution irradiated at 610 nm.

The quantum yields of reaction, Φ_R , were obtained in the presence of O₂ with atmospheric conditions, in degassed solutions (high vacuum line) and in N₂ atmosphere (table 2.2). Degassed solutions enabled to obtain lower levels of O₂ and therefore were considered as the values for Φ_R in the absence of molecular oxygen.

Table 2.2: Quantum yields of reaction, Φ_R , for indigo in DMF at T=293 K, in the presence and absence of molecular oxygen, for more details (see appendix III – Indigo data, section III.1, p. 110, for I_0 and Φ_R).

	Presence O ₂		Absence O ₂	
λ_{irr} (nm)	335	610	335	610
Φ_R	8×10^{-3}	4×10^{-4}	3×10^{-4}	*

* Lower than 10^{-6} , it was not possible to determine with the utilized irradiation set-up.

In the presence of O₂, Φ_R is 20 times lower for irradiation at 610 nm when compared to 335 nm. Also, comparing the values for irradiation at 335 nm with and without oxygen, the difference is similar. It was not possible to compare the Φ_R for irradiation at 610 nm because, in the absence of oxygen the Φ_R was too low ($<10^{-6}$) to be calculated with the available irradiation set-up. Irradiation was also followed by HPLC-DAD and, for both irradiation wavelengths isatin was detected as the major photodegradation product, circa 80% of the relative peak area of total compounds in solution (figure 2.5, see appendix III – Indigo data, section III.2, p.111, for HPLC-DAD calibration curves). Two other minor components with less than 10% of the relative peak area of total compounds in solution (see appendix III-Indigo data) were also formed, see appendix III – Indigo data, section III.3.1, p.112, for indigo HPLC-DAD chromatograms). These compounds, on the basis of their mass spectra and by comparison with HPLC standards, could not be isatoic anhydride (C₈H₅NO₃), anthranilic acid (C₆H₄(NH₂)CO₂H) or tryptanthrin (C₁₅H₈N₂O₂) [98].

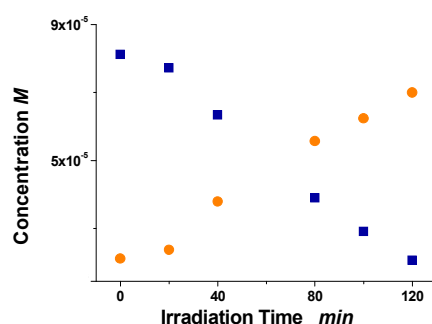


Figure 2.5 – Monitorization by HPLC-DAD of indigo irradiation at 335 nm in homogeneous media: squares – indigotin, circles - isatin.

The results obtained prompt to some caution in what concerns the rationalization of the role played by oxygen. It is possible that irradiation at 335 nm is promoting the homolytic scission of hydroperoxides existing in the DMF, even if existing at very low yields. The radicals formed, OH, could in turn easily attack the double bond, reducing indigo. This reduced intermediate would collapse forming isatin. Nevertheless, a different mechanism of degradation for 335 nm and 610 nm irradiation cannot be excluded.

2.4.1.2 Indigo carmine in DMF and water

The $\Phi_R = 2 \times 10^{-3}$ value for indigo carmine in DMF, in the presence of O₂, with irradiation at 335 nm, is similar to that obtained for indigo. The same cannot be said when irradiation is carried in water, for which a $\Phi_R = 9 \times 10^{-6}$ was obtained. However, the photoproducts formed (isatin sulfonic acid and a higher content of compound 3 and 4) were the same with both solvents with a similar pattern distribution (figure 2.6 and table 2.3). These data confirm that the DMF solvent, when present, is catalyzing indigo degradation, even when solutions with freshly distilled DMF are used.

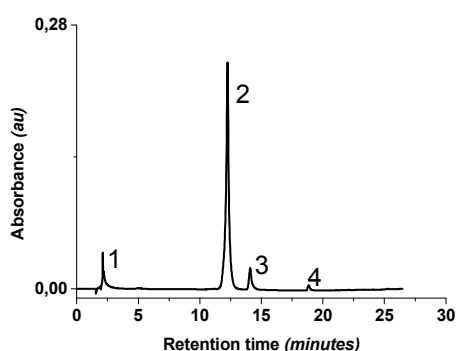


Figure 2.6 - HPLC-DAD chromatogram of indigo carmine $\approx 1 \times 10^{-5}$ M at 275 nm, after the irradiation ($t_{irr}=9$ h). Compounds detected: 1- Isatin sulfonic acid; 2 - indigo carmine; 3 and 4- compounds not identified.

Table 2.3 – Compounds identified by HPLC-DAD with the photodegradation of indigo carmine in water and DMF with 335 nm irradiation. The compounds obtained with the 610 nm irradiation were the same reported for the 335 nm irradiation see appendix III – Indigo data, section III.3.2, p.112 for indigo carmine HPLC-DAD chromatograms).

Compounds	t_r (min)	λ_{max} (nm)	Relative area (%)*	Attribution**
1	2.1	297	<2	Isatin sulfonic acid
2	12.3	610	89	Indigo carmine
3	14.1	604	8	?
4	19.0	620	2	?

* The relative area was calculated at 275 nm.

** For an unequivocal identification LC-MS should be performed.

2.4.2 Monochromatic irradiation in heterogeneous media

Recently, it was demonstrated that it is possible to calculate Φ_R in transparent gel solutions with the same equations and methodology developed for solution, if the active volume of irradiation is considered and the incident light is distributed uniformly over the irradiated surface [110]. It was concluded that the Lambert-Beer's law can be applied whether the concentration is uniform or distributed (i.e., whether in a stirred solution or in a transparent gel), provided that the irradiated volume is defined by the product of the area of the irradiated face and the optical pathway.

Carboxymethylcellulose (CMC) aqueous gels were used to simulate a cellulosic fibre and several commercial gelatines (mostly collagen) the protein based fibres. The commercial gelatines were used as in the literature it was proved that they display good purity and are currently used in research [111,112]. Even so, bacteriological gelatine was also prepared. Gels formulated with these polymers allowed excellent transparency in the visible region. The results obtained in these transparent gels are perhaps what threw more light into the degradation mechanism of indigo (see table 2.4).

Table 2.4 - Quantum yields of reaction, Φ_R , for indigo carmine in aqueous gels and water at T=293 K, in the presence of molecular oxygen, (see appendix III – Indigo data, section III.2, p. 110, for I_0 and Φ_R).

Medium	Φ_R	
	λ_{irr} 335 nm	λ_{irr} 610 nm
H ₂ O	9×10^{-6}	*
DMF	2×10^{-3}	-
CMC	5×10^{-4}	2×10^{-4}
<i>Vahine</i> gelatine	4×10^{-4}	5×10^{-4}
<i>Jerónimos</i> gelatine	9×10^{-4}	4×10^{-4}
Bacteriological gelatine	2×10^{-3}	3×10^{-4}

* Lower than 10^{-6} , it was not possible to determine with the utilized irradiation set-up. The Φ_R of indigo carmine in DMF was not performed.

When photodegradation of indigo carmine in DMF is compared with indigo carmine in water solution (gels), the Φ_R obtained is circa 2 orders of magnitude higher. Taking into account that these gels are water based gels this is an unexpected result, as in more confined environments we would expect to have lower photodegradation reaction rates and not 2 orders of magnitude higher. It is well known that both cellulose based materials and proteinaceous ones are prone in developing hydroperoxides [113]. These, in turn, can absorb light in the visible region and in the excited intermediate state can evolve through intra or intermolecular reactions with the formation of carbonyl groups and other radicals. Carbonyl groups can further act as chromophores and evolve into a series of Norrish reactions, with further bond breaking and formation of other reactive carbonyl functions and radicals. The results obtained with the bacteriological pure gelatine further sustain this line of reasoning; contrary to the other gelatines acquired as tablets, this was sold as a powder that could not be previously washed with cold water (the gel is prepared with warm water), procedure adopted for the commercial gelatines. This washing would enable the quenching of radicals present in the protein structure as well as the removal of degraded material more polar and soluble in water. When irradiated at 610 nm (where the hydroperoxides cannot absorb), the Φ_R obtained is similar to the other gelatines, but when irradiation is carried out at 335 nm, the values are almost one order of magnitude higher for the bacteriological gelatine (figure 2.7).

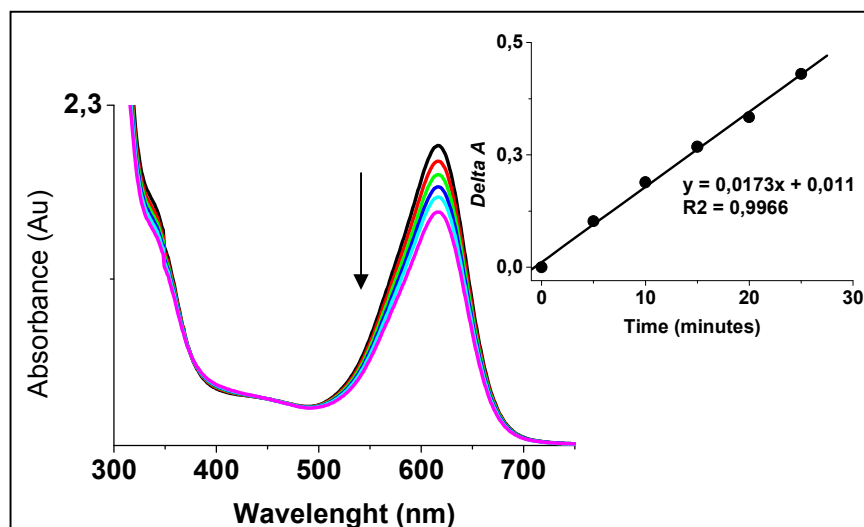


Figure 2.7 – Photodegradation of indigo carmine in bacteriological gelatine with irradiation at 335 nm. In the inset the absorbance variation followed at 610nm, is plotted over time, giving the m parameter of the Φ_R equation, for more details, see Appendix II – Indigo data.

The main products formed in cellulose or proteic gels at both irradiation wavelengths are the same as those obtained for indigo carmine when dissolved in water. Moreover, a similar distribution of the principal compounds could also be found.

2.4.3 Polychromatic irradiation in heterogeneous media

Indigo deposited in creased glass surfaces creating a homogeneous blue surface ($L^*=44.52\pm 0.36$; $a^*=-0.70\pm 0.04$; $b^*=-12.00\pm 0.15$ [114]) was irradiated with a Xenon lamp with a cut-off filter till 300 nm, simulating the sunlight exposure (see appendix I – Experimental section, p. 93). The reaction was followed by periodically measuring colour changes with a colorimeter and the photodegradation profile was characterized as previously by HPLC-DAD, after full extraction of the indigotin with DMF from the glass surfaces. Circa 0.10 mg after 1700 hours/5950 MJ of irradiation faded almost totally ($L=82.00\pm 0.41$, $a^*=-1.95\pm 0.12$, $b^*=3.23\pm 0.16$), corresponding to circa 120 years in a museum display (see appendix III- Indigo data, section III.3, p. 113). It was possible to confirm that the photodegradation of indigo in the solid state was similar to what was observed with monochromatic irradiation, being isatin the major product formed. However, the concentration of isatin formed in the solid state was very low when compared with the indigo in homogeneous media (figure 2.8). One of the reasons for this low content of isatin

can be its possible degradation during the indigo irradiation due to the absorbance of short wavelength radiation by isatin.

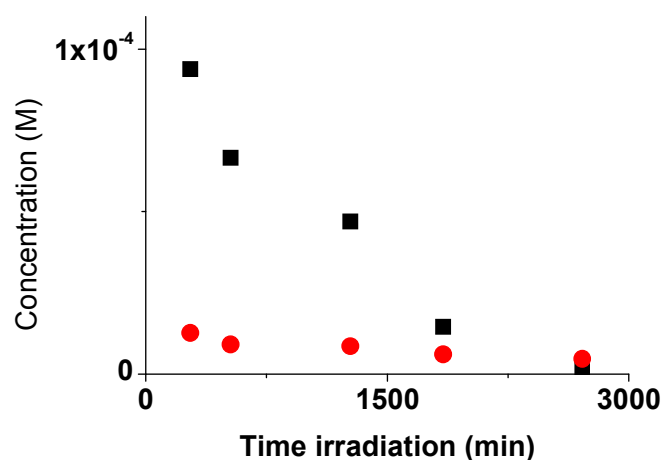


Figure 2.8 - Monitorization by HPLC-DAD of indigo photodegradation in the solid state. Squares – indigotin; Circles – isatin.

2.4.4 Characterization of the degradation products in Andean millenary textiles

The blues from 11 textiles of the pre-Colombian civilization of Paracas, 500 BC – 200 AD, and one of Nasca, 200 AD, in a total of 17 samples, were analysed by HPLC-DAD (see appendix I-experimental section, p.93 for extraction methods).

In all the 19 samples analysed, indigotin ($t_r = 25.00$ min, $\lambda_{max} = 614$ nm) was identified as the main colourant. A high amount of indirubin ($t_r = 26.23$ min, $\lambda_{max} = 544$ nm), as reported by Wouters for textiles from these cultures [115], was also found (see table 2.5 and appendix III-indigo data, section III.4, p. 114, for Andean sample HPLC-DAD chromatogram).

In all the samples analysed, the presence of isatin ($t_r = 8.50$ min, $\lambda_{max} = 242, 302$ nm) and an unknown compound ($t_r = 6.82$ min, $\lambda_{max} = 311$ nm), previously identified in indigo homogeneous and heterogeneous media photodegradation, was detected. This unknown compound was identified in less than 50% of the samples analysed with a relative percentage inferior to 10% and, as its epsilon was not known, it was excluded from table 2.6.

Table 2.5 – Relative concentration of the principal chromophores and main products identified in Andean Textiles by HPLC-DAD.

Textile	Sample	Indigotin (%) [*]	Indirubin (%) [*]	Isatin (%) [*]
Skirt 200BC – 200AD	Dark blue	77	12	11
	Blue	41	20	39
	Blue	58	13	29
Poncho fragment 0 – 100AD	Dark blue	55	21	24
	Light Blue	63	23	14
Man's Poncho, 100 BC – 0	Blue	60	16	24
Fragment, Nasca, 300 AD	Blue	89	3	8
	Dark blue	79	14	7
	Light blue	90	2	8
Border Fragment 0 – 200AD	Dark blue	75	9	16
	Dark blue	73	11	16
Fragment 0 – 200 AD	Light blue	28	17	55
Border Fragment 0 – 50AD	Dark blue	70	8	22
	Dark blue	85	5	10
Mantle Border 100 BC – 100 AD	Blue	51	29	20
Mantle Border 100 BC – 100 AD	Blue	81	11	8
Fragment (100-200 AD)	Light Blue	90	-	10
Turban 100BC – 100AD	Blue	50	45	5

* the respective areas of the compounds were calculated at their maximum wavelength and represented as a function of the concentration, for more details see experimental section.

The identification of the same products in these blue textiles, where isatin was once again the major product formed, confirms the results obtained for indigo photodegradation in liquid and solid media. Isatoic anhydride, tryptanthrin and anthranilic acid, reported in [98], were not found.

2.5 Conclusions

With these results it is possible to conclude that indigo is a stable dye, as referred in the literature [2,3]. It was demonstrated that the main photodegradation reaction that occurs is the cleavage of the central double bond of indigotin, leading to the formation of isatin. This reaction can be promoted by the presence of electron donors such as free radicals that will easily attack the double bond, reducing indigotin. It is in this reduced state, which is more reactive than the indigotin *keto* form, that the central covalent bond will be cleaved forming isatin. This was further confirmed by the indigo carmine photodegradation in cellulosic and

protein based gels which revealed higher Φ_R than those observed for the indigo carmine photodegradation in water, due to the possible presence of radicals. Moreover, when the photodegradation of indigo and indigo carmine were carried out in DMF, it was also verified that both Φ_R obtained were higher than the Φ_R obtained for indigo carmine dissolved in water. Tests, including the irradiation of DMF solvent at 335 nm, revealed that several compounds, possibly hydroperoxides, were formed. The contribution of several radicals for the photodegradation of indigo dye excludes therefore that the main photodegradation mechanism is the oxidative degradation of indigotin through singlet oxygen. Moreover, this explanation did not support the photophysical studies of indigotin, where it was found that the degradation of indigo was unlikely to occur through interactions with triplet oxygen due to the low yields of singlet oxygen formation [106].

Anyway, the best approach to photodegradation of indigo dyed fibres was the photodegradation of indigo carmine in water as it revealed to be very stable, without extra contribution of free radicals. These radicals developed in cellulose and gelatine gels probably will accelerate the indigo photodegradation more than the indigo dyed textiles. It should be stressed that indigo dye is really a stable molecule due to the hydrogen bonds between adjacent carbonyl and N-H groups that keep the molecule in a stable *trans*-planar configuration [105,106] preventing its *photoreactivity*; therefore, low Φ_R can be expected in textile environments.

Chapter 3 - Mauve Dye

3.1 Mauve dye overview

The synthetic colourant mauve was discovered in 23 March 1856 by the eighteen-year-old chemist William Henry Perkin (1838-1907) [1,116,117]. Perkin was trying to synthesize quinine from coal-tar chemicals, although this was just achieved almost a century later by Woodard and Doering [118]. The quinine compound was used against the malaria disease and at that time it was obtained from the bark of chinchona tree [118]. August Hoffman, the director of the Royal College of Chemistry in London, where Perkin studied, suggested that it might be possible to prepare quinine from a suitable amine derivative [119,120]. Perkin tried an oxidative dimerisation of allyltoluidine ($C_{10}H_{13}N$) with potassium dichromate, once the allyltoluidine had almost half of the molecular weight of quinine ($C_{20}H_{24}N_2O$): $2(C_{10}H_{13}N) + O_3 = C_{20}H_{24}N_2O_2 + H_2O$ [119-122]. However, instead of the colourless quinine, Perkin obtained a "dirty reddish brown precipitate". In order to understand the reaction, he repeated the process using a simpler compound, aniline, and once more he obtained a coloured precipitate [119-122]. The majority of his contemporary chemists would have discarded this black precipitate, once the formation of coloured amorphous compounds was considered an indication of non-crystalline compound formation and failure of the reaction [117,120]. For instance, it is known that Hoffman in 1858 obtained accidentally the fuchsine dye (rosaniline); however, he was so concerned with the reaction under study that he regarded it as an impurity [121]. Nevertheless, Perkin treated the black precipitate with water, coal-tar naphtha and methylated spirits of wine (i.e. methanol), obtaining a deep purple solution which dyed silk very well and was resistant to light [119-123]. He sent some specimens of dyed silk to the famous dyers Pullars of Perth that considered the colour as good as one of their best *lilac* [116,117,119,120,122-123]. Furthermore, as they report, at that time the purple color was very fashionable [124]. Moreover, it was obtained with the semi-synthetic murexide dye produced with deposits of bird droppings (guano) or with the vegetable French Purple dye produced with lichen, which faded rapidly [118,125]. Therefore, the discovery of a stable purple colour, not very expensive, would be of great interest for dyers. This was not compatible with the low yield of the reaction (less than five per cent of mauve dye was obtained per each synthesis), the difficulty of obtaining raw-material in relevant amounts and inexpensive manner, the need of large scale-up and finally the difficulties encountered on dyeing with a new class of dyestuffs [116,117,119,120]. For instance, the mauve dye displayed a great affinity to silk fibre which caused unevenness in the dyed textile fabric and in cotton textiles it could not

resist to the action of soap [119,120]. Even so, in 1856 a patent was secured (granted on 26 August 1856 and sealed on 20 February 1857 [126]), and in June 1857 with his father George Perkin and his brother Thomas Perkin, Perkin started the works on the mauve dye in a small factory at Greenford, Middlesex [116,117,119,120]. After six months, the mauve dye, under the name of "Aniline Purple" or "Tryan Purple" (to suggest a connection to the ancient royalty purple colour obtained with thousands of tiny marine molluscs), was being manufactured in an amount enough to supply Thomas Keith's house at Bethnal Green, the largest silk dyer of London [116,117,119,120,125]. The initial problems were rapidly overcome: the Bechamp's discovery of the nitrobenzene conversion into aniline with iron and acetic acid in 1854 [127], were installed at the Greenford Green Factory in 1857 and it was possible to obtain costless aniline [128]. Special apparatuses were developed for the large scale production. It was found that large pieces of silk could be dyed in a soap bath in order to prevent unevenness, and in 1857 Perkin with the dyer Pullar discovered a mordant tannin based process to dye cotton textiles in a permanent way [119,120]. Even the mauve synthesis was optimized in order to obtain a more water soluble colourant and, as a result, the initial amorphous paste sold as sulphate salt was replaced by the soluble mauve acetate salt which required aniline with higher contents of toluidine [129]. It was also noticed that aniline with large amounts of toluidine produced a redder shade of purple, while aniline with little toluidine produced a blue shade of purple and, taking advantage of this, two different products were manufactured [129].

In 1859, Perkin's mauve dye was a success in France, where the name mauveine and mauve were adopted in association with the pale-violet mallow flower (Latin: *malva*). From silk, dyeing was extended to cotton dyeing and calico printing. The purple shade became a favourite colour of Empress Eugenia and Queen Victoria and immediately spread all over France and England, being the mauve apogee in the early 1860s [116,117,121,122,124,125]. Since Perkin was not able to patent the manufacture of his mauve dye in France, the French colourists and chemists started to replicate and improve the mauve dye process during this period. Even in Britain, in 1860, the Roberts Dale & Co. factory started producing mauve dye using copper salts instead of the usual potassium dichromate to oxidise aniline. Although this process was not as efficient as the process developed by Perkin, they started competing with the Perkin's & Sons factory [130,131].

Very soon other synthetic dyes from coal-tar chemicals were also discovered and made available in large scale. The aniline red, also known as magenta (Britain) and fuchsine (France), was discovered in 1859 by Verguin [132,133]. In 1861, aniline red was converted into a blue dye and in 1863 into Hoffman's violets (more brilliant but less resistant to fading

than the mauve dye), which began to threaten the sales of mauve [132,133]. Indeed, after 1863, the production of the mauve dye declined and, although it was used for about 10 years, the production ceased in 1873. In 1 January 1874 Perkin sold his factory and dedicated his full-time to chemical research, being very well known, for instance, his work with alizarin synthesis, among others [116,117,120-122].

All this pioneering work is considered a landmark in the history of chemistry and launched the synthetic dye industry in Europe. Although other synthetic dyestuff had been discovered before mauve (picric acid in 1771 by Woulfe and aurin by Runge in 1834), this was the first industrial multi-step synthesis of an organic compound that immediately spread within the UK, France, Germany, Switzerland and the USA [1,116,117,124]. Thousands of synthetic colours were discovered and made available to everyone, contrarily to the few dozen of natural colours available in antiquity. Furthermore, the mauve dye was also the indirect inspiration for other coal-tar derivatives as the perfumes and explosives. Important contributions can also be found in medicine and other sciences [1,116,117,124]. Therefore, it is undeniable that the mauve dye is a chemical icon and a landmark in the history of science and technology.

3.1. Chemical composition – *pursuing a perfect colour*

To be used as a textile dye, the chromophore should display a desirable colour; it should also be resistant to light-induced and pollution-induced fading and to washing. Mauve, as a successful dye, fulfilled all these criteria.

Perkin performed an extensive research on the chemistry of mauve dye synthesizing different mauveine salts [134,135], among others, in order to obtain a pure compound suitable for structure elucidation, eventually, for patent protection and possibly to improve the dye obtained in the earlier synthesis. According to Perkin, when the mauve dye was first commercialized, it was sold as an amorphous body in the form of sulphate salt [120]; however, in 1863 the mauve dye was sent to the market perfectly pure and crystallized and, as sulphate of mauveine was unsuitable for the dyer, was converted into the soluble acetate of mauveine [120,122,129].

This extensive research can also be seen as part of a programme to synthesise derivatives of mauveine as novel dyes, in the same way the aniline blue and violet derivatives had been obtained by Hofmann and others from aniline red [132,133]. For instance, the oxidation of the mauve dye led to the discovery of aniline pink or safranine ($C_{20}H_{18}N_4Cl$) in 1859 by Greville Williams and in 1863 by Perkin, which due to its price was

not used extensively [120,122]. Another derivative of mauveine was also discovered in 1863 and named dahlia (patented on 6 November 1863) with the proposed empirical formula by Perkin of $C_{27}H_{23}(C_2H_5)N_4HCl$ [120,122].

During his research Perkin concluded that the mauve dye was composed mostly by mauveine, a trimethylated based compound ($C_{27}H_{24}N_4$), and a second colourant named pseudo-mauveine ($C_{24}H_{20}N_4$) [129,135,136]. In 1879 Perkin confirmed that the mauveine compound was derived from aniline and *para*-toluidine and that its formula was indeed $C_{27}H_{24}N_4$ [129]. The C_{27} empirical formula had been initially presented in 19 August 1863 [134,135]. Between 1863 and 1879, Perkin had assigned the $C_{26}H_{24}N_4$ formula to the mauveine compound [129].

The empirical formula of pseudo-mauveine, $C_{24}H_{20}N_4$, was also presented in 1879 and Perkin concluded that this second colourant could even be obtained only with pure aniline, contrarily to mauveine [129]. One secret of the success of the mauve dye first synthesis lies on the fact that the aniline used by Perkin was not totally pure, it was a mixture of aniline with both *ortho* and *para*-toluidine. It was in 1862-63 that Hoffman concluded that commercial aniline obtained from coal tar was contaminated with toluidine [132,133]. The coal tar had both benzene and toluene which after nitration and reduction would give, respectively, aniline and toluidine. Indeed, after 1896, and contrarily to what he presented in 1879 [129] and 1896 [120], Perkin revealed that the mauve dye was not a mixture of two chromophores but three: "mauveine formed from aniline and *p*-toluidine" (the $C_{27}H_{24}N_4$ chromophore), pseudo-mauveine formed from aniline only (the $C_{24}H_{20}N_4$ chromophore) and "a third analogue formed from aniline, *o* and *p*-toluidine" (probably an isomer of the $C_{27}H_{24}N_4$ compound, see section 3.3 for more details). Moreover, Perkin found that the mixture gave better results in the dyeing than the compounds separately [122].

Taking advantage of the impurity of the commercial anilines, Perkin was able to develop two different types of purple: one bluer, obtained with aniline and little toluidine, and a red shade obtained from aniline with large amounts of toluidine. The percentage of toluidine also revealed to be important in the quality of the mauve acetate salts that replaced the initial mauve sulphates; to precipitate mauve dye as acetate salts, anilines with higher contents of toluidine were necessary [129].

Although Perkin also speculated about the structure of the mauve dye, he was not able to find it. It was in 1893 and 1896 with O. Fischer and E. Hepp [136], and R. Nietzki [137], respectively, that the pseudo-mauveine was found to be an N-phenylphenazidium salt derived from pure oxidized aniline (figure 3.1). However, for the mauveine chromophore,

which was also considered a derivative of pseudo-mauveine, they were not able to find the position of the CH₃ groups in its structure.

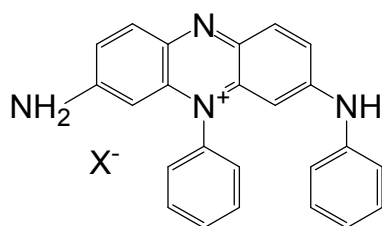


Figure 3.1 – Structure of the N-phenylphenazidinium salt discovered by O. Fischer and E. Hepp and R. Nietzki [125]

The first correct mauveine structure had to wait until 1994 to be revealed by Otto Meth-Cohn and Mandy Smith [138]. In their first pioneering analysis of historic samples, obtained from the Science Museum London and from the Zeneca archives at Blackley, Manchester, two compounds were considered to be the main chromophores, mauveine A (major compound) and mauveine B, respectively C₂₆ and C₂₇ structures, and no pseudo-mauveine was identified [138] (figure 3.2).

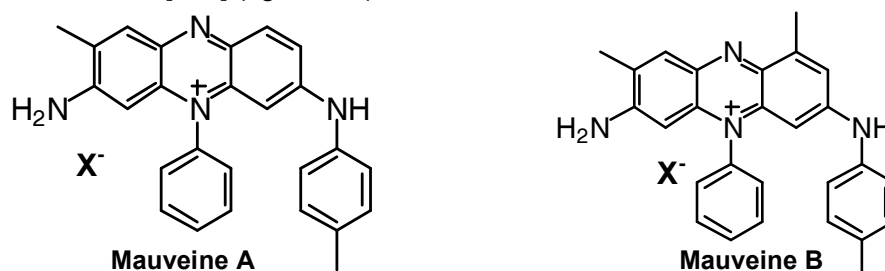


Figure 3.2 – Mauveine structures discovered by Otto Meth-Cohn and Mandy Smith in 1994 [138].

In the present work, using a modern synthesis, it was possible to obtain pseudo-mauveine (C₂₄), mono (C₂₅), di (C₂₆), tri (C₂₇) and tetramethylated (C₂₈) derivatives using as starting materials aniline, *o*-toluidine and *p*-toluidine; depending on the *ortho* to *para* ratios, it was also possible to obtain different isomeric ratios. Two other compounds - mauveine B2 and mauveine C, respectively C₂₇ and C₂₈ compounds - were also discovered during analysis [139].

These data, as well as the early data of Meth-Cohn and Smith [138], contradict Perkin's claim that the definite formula for commercial mauveine was a C₂₇, mauveine B or an isomer, and that the second colouring material was pseudo-mauveine. As it will be shown

in this work, mauveine is a complex mixture and it may be anticipated that both modern authors and Perkin have their credits.

3.3 Results

Mauve synthesis was performed in order to obtain the mauve's chromophores characterization with HPLC-DAD, MS and ¹H-NMR. Afterwards, the analysis of different historic mauve samples -mauveine salts and dyed textiles- was undertaken. Fourteen samples from important museum collections were analyzed with HPLC-DAD, LC-MS and ICP-AES or IC-AEC. Moreover, the study of the photodegradation of dyed mauve textiles was initiated.

3.3.1 Syntheses

In order to obtain the major chromophores of the mauve dye for its characterization, a synthesis as described in the Journal Chemical Education in 1998 [140] was performed (for more details see appendix I – experimental section, p. 94). As the mauve dye obtained with the JCE 1998 synthesis was different from what was reported in the literature [138] (a mauve dye with two major chromophores: mauveine A and B), other syntheses with different proportions of the initial standard materials, namely aniline and toluidine, were also tested (see table 3.1). In synthesis 2 a higher concentration of mauveine A was expected, for synthesis 3 the formation of mauveine B would be increased and in synthesis 5 it was expected to obtain more pseudo-mauveine. Equivalent proportions of the starting materials were also tested in synthesis 4.

Table 3.1 – Syntheses of mauve dye with different ratios of aniline and toluidine.

Synthesis	Aniline (mol)	<i>o</i> -toluidine (mol)	<i>p</i> -toluidine (mol)
1, <i>JCE 1998</i>	1	1	2
2, <i>Mauveine B</i>	1	2	1
3, <i>Mauveine A</i>	2	1	1
4	1	1	1
5, <i>Pseudo-Mauveine</i>	1	0.1	0.1

Of the five syntheses performed, synthesis 1 from JCE 1998 was the most successful, although it was well below the 5% obtained by Perkin in 1856 [120,122,140]. In the other four syntheses, the formation of mauve dye was even lower and in synthesis 3 no purple colour was observed. This can be related with the reaction time; Perkin's synthesis took

one or two days [116,120,122,126] before the final washings and not just 2h as reported in [140]. In the JCE 1998 synthesis, the formation of a black precipitate was really fast, while in syntheses 2 and specially 4 it was slower. Indeed, in all the chromatograms of the synthesized mauve dye, the starting materials were detected, namely aniline and toluidines. Nevertheless, the principal reason for the low yield of the reactions might be the low amounts of $K_2Cr_2O_7$ and H_2SO_4 indicated in [140]. According to a mauve synthesis described in 1876, where the quantities of the starting materials are described [116], the amount of potassium dichromate used is at least 40 times larger than in the JCE 1998 synthesis. Moreover, the stoichiometric equations of the formation of mauveine compounds revealed that a higher amount of $K_2Cr_2O_7$ and H_2SO_4 than what is described in the JCE 1998 synthesis is needed (see Appendix IV-Mauve dye data, section IV.1, p. 115 for stoichiometries of the mauveine chromophores formation). For instance, in the syntheses 2 and 3, almost ten times more amount of H_2SO_4 should be used, compared to what is described in JCE 1998. The insufficient amount of starting materials together with reduced reaction time can explain the lack of success of synthesis 3 and the very low yields in synthesis 2 and 4. Nevertheless, it was still possible to observe that in the three syntheses where a purple colour was obtained, the composition of the mauve dye was related with the proportions of the starting materials used.

In two of the three mauve dye syntheses, the major compounds obtained were mauveine A ($C_{26}H_{23}N_4^+$), B ($C_{27}H_{25}N_4^+$) and isomers, and mauveine C ($C_{28}H_{27}N_4^+$) (see figure 3.3). Other minor purple compounds were also detected but they were only characterized in the historical samples (see next section and Appendix IV-Mauve dye data, section IV.2, p.119 for mauve summarized characterization).

For the **synthesis 1**, the major compound obtained was a new isomer of mauveine B (mauveine B2) together with a new mauveine compound (mauveine C, table 3.2). Both compounds contain two molecules of *p*-toluidine and, therefore, the major amount of this reagent in this synthesis is crucial (table 3.1). Even though they were never identified before, they are always present as minor compounds in Perkin's original samples (see next section).

In the **synthesis 2**, the major chromophores were mauveine B (28%), together with mauveine A (25%). Although more mauveine B was produced in this reaction than in the first synthesis, as expected, the amount of mauveine B2 and mauveine C were still considerable (circa 23% each). Probably, the amount of the starting material *p*-toluidine was too high, inducing the formation of mauveine B2 and C, which competed with the formation of mauveine B. In the original Perkin's samples, such amounts of mauveine C

and B2 compounds were never found, although Perkin in his last communications referred that the mauveine was a mixture of three chromophores [122], the third possibly being an isomer of mauveine B.

In the **synthesis 4**, with a higher content of the starting material aniline, more pseudo-mauveine ($C_{24}H_{20}N_4^+$, circa 46%), with no methyl groups, was obtained, together with two new mono-methylated derivatives ($C_{25}H_{22}N_4^+$, circa 40%). The presence of mauveine A and B was very low (less than 6% each, see table 3.2). This synthesis confirms that it is possible to obtain pseudo-mauveine from “pure aniline” as referred by Perkin. Indeed, in one of the historical samples, the mauveine chromophores distribution is very similar (see next section).

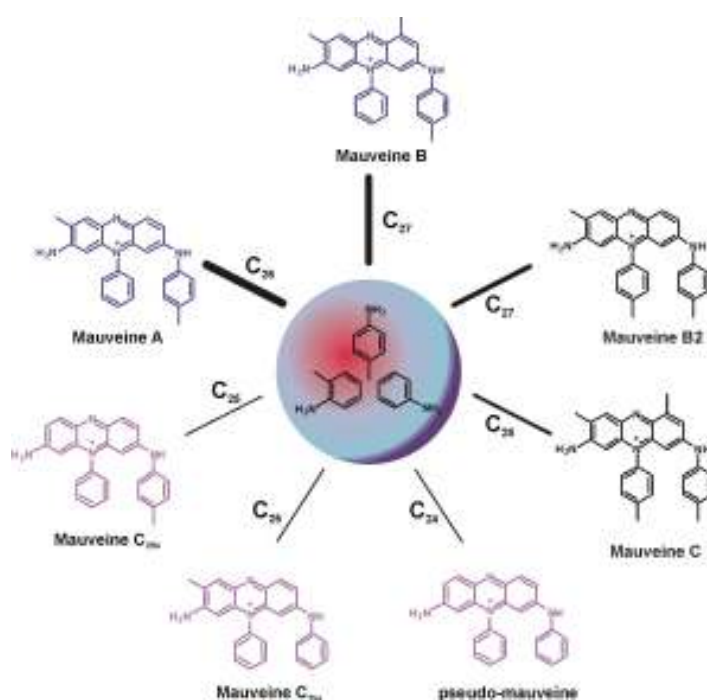


Figure 3.3 - Fully characterised products isolated from modern mauve synthesis and mauve historical salt samples. Depending on the initial ratio of aniline, *o*-toluidine and *p*-toluidine, the proportions of the different mauveine compounds vary. The mauveines A, B and B2, pseudo-mauveine and mauveines C_{25a} and C_{25b} could be isolated in sufficient amount to allow MS and NMR characterization, while seven others could only be characterized by HPLC-MS.

Table 3.2 – Relative percentages of the mauveine chromophores in the synthesized mauve dye.

Synthesis	C_{24}	C_{25}	C_{26}	C_{27}	C_{27}	C_{28}
		$C_{25a}+C_{25b}$	A	B	B2	C
1	-	-	15	24	31	30
2	-	-	25	29	24	22
3*	-	-	-	-	-	-
4*	-	-	-	-	-	-
5**	46	40	5	5	-	-

* No formation of mauve dye was observed in this synthesis.

**In synthesis 5 other minor compounds were also found with less than 4%.

3.3.2 Original samples

All the original mauve samples synthesised and purified by Perkin (as well as the mauve samples synthesised in this work) are complex mixtures of at least thirteen different compounds, all containing the 7-amino-5-phenyl-3-(phenylamino)phenazin-5-ium core. Besides the C_{24} compound with no methyl groups (pseudo-mauveine), two monomethylated C_{25} isomers, named C_{25a} and C_{25b} , dimethylated mauveine A (C_{26}), four trimethylated mauveines (B, B2, B3, B4), two tetramethylated mauveines (C, C1), one pentamethylated (mauveine D) and one hexamethylated (mauveine E) could be identified in the historical samples (see Appendix IV-Mauve dye data, section IV.2, p. 119 for mauve summarized characterization, section IV.3, p. 120 for HPLC-DAD/LC-MS characterization of historical samples and section IV.4 for NMR characterization, p.126). These last two compounds show that the commercial aniline used by Perkin was contaminated not only with toluidines but also with anilines containing two methyl groups in the benzene ring. All these compounds have absorption wavelength maxima (λ_{max}) in methanol solution in the range 540 (mauve E) – 550 (mauve B2) nm. This is also in agreement with a recent chromatographic analysis (by HPLC) of mauveine samples [141].

3.3.2.1 Original mauve textile samples

Some of the original mauve textile samples analyzed can be from the early years of mauve manufacture and in the case of ScMF5 and Perth samples may even be from 1856 [142]. The seven samples analyzed (figure 3.4) can be grouped in two sets of three and four samples. The first group (ScMF5, Perth and ScMF6) is characterized by a high percentage of mauveine A (circa 50%), with the mono-methyl derivative isomers (15-20%), pseudo-

mauveine (5%) and mauveine B (5-12%) also present (table 3.3). In the second group (ScMF1, F2, F3 and F4), samples with mauveine A and B as major chromophores can be found, with the mono-methyl derivatives C25 being present in minor amounts (1-5%) and no pseudo-mauveine (table 3.3). Both data sets are consistent, and, therefore, may reflect standard processes for the production of the mauve dye.

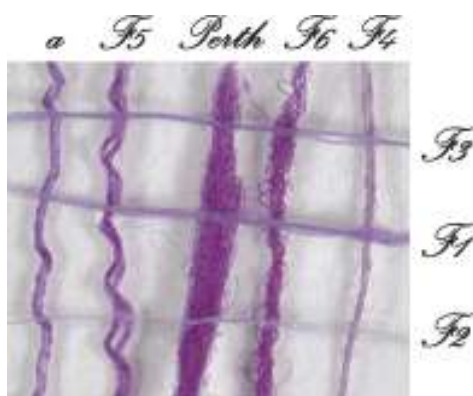


Figure 3.4 - Textile samples from museum collections analysed in this work. The designations are in accordance with those given in Table 3.3. Fibre a corresponds to a fibre dyed with mauveine Science Museum 1, using an original dyeing procedure described by Perkin [119] (for more details about mauve samples, see appendix I- Experimental section, p.94.

Table 3.3 - Relative percentages of the main chromophores of the mauve dyed textile samples.

Textile	C_{24}	C_{25}	C_{26}	C_{27}	C_{27}	C_{27}^{**}	C_{28}	C_{28}^{**}	C_{26}/C_{27}^{***}
		$C_{25a}+C_{25b}$	A	B	B2	B3+B4	C	C1	
ScMF1	-	1	32	36	11	4	7	9	0.6
ScMF2*	-	5	70	13	7	4	1	-	3.0
ScMF3	-	2	61	21	8	5	2	2	1.8
ScMF4	-	2	53	24	9	5	3	4	1.4
ScMF5	5	20	51	5	11	9	-	-	2.1
Perth	4	18	50	12	9	7	-	-	1.8
ScMF6	5	15	51	11	11	7	-	-	1.7
a	<1	2	50	22	11	6	4	5	1.3

* The concentration of mauve in this sample was very low. ** The assignment of these three structures (mauveines B3, B4 and C1) was not made; however, based on the available analytical data, these could be clearly identified as isomers of mauveine B and mauveine C (see appendix IV- Mauve data, section IV.3, p.120 for HPLC-DAD/LC-MS characterization of historical samples and section IV.4 for NMR characterization, p.126). *** Defined as the ratio between the sum of all C_{26} and all C_{27} compounds relative percentages calculated at $\lambda=551\text{nm}$.

3.3.2.1.1 Group I - Perth, Science Museum F5 and F6

The Science Museum has a piece of the first silk fabric dyed on a large scale (ScMF5), which was allegedly presented to Queen Victoria. The museum's inventory record dates this piece to "about **1860**" and this information came probably from the Perkin family. The Perth Museum in Scotland has also a similar piece that was probably from the same silk fabric and for Queen Victoria. However, in this museum it is labelled as "cut from the first length of material dyed by Dr Perkins [sic] by his new process in Pullar's works, Perth in **1856**" [142].

The chromophore fingerprint for the Perth and the ScMF5 samples are very similar, pointing to a common mauve dyeing bath. In order to confirm if they are from the same silk fabric, an analysis of the weaving techniques and pattern is also required.

Since the Perth and the ScMF5 samples are identical, probably they were made in 1856-7, when Perkin was working with the Pullars dyers as reported in the Perth sample label. There is no evidence that Perkin was working with the Pullars in 1860 and therefore the tentative dating of the Science Museum is probably incorrect. Both samples are similar to the ScMF6 sample, the only textile that can be accurately dated to 1862 or slightly earlier once it was displayed in the 1862 exhibition [142] (figure 3.5).



Figure 3.5 – The mauve dyed shawl (a), ScMF6 sample, which was displayed in the 1862 exhibition (b) [142].

The high percentage of mauveine A (circa 50%) together with the mono-methyl derivative isomers (15-20%) and the pseudo-mauveine (5%) in these three samples possibly correspond to the first large scale product introduced in the market, where the commercial mauve appeared as an amorphous body [120,122,129]. In this process, the mauve dye was probably obtained from aniline containing but little toluidine, leading to the formation of a higher content of pseudo-mauveine and mauveine C₂₅ compounds when compared with the samples of the group II (ScMF1, F2, F3 and F4).

In the wool ScMF6 sample, almost 6 mg of iron and aluminium per g of textile were detected by ICP-AES (see appendix IV- Mauve data, section IV.5 p. 131 for mordant analysis). The amounts of aluminium and iron ions are in the concentration range of mordanted wool textiles [143].

In the original patent, Perkin mentions that he found advantageous to boil the wool with the mauve dye and iron sulphate, which can explain the high content of iron in this sample [126]. In the article of 1862 [119], Perkin does not refer the presence of iron sulphate in the mauve dyeing bath of wool and this procedure could have been discarded. Indeed, the mauve colourant is a direct dye for protein based fibres and a mordant is not required to obtain a permanent colour [144]. It would be interesting to analyse the amount of iron and aluminium in older wool textile samples and compare with the present results.

As expected, in the silk sample analysed (Perth), metal ions were not detected in sufficient amount to consider that a mordant was applied to the sample. Only 1 mg of iron per g of textile was found, which is very low for a silk mordanted with iron (around 5 mg of iron per g of textile are needed). This value is also outside of the values expected for non-mordanted silk (0.07 mg of iron per g of textile) [143]. In the cotton sample from group II (ScMF4), a similar amount of iron was also found. One remote hypothesis for the presence of iron is the use of iron vessels to obtain the reagents for the mauve synthesis [120]; other contaminations during the dyeing process can also be considered.

3.2.2.1.2 Group II - ScMF1, F2, F3 and F4

The four samples of this group, all of unknown date but possibly prepared for the 1862 International exhibition [142], display a higher content of mauveine A, mauveine B and even mauveines C when compared with the group I. This is possibly due to a transition from the first process described above to a second process where the mauve dye was sold in the form of the more water-soluble mauveine acetate [122,129]. In order to obtain crystallized mauveine acetate it was necessary to have a mauve dye enriched in methylated derivatives like mauveines A, B or C [145].

In the cotton ScMF4 sample, besides the presence of iron, 10.06 mg of tin per g of textile were detected. Indeed, one year after the mauve discovery, Perkin and the Pullar dyers developed a process based on tannins and stannate of sodium or alum [$KAl(SO_4)_2 \cdot 12H_2O$] to fix the mauve dye to vegetable fibres in such a way that it could resist the action of soap [120].

3.3.2.2 Original mauve salt samples

The mauve salt samples are of an unknown date but probably they were all made after 1860 [142], when the mauve dye was manufactured in the form of acetate salt. It was with some of these salt samples that Perkin perhaps performed his research on the mauveine compound formula until 1879, concluding that it was a $C_{27}H_{24}N_4$ [129].

Although the distribution of the mauveine compounds amongst the salt samples (table 3.4) shows rather large dissimilarities, the two major chromophores present are (with the exception of Schunck's sample) mauveines A (C_{26}) and B (C_{27}). Other C_{27} isomers (mauveines B3 and B4), as well as C_{28} compounds (mauveines C and C1), are also present, with mauveine B2 as the most important of these minor compounds and contributing with *circa* 10% to the overall colour. The pseudo-mauveine and mauveines C_{25a} and C_{25b} are present in minor amounts C (see appendix IV- Mauve data, section IV.3, p.120 for HPLC-DAD/LC-MS characterization of historical samples and section IV.4 for NMR characterization, p. 126).

Table 3.4 - Relative percentages of the main chromophores of the mauveine salt samples and respective counter-ions (A-acetate, S-sulphate).

Salt	C_{24}	C_{25}	C_{26}	C_{27}	C_{27}	C_{27}	C_{28}	C_{28}	C_{26}/C_{27}^*	Anion %
		$C_{25a}+C_{25b}$	A	B	B2	B3+B4	C	C1		
ScM 1	1	2	50	23	10	5	4	5	1.3	97 A
ScM 2	1	3	37	26	13	6	5	8	0.8	98 S
ScM 3	1	2	54	16	9	4	5	8	1.8	67 S
ScM 4	1	2	37	31	12	5	5	8	0.8	82 A
MSIM1	-	2	39	33	12	5	4	6	0.8	86 A
MSIM2	49	41	7	-	3	-	-	-	-	68 A
CM	1	2	50	24	8	4	5	7	1.4	100 A

*Defined as the ratio between the sum of all C_{26} and all C_{27} compounds relative percentages calculated at 550nm.

3.3.2.2.1 Science Museum 1, Chandler Museum and Science Museum 3

The ScM1 sample, an iconic object of the Science Museum of London, has been displayed by the museum as the original mauve dye prepared by Perkin in the Easter of 1856 (figure 3.6 a).



Figure 3.6 – The historical salt mauve samples. a) The Science Museum’s “Original Sample” of Mauve, ScM1. In this work, it is shown that this sample was obtained by a second synthetic process developed by Perkin and therefore cannot be considered as the result of Perkin’s pioneer synthesis. b) The mauve salts (ScM2, ScM3 and ScM4) donated by Miss A. Perkin to the Science Museum.

However, its original date of conception was discussed by P. Morris in 2006 [142], who concluded that this sample could not be earlier than 1862. In the earlier years of production and until 1859, the mauve dye was known as Tryan Purple or Aniline Purple [116,117,120,122,125] and not as mauveine, as written in the original label of the bottle. Moreover, it has also written Sir William Perkin which refers to the knighting of Perkin in 1906 in the mauve jubilee celebrations, fifty years after its discovery. However, the main reason for this sample to be dated after 1862, is that the mauve dye in the bottle is a salt and not an amorphous body as the first batches of the commercial dye described by Perkin [120,122]. Indeed, the first crystalline samples made by Perkin are from 1862 [142]. Curiously, the CM sample which was offered by Perkin to Prof. Chandler in 1906, displays a similar label to the ScM1 sample, where it can be read: “Mauve or aniline purple, Mauveine Acetate presented by Sir William Perkin, October 1906” [142].

In these two salts samples, mauveine A is present in a higher amount, contributing with *ca.* 50% of the overall chromophores. The distribution of all mauveine compounds is very similar in both samples (table 3.4), pointing to a common source. Moreover, they are the only two samples that display such a high amount of acetate, almost 100% C (see appendix IV- Mauve data, section IV.6, p.131 for counter ion analysis).

The presence of acetate, as already mentioned by Morris [142], confirms that these samples cannot be earlier than 1862, as there is no historical evidence for the earlier synthesis of any salts as reasonably pure samples. They could have been made both in France for the jubilee celebrations 50 years after the mauve discovery [125]. If so, they were made after the Perkin's research on the mauveine structure, where in 1879 he concluded that the main chromophore of mauveine was a C₂₇ based compound. Indeed these two samples, as well as the ScM3, display a higher content of mauveine A (C₂₆) and they are the only salt samples where the ratio C₂₆/C₂₇ is higher than one. However, the ScM3 sample displays almost 70% of sulphate and only 20% of acetate ion, which could indicate that this dye was from an earlier period than the ScM1 and CM, when the sulphate salt was being replaced for the more soluble acetate salt and comparable for instance to the period of textiles group I.

As referred before, there was a time when Perkin thought that the mauveine compound had a C₂₆ based formula and in the ScM3 sample, as well as in the ScM1 and CM samples, the ratio C₂₆/C₂₇ higher than one could explain the proposal of a C₂₆H₂₃N₄⁺ formula for the principal mauveine chromophore somewhere between 1863 and 1879. Furthermore, all the textiles samples, except one, present a higher content of mauveine A and a C₂₆/C₂₇ ratio higher than one and, therefore, these salt samples were not a unique case.

3.3.2.2.2 Museum SI Manchester 1, Science Museum 4 and Science Museum 2

ScM1 and MSIM1, samples allegedly from the Perkin's factory [142], were both analysed by Meth-Cohn and Smith in 1994 [138], obtaining identical results for both samples: they identified two chromophores, namely mauveine A (C₂₆H₂₃N₄⁺) and mauveine B (C₂₇H₂₅N₄⁺), and in both samples the major compound was mauveine A.

Although both samples displayed mauveine A as the major compound, the ScM1 sample had circa 50% of mauveine A, while the MSM1 sample had only circa 40%. Moreover, the distribution of all mauveine compounds was quite different in both samples: in the MSM1, the relative percentage of C₂₇ based compounds was superior to mauveine A (C₂₆) contrarily to the ScM1 sample. Although the acetate ion was the major counter-ion found in both samples, in the MSM1 chloride with circa 7% and sulphate with circa 13% were also found. Therefore, they are probably not identical samples as reported by Meth-Cohn and Smith in 1994 [138].

The MSIM1 sample is more similar to the ScM4, as the relative distribution of the mauveine chromophores and the counter-ions composition is similar. In both samples, the

relative percentage of C_{27} based compounds is superior to mauveine A and the C_{26}/C_{27} ratio is less than one. Other sample also with a C_{26}/C_{27} ratio minor than one is the ScM2 sample. The C_{26}/C_{27} ratio minor than one in these three samples can explain why, although mauveine A is the major compound with circa 40% relative percentage of total purple compounds, Perkin concluded that the major mauveine compound was a C_{27} based compound and not a C_{26} . Indeed, the percentage of mauveine B and its C_{27} isomers (more than 45% of the total purple compounds) is superior to mauveine A (C_{26}).

3.3.2.2.3 Museum SI Manchester 2 and JCE 1926

The sample from the Schunk's collection (MSIM2), labelled as mauveine $C_{27}H_{24}N_4$, displays a very different fingerprint from the previously samples. The major purple chromophores present were the C_{24} pseudo-mauveine (49%) together with two mono-methylated derivatives (C_{25a} and C_{25b} , 41%). There was also a minor component of mauveine A (7%) and no evidence for mauveine B or C was found. The major counter-ion was acetate but sulphate (17%) and chloride (13%) in minor amounts were also found.

In order to obtain a higher amount of pseudo-mauveine and mono-methylated derivatives as in this sample, a synthesis with aniline but little toluidine was required, as demonstrated in mauve synthesis 5. As referred before, in the earlier days of mauve production, commercial aniline contaminated with toluidine was used [120]. Some years later, a process with almost pure aniline was developed in order to give blue shades to the mauve dye. Since the fingerprint of this sample (chromophores distribution) is different from the group I textile samples, which are probably the most antique mauve dyed textiles analysed, it is possible that this sample was not from the earlier years of production of the mauve dye. Moreover, the original label, probably made by Schunck or one of his assistants and the presence of acetate in such quantity, points also to a later date of conception. The formula $C_{27}H_{24}N_4$ written in the original label was proposed in 1863, while the pseudo-mauveine formula was only presented in 1879 and for that reason this sample should be dated at least after 1863 and eventually before 1879.

A bluer purple cotton textile ($L^*=31.24\pm 0.03$; $a^*=24.69\pm 0.00$ and $b^*=-30.64\pm 0.01$) from the Journal Chemical Education (JCE) from 1926 [146] was also analysed, revealing the presence of mostly pseudo-mauveine and mono-methylated derivatives. However, in this sample, the percentage of mono-methylated derivatives (80%) is much higher than that of pseudo-mauveine (less than 2%), contrarily to the MSIM2 sample C (see appendix IV-Mauve data, section IV.3, p. 125 for HPLC-DAD characterization).

For the MSIM2 sample, a different synthesis cannot be excluded since its fingerprint was never found in the Perkin's samples analysed; the yield of synthesis 5 was very low and Schunck could be doing an independent synthesis not published in the literature.

3.3.3. Accelerated aging study

A preliminary photodegradation study of mauve dyed textiles in a Solar Box Camera was carried out in order to verify if the relative percentage of mauveine chromophores could change with exposure to light. Four mauve dyed samples (two historic and two reconstructions) were submitted to polychromatic irradiation in the Solar Box Camera and the colour fading was monitored with a colorimeter and HPLC-DAD.

3.3.3.1 Mauve dyed textile reconstruction

The mauve dyed textile reconstruction after 200 h/700 Mj/m² of irradiation revealed an increase of luminosity in 67% and a decrease of the blue component in 90% and of the red component in 65%, which means that after nearly 14 years display in a museum, the mauve dye would have faded almost completely, (see appendix IV – Mauve data, section IV.7 for Solar box exposure, p.133). Significant changes in colour occurred only after 48 h (3 years in a museum display), with the initial purple colour ($L^*=38.93\pm0.80$; $a^*=32.24\pm0.20$; $b^*=-38.18\pm0.05$) changing to a *reddish* colour ($L^*=45.05\pm0.63$; $a^*=26.37\pm0.44$; $b^*=-20.47\pm0.28$) due to the intense decrease of the blue component (see figure 3.7).

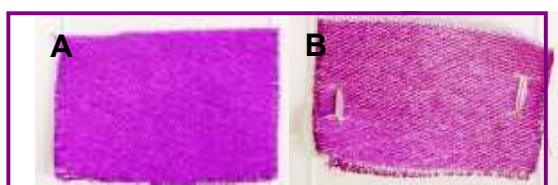


Figure 3.7 – Mauve dyed textile reconstruction before a) and after b) 48h of irradiation (14 years in a museum display) in the solar box camera.

The relative percentage of the principal nine mauveine chromophores analysed by HPLC-DAD remained almost constant during the irradiation. The decrease of mauveine B was slightly superior to mauveine A (less than 2% was observed).

3.3.3.2 Mauve dyed historic textiles

The other two historic mauve dyes (Science Museum F5 and F6) followed the same behaviour of the mauve dyed textile reconstruction, being possible to conclude that the photodegradation does not change significantly the final relative percentages of the mauveine chromophores. The Science Museum F5, less concentrated than the Science Museum F6, as expected faded more rapidly than Science Museum F6. With these preliminary photodegradation results of mauve dyed textiles it can be predicted that the mauve dye is less stable than indigo in heterogeneous media. Light indigo silk dyed textiles (and less concentrated than the mauve dyed textiles) submitted to similar aging conditions of mauve dye, revealed that after 14 years of light exposure in a museum would still have a blue colour.

3.4 Conclusions

Mauve dye can be defined as a complex mixture of methyl derivatives of 7-amino-5-phenyl-3-(phenylamino)phenazin-5-ium in which relative percentages of the purple chromophores vary according to the initial proportion of the starting materials. All the historical samples analysed contained a common fingerprint where mauveine A or mauveine B (and isomers) predominate, with the exception of the mauveine salt from the Schunk collection. New C_{27} isomers, two C_{28} and two C_{25} compounds were for the first time described and characterised in historic mauveine samples. Pseudo-mauveine, described by Perkin as a second colouring material in the mauve dye, was also identified for the first time in historical samples. Mauveines C_{25} can constitute a fingerprint marker for the original synthesis while mauveines C_{27} are markers for a later synthetic process. Depending on the number of methyl groups, the purple colour ranges from a bluish shade as the original textiles group I (mauveine A, C_{26} and pseudo mauveine, C_{25}) to a reddish shade of violet as the original textiles group II (mauveine B, C_{27}). This confirms the existence of two different types of purple as mentioned by Perkin: a bluer shade that was obtained with aniline and little toluidine (inducing a higher content of mauveine A, C_{26} , and pseudo mauveine, C_{25}) and a redder shade that was obtained with large amounts of toluidine (inducing a higher content of mauveines B, C_{27} , and C, C_{28}).

Perkin's original recipe could be identified in three textile samples and, in these cases, mauveine A and mauveines C_{25} were found to be the major chromophores. Therefore, it is expected that during the earlier years of mauve production, when the mauve dye was sold as an amorphous paste in the form of sulphate salt, the bluish shade of

purple was usually obtained. Later and when the mauve sulphate salt was replaced by the soluble mauve acetate salt more suitable for the dyer, large amounts of toluidine were used producing a reddish shade of purple. Nevertheless, it is possible that both processes were used at the same time, mainly when different shades of purple were required.

These differences in the synthesis may explain the different structures of mauveine chromophores presented by Perkin namely, the C₂₆ and C₂₇ structures. Interestingly, only after 1896 Perkin concluded that the mauveine dye was composed by three chromophores, one of them obtained from aniline, *o*-toluidine and *p*-toluidine. It is possible that during a later period a mauve dye enriched in methylated derivatives was used and more mauveines C₂₇ (and even C₂₈) with a higher content of *p*-toluidine were obtained. This was the case of some salt samples, including the one displayed by the Science Museum of London as the original mauve dye synthesized by Perkin in 1856. The counterions analysis of this sample and other salts revealed that the acetate was the major ion (except in two samples), indicating that they were most probably prepared as a textile dye and therefore they should be dated after 1862. As a result, the only mauve dye made according to the original recipe of 1856 exists in three of the textile samples, in group I. These were now shown to be the samples containing the “original mauve”.

General Conclusion

Organic dyes have been used since pre-historic times for artistic purposes, revealing a considerable resistance to light induced fading. However, their initial colour often changes under light exposure, where the initial coloured chromophores are usually transformed into colourless photoproducts. Both the initial chromophores and the photoproducts formed give a kind of fingerprint useful in the characterization and identification of the organic dyes. Moreover, if the photophysical and photochemical properties are known, it is possible to predict the lifetime of these colours and estimate the initial colour. This is also valuable information in order to prevent the colours from fading and improve their lifetime. An approach to the study of organic dyes fading is their characterization at the molecular level as performed in this work for dragon's blood, indigo and mauve dye. This molecular description revealed new insights into the identification and characterization of mauve dye and dragon's blood, whereas for indigo a better understanding of the general photodegradation mechanism was achieved. With it, the importance of these organic dyes can be reevaluated, especially in the cases of dragon's blood and mauve dye. For dragon's blood, its importance as an organic dye can be reconsidered as its identification could have been mislaid during the last decades due to the lack of characterization of the principal red chromophores. For indigo dye, the comprehension of the fading mechanisms can prompt the development of new strategies that will help improve its lifetime. As referred in the introduction, this more in-depth understanding will contribute for a better access, valorization and conservation of these organic dyes.

In order to obtain this characterization at the molecular level of dragon's blood, indigo and mauve dye, a structural analysis of their chromophores was performed and in the case of indigo its photodegradation was studied.

In Chapter 1, with the fingerprint study of the red chromophores from *Dracaena* and *Daemonorops* dragon's blood resins with HPLC-DAD and PCA, it was possible to conclude that different flavylium compounds, two of them identified for the first time (7,4'-dihydroxy-5-methoxyflavylium and 7,4'-dihydroxyflavylium), were responsible for the red colour of the resins. Moreover, 7,6-dihydroxy-5-methoxyflavylium (dracorhodin) and 7,4'-dihydroxy-5-methoxyflavylium (dracoflavylium) are the first natural flavylium compounds for which the base is the major species at biological pH (more than 50%). From circa 50 samples of *known* dragon's blood sources it was possible to select 7,6-dihydroxy-5-methoxyflavylium (dracorhodin), 7,4'-dihydroxy-5-methoxyflavylium (dracoflavylium) and 7,4'-dihydroxyflavylium as species markers for *Daemonorops* spp., *Dracaena draco* and

Dracaena cinnabari, respectively. This method was applied successfully to 37 samples of dragon's blood from the Economic Botany Collections at the Royal Botanic Gardens, Kew (EBC, K).

In Chapter 2 it was possible to conclude that the photodegradation of indigo can be promoted by the presence of electron donors such as free radicals that will easily attack the central double bond, reducing indigotin and leading to the formation of isatin. Therefore, solvents as DMF or media with free radicals can accelerate its degradation. Nevertheless, it was found by comparison with indigo carmine that indigo displays low quantum yields in the homogeneous media, as expected for a molecule which is considered very stable and presents also low photoreactivity.

In Chapter 3 it was possible to conclude that the mauve dye is a complex mixture of methyl derivatives of 7-amino-5-phenyl-3-(phenylamino)phenazin-5-ium, contrarily to what is reported in the literature. By investigating original mauve salt samples and fabric tests dyed with mauve from different sources, it was possible to understand the evolution of mauve as a commercial dye. With the exception of the mauveine salt from the Schunk collection, all samples contained a common fingerprint where mauveine A or mauveine B (and isomers) predominate. Besides these derivatives of pseudo-mauveine with two and three methyl groups, several other methylated derivatives were found (mono, tetra and more) for the first time. Amongst these, mauveine B2 (C₂₇) and mauveines C₂₅ are important markers in the fingerprint of mauveine salts and textiles, respectively. Moreover, it was possible to conclude that the mauve dye made according to the original recipe of 1856 exists only in three of the textile samples analysed.

References and Notes

- [1] Travis, A. *The Rainbow Makers: The Origins of the Synthetic Dyestuffs Industry in Western Europe*. Lehigh University Press: London, 1993.
- [2] Cardon, D. *Natural Dyes- Sources, Tradition, Technology and Science*. Archetype Publications: London, 2007.
- [3] Ferreira, E.; Hulme, A.; McNab, H. *Chemical Society Reviews* **2004**, *33*, 329.
- [4] Verhecken, A.; Wouters, J. *Bulletin Institut Royal du Patrimoine Artistique XXII*. **1988-89**, 207.
- [5] Wouters, J.; Verhecken, A. *Annales de la Société Entomologique de France* **1989**, *25-4*, 393.
- [6] Wouters, J.; Verhecken, A. *Studies in Conservation* **1989**, *34*, 189.
- [7] Zhang, X.; Laursen, R. A. *Analytical Chemistry* **2005**, *77-7*, 2022.
- [8] Constable, O. R. *Trade and Traders in Muslim Spain*. Cambridge University Press: Cambridge, 2003.
- [9] Valeur, B. *Molecular Fluorescence – Principles and applications*. Wiley-VCH: Weinheim, 2002.
- [10] Wells, C. *Introduction to Molecular Photochemistry*. Chapman and Hall: London, 1972.
- [11] Montalti, M.; Credi, A.; Prodi, L.; Gandolfi, M. *Handbook of Photochemistry*. 3rd edition. CRC Press: Boca Raton, USA, 2006.
- [12] Turro, N. J.; Valley, M. *Modern Molecular Photochemistry*. University Science Books: US, 1991.
- [13] Resins can be defined as a lipid-soluble mixture of volatile and non-volatile terpenoid and/or phenolic secondary compounds that are usually secreted in specialized structures located either internally or on the surface of the plant. These compounds apparently play no role in the primary or fundamental physiology of the plant. Its function is more related with protection against injuries, desiccation, high temperatures and ultraviolet radiation, amongst others. In: Langenheim, J. *Plant Resins – Chemistry Evolution Ecology and Ethnobotany*. Timber Press: Cambridge, 2003.
- [14] Pearson, J. *The Horticulturist* **2002**, *10*.
- [15] Pearson, J.; Prendergast, H.D.V. *Economic Botany* **2001**, *55*, 474.
- [16] Pearson, J. *The History, Botany and Analysis of the Dragons Blood Collection at the Royal Botanic Gardens*, Kew Diploma Dissertation 36. Kew Garden: Kew, 2001.
- [17] Mills, J.; White, R. *Studies in Conservation* **1977**, *22*, 12.
- [18] González, G. A. L. *Los Árboles y Arbustos de la Península Ibérica e Islas Baleares*. Ediciones Mundi-Prensa: Madrid, 2001.

- [19] Hernández, J. C.; León, F.; Quintana, J.; Estévez, F.; Bermejo, J. *Bioorganic and Medicinal Chemistry* **2004**, *12*, 4423.
- [20] González, A. G.; Hernández, J. C.; León, F.; Padrón, J. I.; Estévez, F.; Quintana; Bermejo, J. *Journal of Natural Products* **2003**, *66*, 793.
- [21] Mimaki, Y.; Kuroda, M.; Ide, A.; Kameyama, A.; Yokosuka, A.; Sashida, Y. *Phytochemistry* **1999**, *50*, 805.
- [22] Machala, M.; Kubínova, R.; Horavová, P.; Suchy, V. *Phytotherapy Research* **2001**, *15*, 114.
- [23] Shen, C.; Tsai, S.; Wei, S.; Wang, S.; Shieh, V.; Chen, C. *Journal of Natural Products* **2007**, *21*, 377.
- [24] Gong, W. J.; Cao, Y. H.; Wang, Y. *Chromatographia* **2007**, *66*, 767.
- [25] Zhu, Y.; Zhang, P.; Yu, H.; Li, J.; Wang, M.; Zhao, M. *Journal of Natural Products* **2007**, *70*, 1570.
- [26] Zheng, Q.-A.; Li, H.-Z.; Zhang, Y.-J.; Yang, C.-R. *Helvetica Chimica Acta* **2004**, *87*, 1167.
- [27] Salatino, A.; Salatino, M. L. F.; Negri, G. *Journal of the Brazilian Chemical Society* **2007**, *18-1*, 11.
- [28] Jones, K. *The Journal of Alternative and Complementary Medicine* **2003**, *9-6*, 877.
- [29] Cennini, C. *Il Libro dell'Arte*. (Ed.: Brunello, F.) Neri Pozza Editore: Vicenza, 1982.
- [30] Edwards, H. G. M.; Farwell, D. W.; Quye, A. *Journal of Raman Spectroscopy* **1997**, *28*, 243.
- [31] Edwards, H. G. M.; Oliveira, L. F. C.; Quye, A. *Spectrochimica Acta Part A* **2001**, *57*, 2831.
- [32] Edwards, H. G. M.; Oliveira, L. F. C.; Prendergast, H. D. V. *Analyst* **2004**, *129*, 134.
- [33] Govaerts, R.; Dransfield, J. *World Checklist of Palms*. Royal Botanic Gardens: Kew, 2005.
- [34] Machala, G.; Mbugua, P. K. *Flora of Tropical East Africa. Dracaenaceae*. Royal Botanic Gardens: Kew, 2007.
- [35] Bos, J. J. *Agricultural University Wageningen Papers* **1984**, *84*, 1.
- [36] Rustiami, H. *Phenetic Study on Dragon's blood Species of *Daemonorops* Section *Piptospatha* (family *Arecaceae*)*, Thesis (M.Sc.). Royal Botanic Gardens: Kew, 1999.
- [37] Rustiami, H.; Setyowati, F. M.; Kartawinata, K. *Journal of Tropical Ethnobiology* **2004**, *1-2*, 65.
- [38] Adolt, R., Pavlis, J. *Trees* **2004**, *18*, 43.

- [39] Marrero, A.; Almeida, R. S.; González-Martin, M. *Botanical Journal of the Linnean Society* **1998**, *128*, 291.
- [40] Thulin, M. *Flora of Somalia*, 4. Royal Botanic Gardens: Kew, 1995.
- [41] Benabid, A.; Cuzin, F. *Comptes Rendus de l'Académie des Sciences. Sciences de la Vie* **1997**, *320*, 267.
- [42] In <http://www.worldtwitch.com>, April 2008.
- [43] In <http://www.huntington.org/BotanicalDiv/ISI2004/isi/2004-20.html>, April 2008.
- [44] In <http://www.jpib-imagine.com/djibflor/dracaen.html>, April 2008.
- [45] Attorre, F.; Francesconi, F.; Taleb, N.; Scholte, P.; Saed, A.; Alfo, M.; Bruno, F. *Biological Conservation* **2007**, *138*, 430.
- [46] In http://en.wikipedia.org/wiki/Dracaena_%28plant%29, April 2008.
- [47] Rustiami, H. *Gardens' Bulletin, Singapore* **2002**, *54*, 199.
- [48] In <http://content.answers.com/main/content/wp/en-commons/thumb/7/71/240px-Koeh-023.jpg>, April 2008.
- [49] In http://www.ics.trieste.it/MedicinalPlant/_MedicinalPlant.aspx?id=60, April 2008.
- [50] Dobbie, J. J.; Henderson, G. G. *American Journal of Pharmacy* **1884**, 56-6, 4.
- [51] Zheng, Q.; Yang, C. *Journal of Asian Products Research* **2003**, 5-4, 291.
- [52] In <http://striweb.si.edu/ctfs/webatlas/plant.photos/pterof.arq.jpg>, April 2008.
- [53] In <http://www.infojardin.com/foro/showthread.php?t=4197>, April 2008.
- [54] Bensky, D.; Clavey, S.; Stöger, E. *Chinese Herbal Medicine Materia Medica*. 3rd edition. Eastland Press: US, 2004.
- [55] Hernández, J. C.; León, F.; Estévez, F.; Quintana, J.; Bermejo, J. *Journal of Chemistry and Biodiversity* **2006**, *3*, 62.
- [56] Himmelreich, U; Masaoud, M.; Adam, G.; Ripperger, H. *Phytochemistry* **1995**, 39-4. 949
- [57] Masaoud, M.; Ripperger, H.; Porzel, A.; Adam, G. *Phytochemistry* **1995**, 38-3. 745.
- [58] Masaoud, M.; Ripperger, H.; Himmelreich, U.; Adam, G. *Phytochemistry* **1995**, 38-3. 751.
- [59] Masaoud, M.; Schmidt, J.; Adam, G. *Phytochemistry* **1995**, 38-3, 795.
- [60] Cardillo, G.; Merlini, L.; Nasini, G. *Journal of the Chemical Society* **1971**, 3967.
- [61] Arnone, A.; Nasinin, G.; Vajna de Pava, O. *Journal of Natural Products* **1997**, *60*, 971.
- [62] Brockmann, H.; Haase, R. *Berichte der Deutschen Chemischen Gesellschaft, B* **1936**, *69*, 1950.
- [63] Brockmann, H.; Haase, R. *Berichte der Deutschen Chemischen Gesellschaft, B* **1937**, *70*, 1733.

- [64] Brockmann, H.; Junge, H. *Berichte der Deutschen Chemischen Gesellschaft, B* **1943**, 76, 751.
- [65] Robertson, A.; Whalley, W. B. *Journal of the Chemical Society* **1950**, 1882.
- [66] Agbakwuru, E.; Whalley, W. B. *Journal of the Chemical Society, Perkin Transactions 1* **1976**, 1392.
- [67] Olaniyi, A. A.; Powell, J. W.; Whalley, W. B. *Journal of the Chemical Society, Perkin Transactions 1* **1973**, 179.
- [68] Robertson, A.; Whalley, W. B. *Journal of the Chemical Society* **1950**, 3117
- [69] Melo, M. J.; Sousa, M. M.; Parola, A. J.; Seixas de Melo, J. S.; Catarino, F.; Marçalo, J.; Pina, F. *Chemistry – A European Journal* **2007**, 13, 1417.
- [70] Sousa, M. M.; Melo, M. J.; Parola, A. J.; Seixas de Melo, J. S.; Catarino, F.; Pina, F.; Cook, F. E. M.; Simmonds, M. S. J.; Lopes, J. A. *Journal of Chromatography A* **2008**, submitted.
- [71] Büllow, C.; Wagner, H. *Chemische Berichte* **1901**, 34, 1782.
- [72] a) Willstätter, R.; Everest, A. E. *Justus Liebigs Annalen der Chemie* **1913**, 401, 189. b) Willstätter, R.; Mallinson, H. *Justus Liebigs Annalen der Chemie* **1915**, 408, 15 c) Willstätter, R.; Mallinson, H. *Justus Liebigs Annalen der Chemie* **1915**, 408, 147.
- [73] a) Perkin, A. G.; Robinson, R. *Journal of the Chemical Society* **1927**, 3015. b) Pratt, D.; Robinson, R.; Robertson, A. *Journal of the Chemical Society* **1927**, 1975.
- [74] Haslam, E. *Practical Polyphenolics, from Structure to Molecular Recognition and Physiological Action*. Cambridge University Press: Cambridge, 1998.
- [75] Brouillard, J. R.; Dubois, J. E. *Journal of the American Chemical Society* **1977**, 99, 1359.
- [76] McClelland, R. A.; Gedge, S. *Journal of the American Chemical Society* **1980**, 102, 5838.
- [77] a) Pina, F. *Journal of the Chemical Society, Faraday Transactions* **1998**, 94, 2109. b) Pina, F.; Maestri, M.; Balzani in *Handbook of Photochemistry and Photobiology*, vol. 3: *Supramolecular Photochemistry*. (Ed.) Nalwa, H. S. American Scientific Publishers: ?, England, 2003. c) Pina, F.; Melo, M. J.; Parola, A. J.; Maestri, M.; Balzani, V. *Chemistry – A European Journal* **1998**, 4, 2001. d) Pina, F.; Lima, J. C.; Parola, A. J.; Afonso, C. A. *Angewandte Chemie-International Edition* **2004**, 116, 1551. e) Pina, F.; Maestri, M.; Balzani, V. *Chemical Communications* **1999**, 107.
- [78] Anthocyanidins are the aglicones of antocyanins, and this term was proposed by R. Willstätter in 1913 [72a]. The structures identified by Willstätter were the anthocyanidin chromophores. Only with the work of Robinson and others, the sugar substitution was

characterized. It is important to retain that anthocyanidins do not exist in Nature, namely with a free OH in the 3 position the forms in solution will not be stable.

[79] a) Zorn, B.; García-Piñeres, A. J.; Castro, V.; Murillo, R.; Mora, V.; Merfort, I. *Phytochemistry* **2001**, *56*, 831. b) Devia, B. ; Llabres, G.; Wouters, J.; Dupont, V.; Escribano-Bailon, M. T.; Pascual-Teresa, S.; Angenot, L.; Tits, M. *Phytochemical Analysis* **2002**, *13*, 114.

[80] Thulin, M. *Flora of Somalia*, 4. Royal Botanic Gardens: Kew, 1995.

[81] Vaughan, J. *The Pharmaceutical Journal* **1852-1853**, *12*, 385.

[82] Trimble, H. *American Journal of Pharmacy* **1895**, 516.

[83] Pina, F.; Benedito, L.; Melo, M. J.; Parola, A. J.; Lima, J. C.; Maçanita, A. *Anales de Química International Edition* **1997**, *93*, 111.

[84] McClelland, R. A.; Gedge, S. *Journal of the American Chemical Society* **1980**, *102*, 5838.

[85] a) Goto, T.; Kondo, T. *Angewandte Chemie-International Edition* **1991**, *30*, 17. b) Kondo, T.; Yoshida, K.; Nakagawa, A.; Kawai, T.; Tamura, H.; Goto, T. *Nature* **1992**, 358, 515. c) Kondo, T.; Ueda, M.; Yoshida, K.; Titani, K.; Isobe, M.; Goto, T. *Journal of the American Chemical Society* **1994**, *116*, 7457. d) Kondo, T.; Oyama, K.-I.; Yoshida, K. *Angewandte Chemie-International Edition* **2001**, *40*, 894.

[86] For luteolidin the amount of the red quinoid base found in the equilibrium was circa 30%. In Melo, M. J.; Moura, S.; Roque, A.; Maestri, M.; Pina, F. *Journal of Photochemistry and Photobiology A: Chemistry* **2000**, *135*, 33.

[87] Clark, R. J. H.; Cooksey, C. J.; Daniels, M. A. M.; Withnall, R. *Endeavour* **1993**, *17*, 191.

[88] Balfour-Paul, J. *Indigo*. British Museum Press: London, 2000.

[89] Padden, A. N.; Dillon, V. M.; John, P.; Edmonds, J.; Collins, M. D.; Alvarez, N. *Nature* **1998**, *396*, 225.

[90] Fitzhugh, E. (Ed.); *Artists Pigments – A Handbook of Their History and Characteristics*. vol. 3. Oxford University Press: Oxford, 1997.

[91] Wouters, J.; Verhecken, A. *Journal of the Society of Dyers and Colourists* **1991**, *7*, 266.

[92] Orska-Gawrys, J.; Surowiec, I.; Kehl, J.; Rejniak, H.; Urbaniak-Walczak, K.; Trojanowicz, M. *Journal of Chromatography A* **2003**, *989*, 239.

[93] Surowiec, I.; Quye, A.; Trojanowicz, M. *Journal of Chromatography A* **2006**, *112*, 209.

[94] Zhang, X. *Analysis of Natural Yellow dyes using HPLC with Diode Array and Mass Spectrometric Detection*. PhD Thesis. Boston University: Boston, 2007.

- [95] Maugard, T.; Enaud, E.; Choisy, P.; Legoy, M. *Phytochemistry* **2001**, *58*, 897.
- [96] Kuramoto, N.; Kitao, T. *Journal of the Society of Dyers and Colourists* **1979**, *95*, 257.
- [97] Kuramoto, N.; Kitao, T. *Journal of the Society of Dyers and Colourists* **1982**, *98*, 334.
- [98] Novotná, P.; Boon, J. J.; vand der Horst, J.; Pacáková, V. *Coloration Technology* **2003**, *119*, 121.
- [99] Galindo, C.; Jacques, P.; Kalt, A. *Journal of Photochemistry and Photobiology A: Chemistry* **2001**, *141*, 47.
- [100] Wentworth Jr., P; McDuhn, J. E.; Wentworth, A.; Takeuchi, A.; Nieva, J.; Jones, T.; Bautista, T.; Ruedi, J.; Gutierrez, A.; Janda, K.; Babior, B.; Eschenmoser, A.; Lerner, R. *Science* **2002**, *298*, 2195.
- [101] Kettle, A. J.; Clark, B. M.; Winterbourn, C. C. *Journal of Biological Chemistry* **2004**, *279*, 18521.
- [102] Dalmázio, I.; Urzedo, A.; Alves, T.; Catharino, R.; Eberlin, M.; Nascentes, C.; Augusti, R. *Journal of Mass Spectrometry* **2007**, *42*, 1273.
- [103] N. Gandra; Frank, A. T.; Le Gendre, O.; Sawwan, N.; Aebisher, V.; Liebman, J. F.; Houk, K. N.; Greer, A.; Gao, R. *Tetrahedron* **2006**, *62*, 10771.
- [104] Melo, J. S.; Moura, A. P.; Melo, M. J. *Journal of Physical Chemistry A* **2004**, *108*, 6975.
- [105] Melo, J. S.; Rondão, R.; Burrows, H. D.; Melo, M. J.; Navaratnam, S.; Edge, R., Voss, G. *A European Journal of Chemical Physics and Physical Chemistry* **2006**, *7*, 2303.
- [106] Melo, J. S; Rondão, R.; Burrows, H. D.; Melo, M. J.; Navaratnam, S.; Edge, R. Voss, G. *Journal of Physical Chemistry A* **2006**, *110*, 13653.
- [107] Bond, A. M.; Marken, F.; Hill, E.; Compton, R. G.; Hügel, H. *Journal of the Chemical Society, Perkin Transactions 2* **1997**, 1735.
- [108] Roessler, A.; Crttenand, D.; Dossenbach, O.; Marte, W.; Rys, P. *Electrochimica Acta* **2002**, *47*, 1989.
- [109] Feller, R. *Accelerated aging – Photochemical and Thermal aspects*. The Getty Conservation Institute: US, 1994.
- [110] Pina, F.; Hatton, T. A. *Langmuir* **2008**, *24*, 2356.
- [111] Kobzar, K.; Kessler, H.; Luy, B. *Angewandte Chemie International Edition* **2005**, *44*, 3145.
- [112] Schloddera, E.; Shubinb, V.; El-Mohsnawyc, E.; Roegnerc, M. *Biochimica et Biophysica Acta – Bioenergetics* **2007**, *1767-6*, 732.
- [113] Wach, R.; Mitomo, H.; Nagasawa, N.; Yoshii, F. *Radiation Physics and Chemistry* **2003**, *68*, 771.

- [114] The L^* , a^* and b^* are coordinates used in the system CIELAB to characterize a colour. L^* represents the difference between light ($L^*=100$) and dark ($L^*=0$), a^* represents the difference between green ($-a^*$) and red ($+a^*$), and b^* represents the difference between yellow ($+b^*$) and blue ($-b^*$) in Berns, R. *Billmeyer and Saltzman's Principles of Color Technology*. 3rd edition. John Wiley & Sons: US, 2000.
- [115] Wouters, J.; Rosario-Chirinos, N. *Journal of the American Institute for Conservation* **1992**, 31-2, 237.
- [116] Travis, A. S. *History and Technology* **2006**, 22, 131.
- [117] Holme, I. *Coloration Technology* **2006**, 122, 235.
- [118] Read, J. *The Life and Work of Perkin* in Perkin Centenary London -100 years of Synthetic dyestuffs. Pergamon Press Ltd.: Great Britain, 1958.
- [119] Perkin, W. H. *Journal of the Chemical Society* **1862**, 14, 230.
- [120] Perkin, W. H. *Journal of the Chemical Society Transactions* **1896**, 596.
- [121] Meldola, R. *Proceedings of the Royal Society of London. Series A, Containing Papers of a Mathematical and Physical Character* **1908**, 80-542, 38.
- [122] Rowe, F. M. *The Journal of the Society of Dyers and Colourists* **1938**, 54-12, 551.
- [123] Perkin, W. H. *Science* **1906**, 24, 488.
- [124] Garfield, S. *How one Man Invented a Colour that Changed the World?* Faber and Faber Limited: London, 2000.
- [125] Travis, A. S.; Meth-Cohn, O. *Chemistry in Britain* **1995**, 547.
- [126] Perkin, W. H. *BP1984*, 1863.
- [127] Travis, A. S. *Chemistry and Industry* **1988**, 508.
- [128] Perkin would not license his process to other British chemical manufacturers but Simpson, Maule & Nicholson started to produce the intermediates nitrobenzene and aniline, making great improvement in the scale up and as a result aniline was exported for all France in 1859.
- [129] Perkin, W. H. *Journal of the Chemical Society Transactions* **1879**, 717.
- [130] Travis, A. S. *Ambix* **1991**, 38-3, 113.
- [131] Travis, A. S. *Die Allianz Von Wissenschaft under Industrie: August Wilhelm Hofmann (1818-1892): Zeit, Werk Wirkung*. (Eds.) Christopher Meinel and Harmul Scholz. Weinheim VCH: Weinheim 1992.
- [132] Travis, A. *The British Journal for the History of Science* **1992**, 25, 27.
- [133] Travis, A. *Endeavour* **1992**, 16, 59.
- [134] Perkin, W. H. *Proceedings of the Royal Society of London* **1862-3**, 13, 170.
- [135] Perkin, W. H. *Proceedings of the Royal Society* **1864**, 713.

- [136] Fischer, O.; Hepp, E. *Chemische Berichte* **1893**, 26, 1194.
- [137] Nietzki, R. *Chemische Berichte* **1896**, 29, 1442.
- [138] Meth-Cohn, O.; Smith, M. *Journal of the Chemical Society-Perkin Transactions 1* **1994**, 5.
- [139] Melo, J. S.; Takato, S.; Sousa, M.; Melo, M. J.; Parola, A. J. *Chemical Communications* **2007**, 2624.
- [140] Scaccia, R.; Coughlin, D.; Ball, D. *Journal of Chemical Education* **1998**, 75-6, 769.
- [141] Bommel, M. R.; Berghe, I. V.; Wallert, A. M.; Boitelle, V.; Wouters, J. *Journal of Chromatography A* **2007**, 1157, 260.
- [142] Morris, P. J. T. *History and Technology* **2006**, 22, 119.
- [143] Sousa, M.; Melo, M. J.; Aguiar-Ricardo, A.; Cruz, P. *The 14th Triennial Meeting the Hague Preprints, ICOM Committee for Conservation*, **2005**, 2, 944.
- [144] Tímár-Balázsy, Á.; Eastop, D. *Chemical Principles of Textiles Conservation*. Elsevier Butterworth Heinemann: Oxford, 1998.
- [145] From the 5 synthesis performed, the most similar with this one would be synthesis 1 and 2, where in both cases, a mauve dye enriched in methylated derivatives was expected.
- [146] Rose, R. *Journal of Chemical Education* **1926**, 3-9, 973.

Appendix I: Experimental section

I.1 General

All reagents and solvents used were of analytical grade.

I.2 Instrumentation

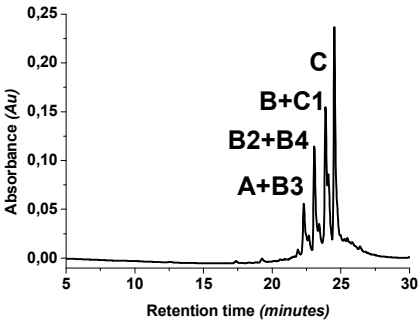
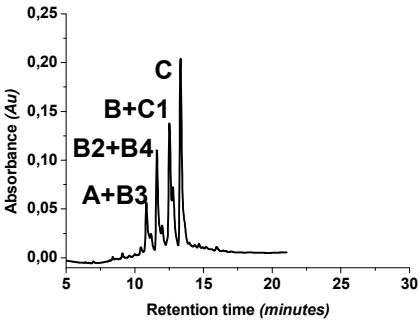
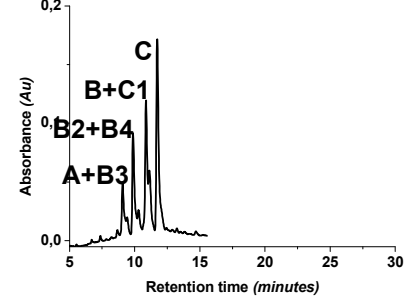
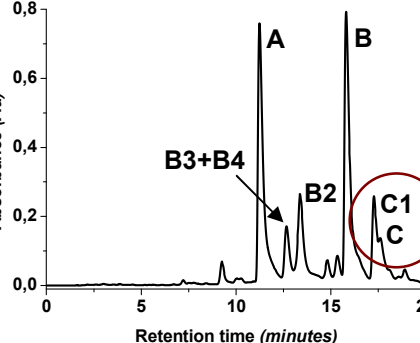
I.2.1 HPLC-DAD

The dye analyses were performed in an analytical ThermoFinnigan Surveyor HPLC-DAD system with a PDA 5, using a RP-18 analytic column (250x4.6 Nucleosil 300-5 C18). The purification of the dyes chromophores in large amounts was performed in a semi-preparative 6000 Merck Hitachi HPLC-DAD system with a L-6200 A Intelligent Pump, a L-5025 Column Thermostat and a L-4500 DAD. The separations were carried out using a RP-18 semi-preparative column (250x10 Nucleosil 300-7 C18). In both HPLC systems the column was kept at controlled temperature (35 °C). In the analytical system the samples were injected onto the column via a Rheodyne injector with a 25 μ L *loop* and in the semi-preparative system a 200 μ L *loop* was used. The system was re-equilibrated at the starting eluent composition for 3-5 min before next injection. Several elution gradients were used for the dye analyses and compounds purification:

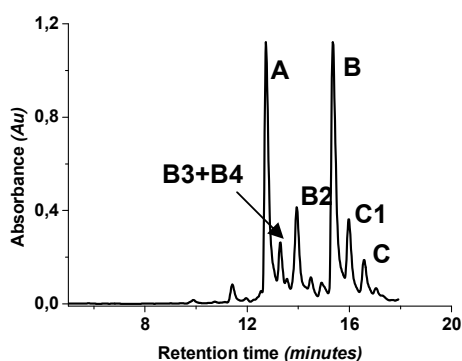
1) General dye analysis with analytical HPLC-DAD: A solvent gradient of **A**-pure methanol and **B**-0.15% aqueous perchloric acid 70% (v/v) was used at a flow rate of 1.7 ml/min; 0-2 min 7A:93B isocratic, 8 min 15A:85B linear, 25 min 75A:25B linear, 27 min 80A:20B linear, 29-40 min 100A isocratic [1].

2) Mauve dye analysis with analytical HPLC-DAD: A solvent gradient with **A** - Methanol, **B** -CH₃COONH₄ 0.05 M, **C** - CH₃CN with a flow rate of 1.7 mL/min for the chromophores separation was developed [2] (see table I.1): 0-2 min 20A: 50B: 30C isocratic; 10 min 25A: 35B: 40C linear; 20 min 40A: 20B: 40C linear; 25 min 50A:50C linear; 25-30 min 50A:50C isocratic.

Table I.1 – Elution gradients used for mauve dye analysis.

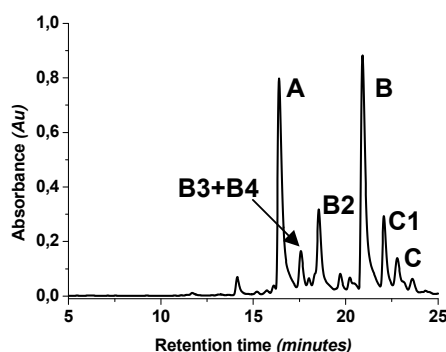
Elution gradient	Chromatogram	Observations
<p>A-pure methanol and B-0.15% aqueous perchloric acid 70% (v/v) with a flow rate of 1.7 ml/min; 0-2 min 7A:93B isocratic, 8 min 15A:85B linear, 25 min 75A:25B linear, 27 min 80A:20B linear, 29-40 min 100A isocratic.</p>	 <p>A chromatogram plot with 'Absorbance (Au)' on the y-axis (0.00 to 0.25) and 'Retention time (minutes)' on the x-axis (5 to 30). Four peaks are labeled: 'A+B3' at ~12 min, 'B+C1' at ~14 min, 'B2+B4' at ~16 min, and 'C' at ~24 min.</p>	<p>Current solvent gradient used for all dye analysis in the DCR laboratory. The mauveine chromophores of a synthesized mauve dye sample were eluted very late and their separation was poorly resolved.</p>
<p>A-pure methanol and B-0.15% aqueous perchloric acid 70% (v/v) with a flow rate of 1.7 ml/min; 0-2 min 7A:93B isocratic, 5 min 20A:80B linear, 23 min 75A:25B linear, 27 min 75A:25B linear, 29-40 min 100A isocratic.</p>	 <p>A chromatogram plot with 'Absorbance (Au)' on the y-axis (0.00 to 0.25) and 'Retention time (minutes)' on the x-axis (5 to 30). Four peaks are labeled: 'A+B3' at ~12 min, 'B+C1' at ~14 min, 'B2+B4' at ~16 min, and 'C' at ~24 min.</p>	<p>Optimization of the previously elution gradient. The mauveine chromophores were eluted earlier than the previously test, however the separation of the mauveine chromophores was not improved.</p>
<p>A-pure methanol and B-0.15% aqueous perchloric acid 70% (v/v) with a flow rate of 1.7 ml/min; 0-2 min 7A:93B isocratic, 5 min 30A:70B linear, 23 min 95A:5B linear, 27 min 95A: 5B linear, 29-40 min 100A isocratic.</p>	 <p>A chromatogram plot with 'Absorbance (Au)' on the y-axis (0.0 to 0.2) and 'Retention time (minutes)' on the x-axis (5 to 30). Four peaks are labeled: 'A+B3' at ~12 min, 'B+C1' at ~14 min, 'B2+B4' at ~16 min, and 'C' at ~24 min.</p>	<p>Optimization of the previously elution gradient. The mauveine chromophores were eluted earlier than the previously test, however the separation of the mauveine chromophores was not improved.</p>
<p>A - CH₃COONH₄ 0.05 M , B - CH₃CN with a flow rate of 1.7 mL/min: 0-10 min 35A: 65B isocratic; 20-25 min 25A: 75B isocratic; 30 min 20A:80B linear.</p>	 <p>A chromatogram plot with 'Absorbance (Au)' on the y-axis (0.0 to 0.8) and 'Retention time (minutes)' on the x-axis (0 to 20). Six peaks are labeled: 'B3+B4' at ~12 min, 'A' at ~13 min, 'B2' at ~14 min, 'B' at ~16 min, 'C1' at ~18 min, and 'C' at ~19 min. The 'C1' and 'C' peaks are circled in red.</p>	<p>Elution gradient reported in literature [2] tested in SCM1 mauve salt. The introduction of the aqueous ammonium acetate solvent allowed a better separation of the mauveine chromophores; however the mauveines C1 and C were not separated.</p>

A - Methanol, **B** -CH₃COONH₄ 0.05 M , **C** - CH₃CN with a flow rate of 1.7 mL/min: **0-2 min 20A: 50B: 30C isocratic; 10 min 50A: 20B: 30C linear; 20 min 40A: 10B: 40C linear; 25 min 50A:50C linear; 25-30 min 50A:50C isocratic.**



Optimization of the previously elution gradient. The introduction of acetonitrile allowed the separation of mauveines C1 and C, however the separation of mauveines B2 and B3 and B4 was worst than the previous test

A - Methanol, **B** -CH₃COONH₄ 0.05 M , **C** - CH₃CN with a flow rate of 1.7 mL/min: **0-2 min 20A: 50B: 30C isocratic; 10 min 25A: 35B: 40C linear; 20 min 40A: 20B: 40C linear; 25 min 50A:50C linear; 25-30 min 50A:50C isocratic.**



Optimization of the previously elution gradient. A better separation of all mauveine chromophores was achieved.

3) Compounds purification with semi-preparative HPLC-DAD: A solvent gradient of A- pure methanol and B-10% aqueous formic acid 99,9% (v/v) with a flow rate of 9 ml/min was developed: 0-2 min 15A:85B isocratic, 3 min 50A:50B linear, 5 min 70A:30B linear, 7 min 90A:10B linear, 29-40 min 100A isocratic. This elution gradient was obtained following a similar procedure reported for mauve dye analysis.

1.2.2 LC-MS

The LC-MS analyses were performed on a HPLC-MS instrument with a ProStar 410 autosampler, two 212-LC chromatography pumps, a ProStar 335 diode array detector and a 500-MS ion trap mass spectrometer with an ES ion source (Varian, Inc.). The LC separations were carried out using a Polaris C18-A column, with 5 μm of particle size (150X2 mm). For the mauve dye analyses the mobile phase was composed by MeOH (A) and 0.08% (v/v) formic acid (aq.) (B). The following gradient, adapted from the method 2 described above, was used at a flow rate of 0.03 mL/min: 0-2 min 50A: 50B isocratic; 10 min 60A: 40B: linear; 20 min 75A: 25B linear; 30-35 100A isocratic.

The mass spectra were obtained in the 500-MS ion trap mass spectrometer with an ES ion source and acquired in positive ion mode. The operating parameters were optimized for

the sample Science Museum F1: the spray needle voltage was set at positive ion mode 5.7 kV, nitrogen was used both as nebulising and as a drying gas (35 psi and 15 psi, respectively), drying gas temperature 350 °C ; capillary voltage 157 V and RF loading of 94 V.

I.2.3 MS

Field-desorption mass spectra (FD/MS) were run on a Micromass GC-TOF spectrometer in positive ion mode.

High-resolution mass spectra (HRMS) were obtained by laser desorption/ionization (LDI) with a Finnigan FT/MS 2001-DT Fourier transform ion cyclotron resonance mass spectrometer (FTICRMS), equipped with a 3 Tesla superconducting magnet and coupled to a Spectra-Physics Quanta-Ray GCR-11 Nd:YAG laser operated at the fundamental wavelength (1064 nm).

I.2.4 NMR spectrometry

Compounds isolated from HPLC were lyophilized and further dried under vacuum at room temperature. All compounds were dissolved in CD₃OD, and the residual solvent peak was used as a reference to calibrate spectra. The NMR spectra in CD₃OD at 298.0 K were obtained either on a Bruker AMX400 operating at 400.13 MHz (¹H) and 100 MHz (¹³C) or on a Bruker Avance 600 operating at 600.13 Hz (¹H) and 150.91 Hz (¹³C). For each compound, ¹H, ¹³C, COSY, HSQC or HMQC, HMBC and eventually NOESY NMR spectra were run. Proton assignments were done on the basis of chemical shifts and COSY spectra; to confirm these assignments, NOESY spectra were run on one of the samples, fully confirming the assignments. Carbon assignments were made on the basis of chemical shifts, HSQC or HMQC, and HMBC NMR spectra.

I.2.5 IC-AEC

The counter-ions of mauve dye crystalline samples were identified in a 3000 Dionex ion chromatography system with continuously regenerated trap column for reagent free ion chromatography (ICS 3000 CR-TC RFIC), a ICS-3000 Conductivity Detector, a ICS-3000 Pump and a Ion Pack® CG 16 column with 5x50 mm guard column, using 37.5 mM KOH as an eluent suppressor.

I.2.6 ICP-AES

The mordants analyses for mauve dye were performed in a Jobin-Yvon Ultima ICP-AES (Inductively Coupled Plasma- Atomic Emission Spectroscopy), with a RF 40, 68 MHz generator and a Czerny-Turner 1.00 m monochromator. The conditions used were: power 1000 kW; 12 L/min of argon flow, Meinhard nebuliser with 3 bar pressure; pump velocity of 20 rpm; 10ml/min of sample flow debit with three analyses for each sample. Before the ICP-AES injection, calibration curves were constructed with ICP standards and the correlation coefficients for the calibration curves were 0.99 for the range studied (0,2-1 ppm for iron and copper; 0.01-0.35 ppm for aluminium).

I.2.7 Optical Microscopy

The optical analysis were carried out in an optical Zeiss Axioplan Z Imaging microscope with a Nikon digital camera DMX 1200F and in a Leica MZ16 stereomicroscope with a Leica digital camera (Digilux 1) with fiberoptic light Leica system (Leica KI 1500 LCD).

I.2.8 Monochromatic irradiation

The monochromatic irradiations were performed in a xenon arc lamp with a Jobin Yvon Divisional Instruments SA monochromator.

I.2.9 Solar Box Camera

The polychromatic irradiation was performed in a 3000e irradiation camera, with a xenon lamp ($\lambda > 300\text{nm}$), intensity of 800W/m² and 70°C BST.

I.2.10 UV/Vis spectroscopy

UV/Vis absorption spectra were recorded on a Cary 100 Bio UV-Vis Varian spectrophotometer at room temperature.

I.2.11 Colorimeter

Colour determinations were made using a *Datacolor International* colorimeter. The optical system of the measuring head uses diffuse illumination from a pulsed Xenon lamp over a 8 mm-diameter measuring area, with a 10° viewing angle geometry. The reference source was D65 and the calibration was performed with a white bright tile standard plate and with a black trap standard.






I.3 Methods

I.3.1 Dragon's Blood

I.3.1.1 Resin samples

Eighty-three samples were analysed by HPLC-DAD; 37 from EBC, K (for more details see chapter 1, section 1.3) were from items labelled: *Daemonorops draco* (5), *Daemonorops propinqua* (a synonym of *Daemonorops draco*) (3), *Daemonorops sp.* (1), *Dracaena cinnabari* (15), *Dracaena draco* (7), *Dracaena schizantha* (a synonym of *Dracaena ombet*) (1), and *Dracaena sp.* (5). Other samples of *Dracaena draco* were from the Botanic garden of Ajuda (2); Botanic garden of Lisbon (2); Botanic garden of Funchal, Madeira (9); Natural Reserve of Dragon's tree – Neves, Madeira (NRDT), (2); from different places/gardens of Lisbon and Madeira (17) and from Cape Verde (1). 9 *Dracaena cinnabari* samples from Socotra were made available by J. Pavlis [3]. Furthermore, 4 samples were purchased from Kremer (2 *Dracaena cinnabari* samples), Zecchi (1 *Daemonorops draco* sample: Sumatra and Borneo) and from Healing Waters & Sacred Spaces (1 *Daemonorops draco* sample: Indonesia). From the 83 samples described above, only 46 samples were used to build the dragon's blood HPLC-DAD library, previously to EBC, K analysis, see table I.2.

Table I.2 - Library samples analysed by HPLC-DAD.

ID	Species	Source	Estimated age/ Observations	Dragon tree photo
1	<i>Dracaena draco</i>	Botanical garden of Ajuda, Lisbon (BGAL)	Centenary tree (300-360 years old)	
2	<i>Dracaena draco</i>	BGAL	Centenary tree (150 years old)	
3	<i>Dracaena draco</i>	Botanical garden of Lisbon	Centenary tree (circa 130 years old)	
4	<i>Dracaena draco</i>	Botanical garden of Lisbon	Centenary tree (less than 200 years old)	
5	<i>Dracaena draco</i>	Botanical garden of Funchal (BGF)	Less than 100 years old This is the oldest dragon tree in BGF.	

6 *Dracaena draco* BGF Less than 100 years old



7 *Dracaena draco* BGF Less than 100 years old



8 *Dracaena draco* BGF Less than 100 years old



9 and
10 *Dracaena draco*

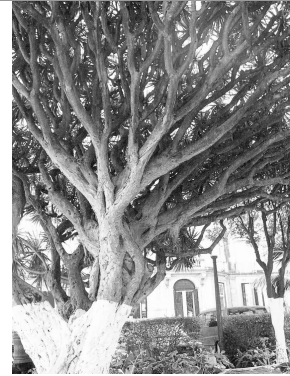
BGF

These dragon trees were the
branches of older dragons that
were recently planted in BGF.



11	<i>Dracaena draco</i>	BGF	This dragon tree was the branches of an older dragon tree that was recently planted in BGF.	
12	<i>Dracaena draco</i>	BGF	Less than 10 years old	
13	<i>Dracaena draco</i>	BGF	Less than 10 years old	
14 and 15	<i>Dracaena draco</i>	Natural Park Madeira	Centenary tree	
16	<i>Dracaena draco</i>	Lisbon, Palace of Necessity	Centenary tree	
17	<i>Dracaena draco</i>	Lisbon, Ultramarine Historic Archive	Centenary tree	

18 *Dracaena draco* Lisbon, Military Govern Centenary tree



19 *Dracaena draco* Lisbon, Ribamar house Centenary tree



20 *Dracaena draco* Lisbon, Ribamar house Centenary tree



21 *Dracaena draco* Lisbon, Ribamar house Centenary tree



22 *Dracaena draco* Lisbon, Ribamar house Centenary tree



23	<i>Dracaena draco</i>	Lisbon, Algés	Centenary tree	
24	<i>Dracaena draco</i>	Lisbon, Carnide house	Less than 100 years old	
25	<i>Dracaena draco</i>	Lisbon, Almada Seminary	Centenary tree	
26	<i>Dracaena draco</i>	Lisbon, Garden of Cidade Universitaria	65 years old	
27	<i>Dracaena draco</i>	Madeira, Museum of Quinta das Cruzes	Centenary tree	

28	<i>Dracaena draco</i>	Madeira, Museum of Quinta das Cruzes	Less than 100 years	
29	<i>Dracaena draco</i>	Madeira, Park of Santa Catarina	Less than 20 years old	
30	<i>Dracaena draco</i>	Madeira, Park of Santa Catarina	Less than 30 years old	
31	<i>Dracaena draco</i>	Madeira, Garden of IBTAM	Centenary tree	
32	<i>Dracaena draco</i>	Madeira, Garden of Avenida do Mar	Less than 50 years old	

33

Dracaena draco

Cape Verde
(Figueiral do Paul)

Less than 30 years old



34-42

Dracaena cinnabari

Socotra

Centenary trees



43

Daemonorops

Kremer

-

44

draco (as Calamus draco)

Zecchi

-

-

45

Daemonorops draco

Indonesia

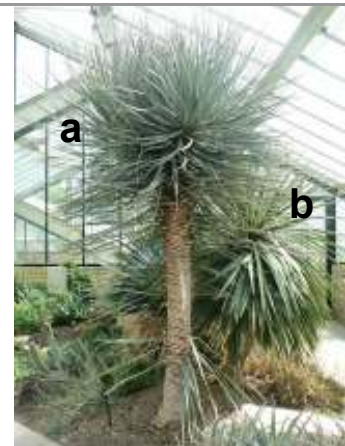
-

46

Dracaena Schizantha

Kew garden, from Ethiopia

29 years old.
Behind the *Dracaena schizantha* (a) there is a *Dracaena cinnabari* whit 41 years old (b).



I.3.1.2 Collection/sampling of resins

The resin samples collected in Portugal were obtained directly from botanically verified dragon trees of different ages (from 10 to circa 200/350 years old, see table I.2), in three different injured areas of the stem and branches (figure I.1). When possible, the samples were also collected in different seasons of the year (summer and winter) and the results were consistent.

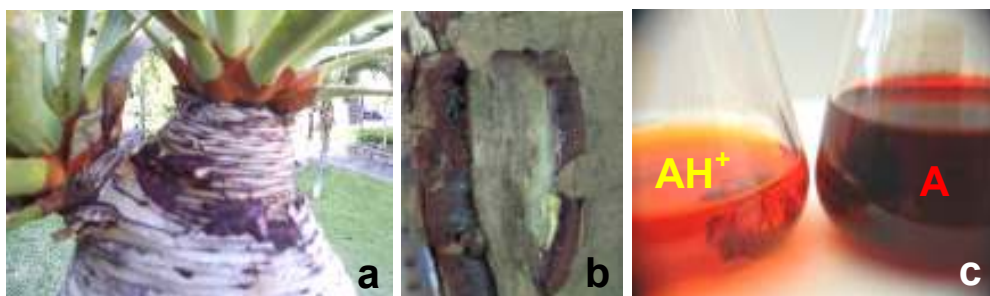


Figure I.1 – a) Resin collected from the branch; b) Resin collected from the stem; c) Extraction of the resin with acidified MeOH (AH^+) and MeOH (A).

From the EBC, K, 50 mg samples were taken for detailed characterization from items labeled *Daemonorops draco* (3), *Daemonorops propinqua* (a synonym of *Daemonorops draco*) (2), *Dracaena cinnabari* (3), *Dracaena draco* (2) and *Dracaena sp.* (3). From the remaining 24 samples of the collection only 0.5 mg were sampled.

The *Dracaena* collection of EBC, K is very heterogeneous, presenting different grades of resin, namely a higher, valuable and pure grade [4] composed of tears of resin - “*Edah amsellah*” - (e.g. 36611, figure I.2a) or fine marbles of resin; a second grade composed of resin attached to bark or red powder - “*Edah dukkah*” – and also a third grade composed of mixtures of resin, bark and powder - “*Edah mukdehah*” (e.g. 36809, figure I.2b). Large pieces of red wood (e.g. 26421) were also found.

In the *Daemonorops* collection, the resin samples were very heterogeneous being composed usually of a mixture of resin fruit scales, and other contaminants. The extraction and processing of the resin into moulded cakes or sticks can incorporate a considerable amount of impurities. Consequently, analysis from resin extracted directly from the fruit's scales was also performed (e.g. 35499, figure I.2c); for more details see chapter 1, section 3.1.



Figure I.2- a) *Dracaena draco*, tear resins, sample 36611 (magnification 7x); b) *Dracaena cinnabari*, composed resin (resin, pigment and wood); sample 36809 (magnification 7x); *Daemonorops draco*, fruits scales with resin, sample 35499 (magnification 7x).

I.3.1.3 Extraction of the dragon's blood dye chromophores, purification and characterization of the natural flavylum markers

The extraction conditions of the coloured compounds of dragon's blood resins are a crucial step in the resins distinction. Special attention should be paid in its identification in works of art, where usually small samples can be taken for a single analysis and low concentrations should be expected. An extraction with at least an acidic pH should be performed in order to avoid the complex network of chemical reactions in which the flavylum compounds are involved and obtain the single flavylum cation which allows the rapid and easy identification of the resin as described in Chapter 1, section 3.1. Therefore, the red colorants of the dragon's blood resin samples were extracted with methanol acidified with perchloric acid in water, $\text{pH} \approx 1$, for less than 2 minutes (figure I.1c).

The samples were filtered and analyzed by analytical HPLC-DAD. All the resin samples were injected at least three times in HPLC-DAD, with exception of small samples from the EBC, K, where less than 0.2 mg of resin was used in one HPLC-DAD analysis.

For the NMR and MS characterization of the flavylum markers, several runs with dragon's blood resins used in the HPLC-DAD library were performed in the preparative HPLC-DAD system as reported above. Moreover, the dracorhodin network of chemical reactions characterization was also performed with the flavylum isolated from the dragon's blood resin with HPLC-DAD.

The identification of the isolated flavylum markers was made on the basis of MS and NMR (see appendix II – Dragon's blood data), although the complete structure confirmation of the 7,4'-dihydroxy-5-methoxyflavylum and the 7,4'-dihydroxyflavylum required their synthesis [5-6].

1.3.1.4 PCA analysis

Principal components analysis (PCA) of dragon's blood resins were carried out using Matlab version 6.5 release 13. The PCA algorithm was written in-house. Given the multivariate nature of the resin samples' chromatograms, multivariate data analysis was required in order to analyse samples. PCA was selected to perform a similarity analysis [7]. Similarity between the dragon's blood resin samples was assessed with the chromatogram data between 15.3 and 28.9 minutes (all peaks were found to be within this region). Prior to PCA, chromatograms were pre-processed using the standard normal variate method and subjected to mean centering [7].

PCA results were analysed on the basis of the principal components retaining the major part of the original chromatogram data variance. Since principal components represent the original chromatograms in a smaller dimension, space scatter plots can be used to visualize the original data.

1.3.1.4 Characterization of the network of chemical reactions of flavylum compounds

The characterization of the network of chemical reactions of flavylum compounds was performed in 99% water/MeOH (v/v) at 25 °C with the UV/Vis spectrophotometer. The 7,4'-dihydroxy-5-methoxyflavylum displayed low solubility in water and, as a result, the final concentration of the solution after filtering with 0.45 µm acrodisc filters was very low (circa 1×10^{-6} M). The concentration of the dracorhodin flavylum was also very low, as it was obtained from the dragon's blood resins after HPLC separation.

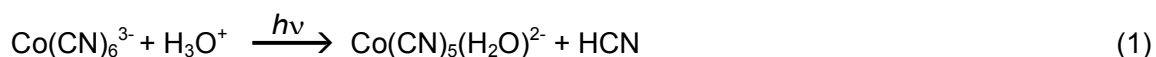
The pH of the solutions was adjusted with the addition of HClO₄ or NaOH solutions and universal buffer, and measured by a Metrohm 713 pH meter. The reaction kinetics were monitored by UV/Vis absorption.

1.3.2 Indigo

1.3.2.1 Actinometry

For the monochromatic irradiation at 335 nm, the intensity of the incident light (I_0) was calculated with the potassium hexacyanocobaltate(III) actinometer ($[\text{Co}(\text{CN})_6]^{3-}$) [8], whereas in the irradiation at 610 nm the Reinecke's salt actinometer ($[\text{Cr}(\text{NH}_3)_2(\text{SCN})_4]^-$) was used [9].

To obtain the lamp I_0 at 335 nm, a 3 mL solution of potassium hexacyanocobaltate(III) actinometer 10^{-2} M in water, pH=2, was irradiated in a quartz cell with 1 cm optical path under constant agitation during 10 minutes. Every 2 minutes, a UV/Vis spectrum of the solution was obtained. The formation of the pentacyanocobaltate(II) product ($[\text{Co}(\text{CN})_5(\text{H}_2\text{O})]^{2-}$), according to equation (1), was followed at 380 nm, with a quantum yield of 0.31 [8].

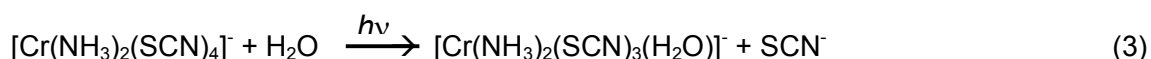


To calculate the intensity of light, the following expression was used:

$$I_0 = \frac{V_{\text{sol}} \cdot (\Delta A / \Delta \varepsilon)}{1000 \cdot \Phi_R \cdot \Delta t} \quad (2)$$

V_{sol} is the volume of irradiated solution in mL (3 mL), ΔA is the change in absorbance at the monitoring wavelength (380 nm) over the irradiation time period, Δt , corrected by the light absorption of the reagent at 335 nm (λ_{irr}), $\Delta \varepsilon$ is the difference between the molar absorption coefficients of reagent ($\varepsilon(\text{R})=10 \text{ M}^{-1}\text{cm}^{-1}$) and product ($\varepsilon(\text{P})=280 \text{ M}^{-1}\text{cm}^{-1}$) at the monitoring wavelength (270 nm), and Φ_R is the quantum yield of reaction (1) ($\Phi_R=0.31$). The I_0 was calculated with the program Moggicor.

To obtain the lamp I_0 at 610 nm, a solution of $[\text{Cr}(\text{NH}_3)_2(\text{SCN})_4]^-$ 0.05 M in water, pH=5.3 (natural pH of Reinecke's salt in water), previously recrystallized also with water at 40 °C in the dark, was irradiated under constant agitation for 2, 4 and 6 minutes, corresponding each irradiation time to an individual 3 mL quartz cell. Moreover, a thermal blank was kept in the dark for comparison with the irradiated samples. The irradiation of the Reinecke's salt causes the substitution of a SCN- ligand by a water molecule:



To obtain the lamp I_0 , the released SCN^- is complexed with ferric nitrate forming a red compound:



Therefore, 2 mL of each irradiated solution and the blank were diluted with 0.1 M Fe(NO₃)₃ in 0.5 M HClO₄ to a final volume of 5 mL in a volumetric flask. Finally, the UV/Vis spectra of the solutions with the resulting iron (III) thiocyanate complex were traced and the formation of the product was followed at 450 nm (equation (4)). This actinometry was performed twice, being the results very similar. However, in the second time, a higher amount of thiocyanate ion was present in the starting Reinecke's salt solution.

The intensity of light was calculated with equation (2), where the V_{sol} considered took into account the dilution performed with 2 mL of the irradiated solution, as described above (V_{sol}=3x(5/2)), ΔA was the absorbance variation at 450 nm corrected by the light absorption of the reagent at 610 nm, Δε used was 4270 M⁻¹cm⁻¹ (ε_P⁴⁵⁰=4300 M⁻¹cm⁻¹ and ε_R⁴⁵⁰=30 M⁻¹cm⁻¹), and the φ_R used was 0.31 [8].

1.3.2.2 Homogeneous media – monochromatic irradiation

1x10⁻⁴ M Indigo/DMF solutions in 3 mL quartz cells with 1 cm optical path and very well-stirred were submitted to monochromatic irradiation at 335 and 610 nm in the presence of O₂ with atmospheric conditions, in degassed solutions (high vacuum line) and in N₂ atmosphere. Degassed solutions enabled to obtain lower levels of O₂ than N₂ bubbling and therefore were chosen for the φ_R in the absence of molecular oxygen.

For the O₂-free atmosphere, the indigo/DMF solution was submitted to circa 0.5 h of freezing and de-freezing cycles (3) with liquid nitrogen in the high vacuum line. In the argon atmosphere, the indigo/DMF solution was submitted to 15 min of bubbling with argon, to assure that O₂ was not present.

1x10⁻⁴ M indigo carmine dissolved in DMF or in water was irradiated in 3 mL quartz cells with 1 cm optical path and very well-stirred at 335 and 610 nm in the presence of oxygen. The I₀ was obtained as reported for Indigo.

For indigo photodegradation studies, small aliquots of the irradiated solution (50 μL) were analysed with HPLC-DAD at each irradiation time. In indigo carmine photodegradation, only the last irradiation time was analysed by HPLC-DAD.

1.3.2.2.1 Quantum yield

The quantum yield was calculated with the following expression:

$$\phi_R = \frac{V_{sol} \cdot (\Delta A / \Delta \epsilon)}{1000 \cdot I_{abs} \cdot \Delta t} \quad (5)$$

I_{abs} is the total light absorbed by the solution at the irradiation wavelength; the I_{abs} is equal to $I_0 \times (1 - 10^{-A_{\text{irr}}})$ when $A < 2$ or $I_{\text{abs}} = I_0$ when $A > 2$. The other terms were obtained as reported for equation 2. The $\Delta\varepsilon$, calculated at the monitoring wavelength (610 nm for indigo and 617 nm for indigo carmine), only considered the ε of the reagent as the main product formed is colourless. The program Moggiccor was also used to obtain the Φ_R .

1.3.2.3 Heterogeneous media – monochromatic irradiation

Solid gels of indigo carmine in carboxymethylcellulose (M.W. 270000) and commercial gelatine (Vahine and Jerónimos), as well as bacteriological gelatine (Aldrich), were irradiated at 335 and 610 nm in the presence of oxygen. For the cellulose based gel, 0.4 g of CMC was dissolved in 4 mL of hot water (at circa 90 °C) with constant agitation and the help of an ultrasonic bath, when necessary. 4 mL of indigo carmine 1×10^{-4} M in water were added to the CMC gel and the resulting mixture was submitted to the ultrasonic bath until the air bubbles disappeared. Finally, circa 3 mL of CMC gel were placed in a 3 mL quartz cell for monochromatic irradiation and other 3 mL were kept in the dark for thermal control. The Vahine and Jerónimos gelatine sheets were kept in a cold water bath overnight, previously to the formation of solid gels with indigo carmine, in order to remove impurities as sugars or other additives.

0.4 g of washed gelatine was dissolved in hot water (at circa 90 °C) under constant agitation. After its complete dissolution, 4 mL of indigo carmine 1×10^{-4} M in cold water was added. Before the gelatine solidification, the solution was transferred to a 3 mL quartz cell, as reported for the CMC gel. The irradiation path was the same as for the CMC gel. The procedure for bacteriological gelatine was the same reported for Vahine and Jerónimos gelatines; however, this gelatine was not submitted to a cold water bath overnight as it promoted the gelatine dissolution.

The final irradiated gels were dissolved in MeOH, filtered with 0.45 μm acrodisc filters and analysed by HPLC-DAD.

1.3.2.3.1 Quantum yield

The quantum yield in heterogeneous media was calculated as in the homogeneous media using equation (5). However, only half volume of the gel was irradiated (see figure I.3) and, therefore, the volume considered was 1.45 mL (calculated through the measurement of the optical path exposed to light) [9].



Figure I.3 – Gelatine indigo carmine gel before a) and after b) 335nm irradiation.

I.3.2.4 Heterogeneous media - polychromatic irradiation

Circa 0.10 mg of indigo were deposited on a creased glass surface (1 cm²) with a small brush and irradiated in the Solar Box camera during 2700 hours, see figure I.4. Three cells were taken at circa each 500 hours of irradiation. The final colour was measured with the colorimeter prior to HPLC-DAD analysis. The indigo was extracted from the cells with DMF and immediately analysed by HPLC-DAD to prevent further deterioration.



Figure I.4 – Indigo cells irradiated in the solar box.

I.3.2.5 Indigo photodegradation HPLC-DAD calibration curves

Previously to analysis of indigo photodegradation in liquid and solid state, calibration curves were made with indigo and isatin standards dissolved in DMF for the concentration range expected (from 1×10^{-4} M to 1×10^{-6} M). Afterwards, the respective areas of the compounds were calculated at their maximum wavelength with the chromatographic program Chromquest and represented as a function of the concentration. The correlation coefficients for all the calibration curves were good, ≥ 0.98 , for the concentration range studied.

I.3.2.6 Andean indigo dyed fibres extraction

The dyes were extracted from circa 0.3 mg of fibre with 400 μ L of DMF and heating for 30 min at 60 °C with magnetic stirring in a glass vial. Before the extraction, the vial was submitted to 5 minutes of vacuum and argon cycles to assure that O₂ was not present. After the extraction, the solvent was evaporated under vacuum. The residue was dissolved

in 40 μL of DMF and then centrifuged to separate the particulate matter. The upper 30 μL of solution were removed and analysed in the HPLC-DAD. The extract was analysed immediately after the concentration, to reduce the risk of degradation.

I.3.3 Mauve dye

I.3.3.1 Syntheses

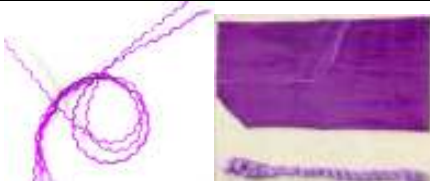
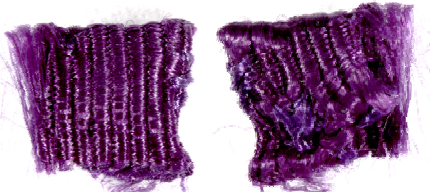


The several syntheses of mauve dye followed the same basic procedure as described in [10], where different proportions of the starting materials were used (for more details, see chapter 3, section 3.3):

The *p*-toluidine was dissolved in water around 30 °C with a large spin vane. Afterwards, aniline, *o*-toluidine and 1M sulphuric acid were added. When all the compounds were dissolved, potassium dichromate dissolved in water was added to the mixture. The solution was stirred for two hours under constant temperature (circa 30 °C) and then filtered. The crude product obtained was washed under suction with water, hexane and finally 25% MeOH/H₂O. In between the three washings, the residue was dried at circa 110 °C first for 30 min and then for 10 min.

I. 3.3.2 Mauve dye sources

20 mauve samples were analysed by HPLC-DAD: 4 different mauve dyes synthesized as described in chapter 3, section 3.1; 7 historic mauveine salts and 7 historic textile samples dyed with mauve from important museums, 2 mauve dyed textiles from the JCE 1926 and DHA 2001 books and a mauve dyed silk textile according to the original Perkin's recipe; for more details table I.3.

Table I.3 – Historical mauve samples

Sample ID	Description	Date attribution in the literature [11]	Labels/Other information from the Museums/ Observations	Photo
TEXTILES SAMPLES				
<i>Science Museum F5</i> 1947-117	Silk. Dark red purple colour. 10 cm of width 1.19 mg.	1856-7 (?)	Small piece of silk fabric dyed with mauve of pattern supplied allegedly to Queen Victoria about 1860.	
				Sample sent by the SM (left), magnification 7x; silk fabric (right) [12].
<i>Perth Museum</i>	Silk. Dark red purple colour. Colour not homogeneous on the back. 0.5 cm ² 8.19 mg.	1856-7 (?)	Gift by the Pullar family in 1938 to the PM and in the register notes it is written that this sample was "cut from the first length of material dyed by Dr Perkins [sic] by his new process in Pullar's works, Perth in 1856".	
				Front (left) and Back (right), magnification 7x
<i>Science Museum F6</i> 1947-333	Wool. Dark red purple colour. 25.46mg.	1862	Mauve dyed shawl exhibited at International Exhibition of 1862.	
				Sample sent by the SM (left), magnification 7x; shawl (right) [12].
<i>Science Museum F1</i> 1947-116, <i>Pt1</i>	Silk. Dark red purple colour. 10 cm of width 0.32 mg.	1860 (?)	Possibly made for the 1862 International Exhibition and given to SM by Miss A. F. Perkin in 1947.	
				Magnification 16x.
<i>Science Museum F2</i> 1947-116, <i>Pt2</i>	Silk. Pale purple colour. 5 cm of width 0.16 mg			

Science
Museum
 F3
 1947-116,
 Pt3

Silk. Dark red
 purple colour.
 10 cm of width
 0.45 mg.

Mounted mauve silk skein.
 Possibly made for the 1862
 International Exhibition and
 given to SM by Miss A. F.
 Perkin in 1947.



Magnification 7x

Science
Museum
 F4
 1947-116,
 pt4

Cotton.
 Heterogeneous
 colour.
 10 cm of width
 2.29 mg.

Possibly made for the 1862
 International Exhibition and
 given to SM by Miss A. F.
 Perkin in 1947.



Magnification 7x

SALTS SAMPLES*

Science
Museum 1
 (1952-175)

Dark black
 purple colour.
 High content of
 rectangular
 particles.

"Original Mauveine Prepared
 by Sir William Henry Perkin in
 1865".
 Formerly in Imperial College,
 donated in 1952 to the Science
 Museum. Analysed by Meth-
 Cohn and Smith [13].

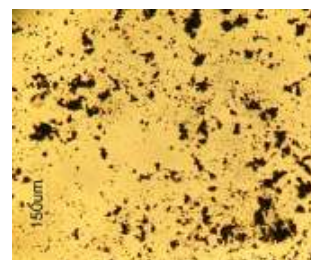


Magnification 200x, transmitted light

Science
Museum 2
 (1947-
 115/1)

Dark black
 purple colour.
 Irregular
 spherical
 particles.

"Mauveine Salt".
 Donated to the SM by Miss A F
 Perkin in 1947.



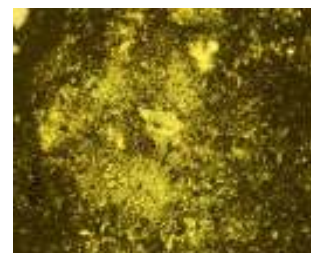
Magnification 100x, transmitted light

1862 (?)

Science
Museum 3
 (1947-
 115/2)

Dark black
 purple colour.
 Irregular
 spherical
 particles.

"Mauveine HCl".
 Donated to the SM by Miss A F
 Perkin in 1947.



Magnification 100x, reflected light-dark ground


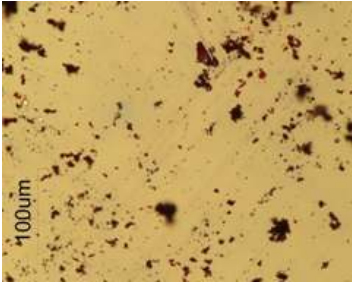

Science
Museum 4
 (1947-
 115/3)

Dark black
 purple colour.
 Irregular
 spherical
 particles.

"Mauveine acetate".
 Donated to the SM by Miss A F
 Perkin in 1947.



Magnification 100x, transmitted light

<p><i>Museum SI Manchester 1</i></p>	<p>Dark black purple colour. Irregular spherical particles and or agglomerates.</p>	<p>1862 (?) 1906 (?)</p>	<p>Given by the Kirkpatrick branch of the Perkin family to ICI and subsequently transferred to the MSIM. It has a broken factory seal on the cork and appears to come from the Grenford Green works of Perkins & Sons. It is labelled as "Crude Mauveine Acetate" "([Perkin&Sons/P]atent[Anil]ine Pur[ple])", 1862 Manchester Museum of Science and Industry, Manchester (Inv. No L1999.2.8). Analysed by Meth-Cohn and Smith [13].</p>		<p>Magnification 100x, reflected light –white ground</p>
<p><i>Museum SI Manchester 2</i></p>	<p>Dark black purple colour. Irregular spherical particles.</p>	<p>-</p>	<p>From the Schunck collection of MSIM and is labelled as "mauveine C₂₇ H₂₄ N₄". The handwriting looks like other samples in the collections and was probably written by Schunck or his assistant.</p>		<p>Magnification 100x, transmitted light</p>
<p><i>Chandler Museum 1</i></p>	<p>Dark black purple colour. High content of rectangular particles</p>	<p>1906 (?)</p>	<p>From the CM at Columbia University, New York City and given to Professor Charles Chandler by W. H. Perkin during his visit to New York in October 1906.</p>		<p>Magnification 400x, reflected light – dark ground</p>

MAUVE FROM OTHER SOURCES

<p>JCE</p>	<p>Blue shade of purple colour. Circa 2.5cm of width and 1cm of height.</p>	<p>1926</p>	<p>L*=31.24±0.03; a*=24.69±0.00; b*=-30.64±0.01**</p>
------------	---	-------------	---



DHA Red shade of purple colour. Circa 2.5cm of width and 1cm of height. 2001 $L^*=45.43\pm 0.17$; $a^*=19.19\pm 0.07$; $b^*=-20.92\pm 0.06^{**}$



SYNTHESIZED MAUVE AND MAUVE DYED TEXTILE AT FCT-UNL

FCT Red shade of purple colour. Circa 2cm of width and 1.5cm of height. 2007 $L^*=44.93\pm 0.61$; $a^*=19.21\pm 0.35$; $b^*=-11.30\pm 0.37^{**}$



Synthesis JCE 1998 Colour obtained: 1, dark purple; 2, purple; 3, brown; 4, brown; 5 light purple

2006 Major compounds: 1, Mauveine B2 and C 2, Mauveine B 3, no formation of mauve dye

2007 Major compounds: 4, no formation of mauve dye 5, Pseudo-mauveine



* The colours of the salt samples in the optical microscope were always golden-green with reflected light and black with transmitted light for minor magnifications.

** The L^* , a^* and b^* are coordinates used in the system CIELAB to characterize a colour. L^* represents the difference between light ($L^*=100$) and dark ($L^*=0$), a^* represents the difference between green ($-a^*$) and red ($+a^*$), and b^* represents the difference between yellow ($+b^*$) and blue ($-b^*$) [14]

1.3.3.3 Extraction and characterization of mauve dye

Prior to HPLC-DAD and/or LC-MS analysis, the mauve salt samples were dissolved in methanol while the chromophores recoveries from fibres with less than 0.2 mg were obtained using soft extraction methods.

Six extraction procedures to enable the recovery of all mauveine chromophores were tested in textile historical reconstructions, that is, silk textiles dyed with *Science Museum 1* according to Perkin's recipes[15]: **extraction 1**: MeOH; **extraction 2**: MeOH / H₂O (25:75, v/v); **extraction 3**: MeOH / HCOOH 98 % (95:5, v/v); **extraction 4**: 0.2 M oxalic acid /

MeOH / acetone / water (1:3:3:4, v/v/v/v); **extraction 5:** MeOH + 1 drop of 0.01 M HCl / H₂O (pH = 2); **extraction 6:** MeOH + 1 drop of NaOH / H₂O (pH = 10). The extraction procedures were carried out as follows: a small sample of thread (around 0.1 mg) was extracted with 400 µL of the solution mixture in 1.5 ml eppendorfs for 30 min at 60 °C (water bath) under constant stirring [16]. After extraction, each extract was dried in a vacuum system, where the resulting dry residues were reconstituted with 50 µL of methanol and then centrifuged to separate the particulate matter. The upper 30 µL solutions were removed and analysed with HPLC-DAD.

All the mauve-dyed samples were extracted with method 5 which revealed to be the most efficient method (see table I.4 and figure I.5). Moreover the colored extract obtained from the mauve dyed fabric with this method revealed that the mauveine chromophores from the dyeing bath were absorbed homogeneously, this is in equal proportion by the textile (table I.5). When there was enough sample amount, methods 3 and 1 were also applied and standard deviation values calculated.

Table I.4 –Extraction methods tested in mauve dyed silk textile according to Perkin’s recipes.

Extraction method	Mauveine A and B (%)*
1	53
2	25
3	65
4	-
5	100
6	-

*The peak areas were measured at 551nm. The areas were then normalized with the major compound area. Correction is made by dividing the raw area by the fiber weight.

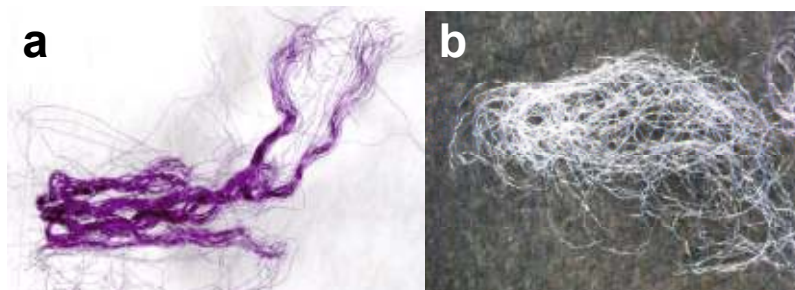


Figure I.5 – Perth Museum sample before (a) and after (b) extraction with MeOH / HCOOH 98 % (95:5, v/v).

Table I.5 – Mauveine chromophores distribution in mauve dyed textile after dyes recovery and in ScM1 salt sample.

Mauveine	Mauve dyed textile	ScM1 salt
pseudo-mauveine	<1	1
mauveine C _{25a} +C _{25b}	2	2
mauveine A	50	50
mauveine B	22	23
mauveine B2	11	10
mauveine B3+B4	6	5
mauveine C	4	4
mauveine C1	5	5

For the mass spectrometry (FDMS and FTICRMS) and NMR (¹H and ¹³C) characterization, several runs with the mauve dye obtained from synthesis 1 (see table I.3 and chapter 3, section 3.3) [10] in the semi-preparative HPLC-DAD, as described in section I.2.1, were performed. The *Science Museum F6*, *Science Museum F1* and *Museum SI Manchester 2* samples were also characterized by LC-MS.

The counter-ions analysis of mauve historic salts 1X10⁻⁵ M in water was performed with HPLC anion exchange chromatography. Previously, a data base with ion standards dissolved in water were also analysed (see table I.6).

Table I.6. Ion standards and respective retention times (t_r) in water*.

Standard (M)	t_r (min)
Acetate (5×10 ⁻⁵)	4.8±0.1
	9.5±0.3
Chloride (5×10 ⁻⁴)	8.1±0.2
Sulphate (5×10 ⁻⁴)	12.4±0.4
Nitrate (5×10 ⁻⁴)	21.7±0.3

*The standards were dissolved in water since with methanol the acetate standard precipitates giving rise to a broad band, masking the identification of other ion standards.

I.3.3.4 Mordant analysis

Fe, Al, and Sn mordant identification was performed in three mauve-dyed textile samples (*Science Museum F4*, *Science Museum F6* and *Perth Museum*) using ICP-AES. Circa 1-3 mg of fibre were digested with HNO₃ 65% for 1h in the ultrasonic bath. After complete

dissolution, the HNO₃ was diluted with water to a total volume of 4 mL and 9% concentration (v/v).

I.3.3.5 Polychromatic irradiation

Two mauve yarns dyed as in the original recipes [15] (see table I.3 and I.5), and two yarns from the SCMF5 and SCMF6 textiles samples were submitted to an accelerated aging study in the Solar Box camera during 200 h at 700 MJ/m². The colour fading was monitored with the colorimeter and HPLC-DAD approximately every 12 h.

References

- [1] Castele, K. V.; Geiger, H.; Loose, R.; van Sumere, C. F. *Journal of Chromatography A* **1983**, 259, 291.
- [2] This method was created after a research on HPLC methods used for similar organic dyes as methyl violet: a) Tarbin, J. A.; Barnes, K.A.; Bygrave, J.; Farrington, W.H.H., *Analyst* **1998**, 123, 2567. b) Samanidou, V. F.; Nikolaidou, K. I.; Papadoyannis, I.N., *Journal of Liquid chromatography and Related Technologies* **2004**, 27-2, 215.
- [3] Adolt, R.; Pavlis, J. *Trees* **2004**, 18, 43.
- [4] Pearson, J.; Prendergast, H.D.V. *Economic Botany* **2001**, 55, 474.
- [5] Melo, M. J; Sousa, M. M; Parola, A. J; Seixas de Melo, J. S.; Catarino, F.; Marçalo, J.; Pina, F. *Chemistry – A European Journal* **2007**, 13, 1417.
- [6] Pina, F.; Benedito, L.; Melo, M. J.; Parola, A. J.; Lima, J. C.; Maçanita, A. *Anales de Química Internacional Edition* **1997**, 93, 111.
- [7] Naes, T.; Isaksson, T.; Fearn, T.; Davies, T. *Multivariate Calibration and Classification*, NIR Publications, Chicester: UK, 2004.
- [8] Pina, F.; Moggi, L.; Manfrin, M.; Balzani, V.; Hosseini, M.; Lehn, J. M. *Gazzeta Chimica Italiana* **1989**, 119, 65.
- [9] Montalti, M.; Credi, A.; Prodi, L.; Gandolfi, M. *Handbook of Photochemistry*. 3rd edition. *CRC Press, Boca Raton: US*, 2006.
- [10] Pina, F.; Hatton, T.A. *Langmuir* **2008**, 24, 2356.
- [11] Scaccia, R.; Coughlin, D.; Ball, D. *Journal of Chemical Education* **1998**, 75-6, 769.
- [12] Morris, P. J. T. *History and Technology* **2006**, 22, 119.
- [13] In <http://www.sciencemuseum.org.uk> , April 2008.
- [14] Meth-Cohn, O.; Smith, M. *Journal of the Chemical Society-Perkin Transactions 1* **1994**, 5.
- [15] Perkin, W. H. *Journal of Chemical Society* **1862**, 14, 230.
- [16] Zhang, X.; Laursen, R. A. *Analytical Chemistry* **2005**, 77, 2022

Appendix II – Dragon’s Blood data

II.1. NMR and MS characterization

II.1.1 7,4'-dihydroxy-5-methoxyflavyliu (*dracoflavylium*)

For the first time, the 7,4'-dihydroxy-5-methoxyflavylium (*dracoflavylium*) was isolated with HPLC from *Dracaena draco* dragon’s blood resins and characterized by HRMS (calculated for $C_{16}H_{11}O_4^-$, 267.06628); m/z 253.04991 $[M-CH_3]^-$ (calculated for $C_{15}H_9O_4^-$, 253.05063). The results obtained were compared with the synthesized flavylium, as the natural *dracoflavylium* separated by HPLC-DAD revealed the presence of minor impurities. The isolated compound had the same retention time, UV-Vis spectra by HPLC-DAD (20.50 min, $\lambda_{max}=477$ nm) and the same molecular mass peaks (HRMS: m/z 267.06646 $[M-H]^-$ (calculated for $C_{16}H_{11}O_4^-$, 267.06628); m/z 253.05025 $[M-CH_3]^-$ (calculated for $C_{15}H_9O_4^-$, 253.05063) of the synthesised flavylium.

The 1H NMR spectra of the isolated and of the synthesised compounds in acidic CD_3OD are identical, except for some peak overlap due to the presence of minor impurities in the isolated sample.

Elemental analysis for the synthesized compound: exp. (calc. for $C_{16}H_{14}O_8S \cdot 3.5H_2O$; $FW=429.40$ g mol $^{-1}$) %C 44.91 (44.76), %H 4.02 (4.93), %S 7.35 (7.47). 1H NMR (400 MHz, CD_3OD/CF_3CO_2D , 30 °C, AH^+ form): see figure II.1 and table II.1; in agreement with published data for this compound [1]; ($D_2O/NaOD$, $pD>12$, 30 °C, equilibrated, C_t^{2-} form): δ/ppm 3.59 (s, 3H, OCH_3), 5.33 (s, 1H, H6 or H8), 6.37 (d, $J=9.0$ Hz, 2H, $H3'+H5'$), 7.51 (d, $J=15.9$ Hz, 1H, H3), 7.58-7.63 (m, 3H, H6 or H8, $H2'+H6'$), 8.09 (d, $J=15.9$ Hz, 1H, H4).

Figure II.1 - 7,4'-dihydroxy-5-methoxyflavylium hydrogen sulphate

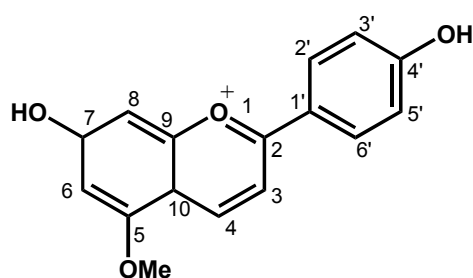


Table II.1 – ^1H and ^{13}C -NMR data for 7,4'-dihydroxy-5-methoxyflavylium hydrogen sulphate. ^[a]

Position	^1H δ /ppm (J/Hz)	COSY	^{13}C (δ /ppm)	HMBC ^[b]
2			173.1	
3	8.09 (d, 9.2)	4	111.1	C2, C10
4	9.08 (d, 9.2)	3	149.1	C2, C9, C5
5			161.0	
6	6.78 (s)	8	100.9	C5, C10, C8
7			160.3	
8	7.03 (s)	6	96.7	C7, C10, C6
9			172.4	
10			113.8	
1'			121.0	
2',6'	8.32 (d, 9.3)	3',5'	133.4	C2, C4', (C2', C6')
3',5'	7.07 (d, 9.3)	2',6'	118.5	(C3', C5'), C1'
4'			167.6	
5-OCH ₃	4.09 (s)		57.8	C1

[a] Data recorded at 400/100 MHz in CD₃OD/CF₃CO₂D [b] Correlation from H to the indicated carbons.

II.1.2 7-hydroxy-5-methoxy-6-methylflavylium (*dracorhodin*)

The occurrence of 7-hydroxy-5-methoxy-6-methylflavylium (*dracorhodin*) in dragon's blood resins was confirmed by isolation with HPLC and characterization by HRMS (m/z [M-H]⁻ 265.09516, [M-H]⁻; calcd. for C₁₇H₁₃O₃⁻: 265.09484; M is the quinoid base) and ^1H and ^{13}C NMR (see figure II.2 and table II.2); to our best knowledge, this is the first full spectroscopic characterization of this compound.

Figure II.2 - 7-hydroxy-5-methoxy-6-methylflavylium.

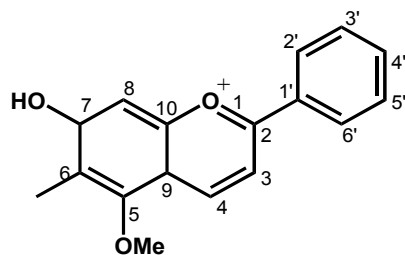


Table II.2 – ^1H and ^{13}C -NMR data for 7-hydroxy-5-methoxy-6-methylflavylium (dracorhodin) isolated from a *Daemonorops* sp. commercial resin by HPLC-DAD.^[a]

Position	^1H δ /ppm (J/Hz)	^{13}C (δ /ppm)	HMBC ^[b]
2		171.8	-
3	8.31 (d, 8.6)	113.2	C2, C10
4	9.20 (d, 8.6)	151.1	C2
5		158.5	
6		125.3	
7		172.0	
8	7.31	99.3	[c]
9		[c]	
10		117.9	
1'		130.5	
2',6	8.36 (d, 7.6)	129.9	C2, C4', (C2', C6')
3',5'	7.07 (t, 7.5)	130.9	C1', (C3', C5')
4'	7.74 (t, 7.4)	136.4	C2', C6'
5-OCH ₃	3.99	64.0	C5
6-CH ₃	2.28	22.4	C5, C6, C7

[a] Data recorded at 400/100 MHz in CD₃OD/DCI (pD ~ 0.1); [b] Correlation from H to the indicated carbons; [c] These signals could not be detected at the level of accumulation used.

II.1.2 7,4'-dihydroxyflavylium

For the first time, the 7,4'-dihydroxyflavylium was identified in *Dracaena cinnabari* resins after isolation by HPLC and characterization by HRMS (m/z 237.07512, [M-H]⁻; calcd. for C₁₅H₉O₃⁻: 237.07725; M is the quinoid base) and ^1H and ^{13}C NMR. The structure assignment was confirmed with synthesised 7,4'-dihydroxyflavylium chloride [2] whose MS and NMR data (see figure II.3 and table II.3) were identical to those of the isolated compound. Also, the isolated compound had the same retention time in HPLC-DAD (18.03 min) and the same $\lambda_{\text{max}} = 462$ nm of the synthesised flavylium.

Figure II.3 - 7,4'-dihydroxyflavylium.

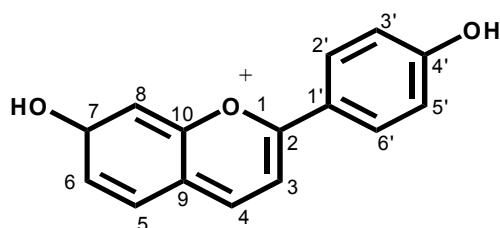


Table II.3 ^1H and ^{13}C NMR data for 7,4'-dihydroxyflavylium isolated from a *Dracaena cinnabari* commercial resin by HPLC-DAD. [a]

Position	^1H δ/ppm (J/Hz)	^{13}C (δ/ppm)	HMBC [b]
2		173.7	
3	8.24 (d, 8.7)	113.3	C2, C10
4	9.00 (d, 8.7)	154.4	C2, C5, C9
5	8.09 (d, 8.9)	133.9	C4, C7, C9, C10
6	7.36 (dd, 2.0, 8.9)	122.3	C8, C10
7		170.1	
8	7.44 (d, 2.0)	103.7	C7, C9, C10
9		160.1	
10		119.9	
1'		121.2	
2',6'	8.36 (d, 8.9)	134.0	C2, C4', (C2', C6')
3',5'	7.04 (d, 8.9)	118.6	C1', C4', (C3', C5')
4'		168.0	

[a] Data recorded at 400/100 MHz in CD₃OD/DCI (pD ~ 0.1); [b] Correlation from H to the indicated carbons.

II.2 PCA analysis

The PCA analysis of *Daemonorops draco* and *Daemonorops propinqua* samples (figure II.4) revealed that it is not possible to distinguish between them. These results confirmed the recent studies of Rustiami [3] and, as a result, the world check list of these plants was updated [4]. For *Dracaena ombet*, the situation was different, as a specimen correctly identified from this species could be distinguished from *Dracaena cinnabari* species (figure II.5; for more details see chapter1, section, 3.3).

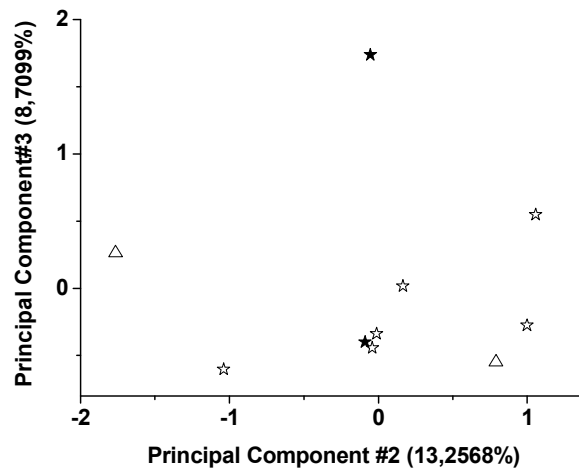


Figure II.4 - PCA analysis of samples from EBC, K (open stars) and HPLC library samples labelled *Daemonorops draco* (solid stars) and *Daemonorops propinqua* (triangles). All the samples fall in the same area and it was not possible to distinguish between the two, which fits in with the recent assignment of *D. propinqua* as a synonym of *D. draco* [3].

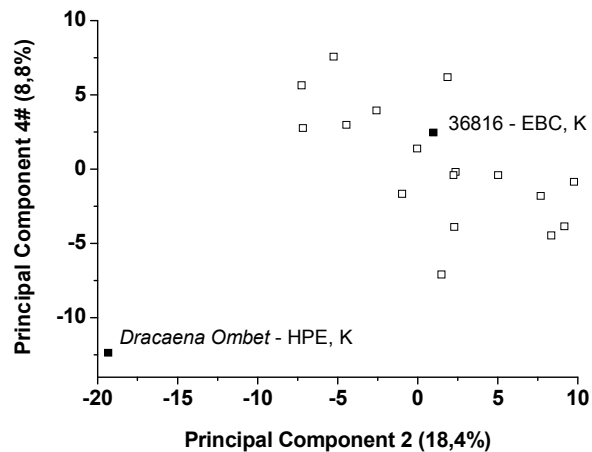
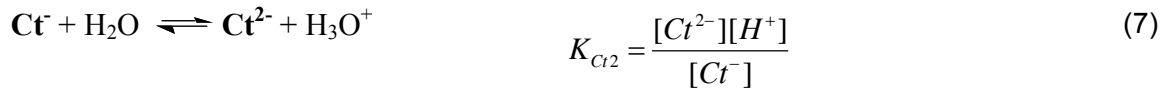
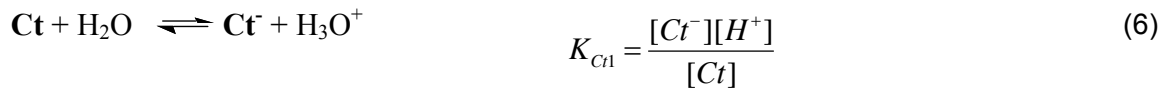
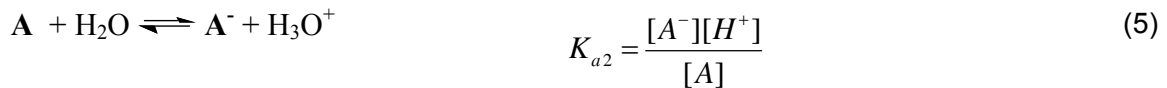
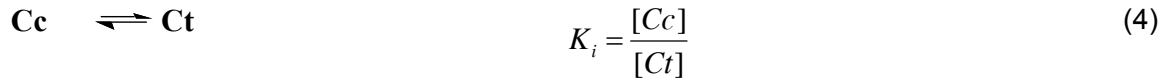
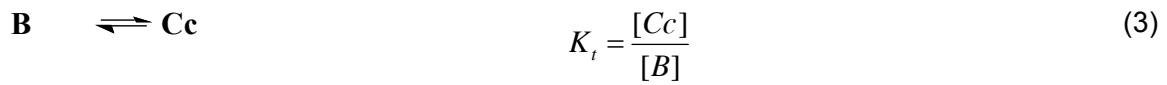
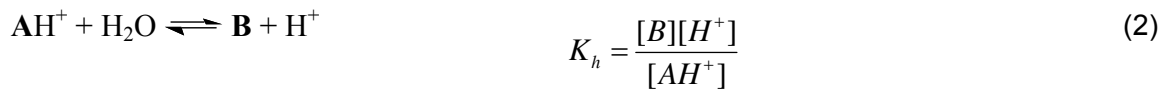
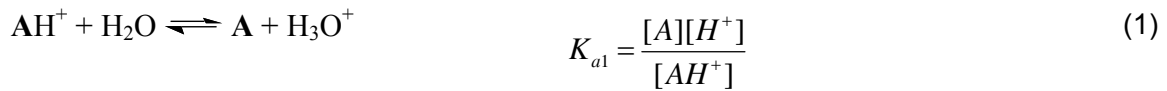


Figure II.5 - PCA analysis of samples labelled *Dracaena cinnabari* and *Dracaena schizantha* from EBC, K and HPE, K. The sample from the living *Dracaena ombet* (synonym *D. schizantha*) is clearly different from the EBC, K 36816 sample which is labelled as *Dracaena schizantha*. The *D. schizantha* is identical to the other *dracaena cinnabari* EBC, K samples.

II.3 Network of Chemical reactions

II.3.1 Dracoflavylum

The network of chemical reactions reported for dracoflavylum (fig. 1.14, Chapter 1, p. 13) can be accounted by the following set of equations:



Considering that at the equilibrium the concentration of B and Cc is negligible, (as observed experimentally), C_0 is the summation of the concentration of all species at the equilibrium:

$$C_0 = [\text{AH}^+] + [\text{A}] + [\text{Ct}] + [\text{A}^-] + [\text{Ct}^-] + [\text{Ct}^{2-}] \quad (8)$$

It can be easily demonstrated that the mole fraction distribution of each species at the equilibrium is given by:

$$\frac{[\text{AH}^+]}{C_0} = \frac{[\text{H}^+]^3}{D} \quad (9)$$

$$\frac{[\text{A}]}{C_0} = \frac{K_{a1}[\text{H}^+]^2}{D} \quad (10)$$

$$\frac{[Ct]}{C_0} = \frac{K_h K_t K_i [H^+]^2}{D} \quad (11)$$

$$\frac{[A^-]}{C_0} = \frac{K_{a1} K_{a2} [H^+]}{D} \quad (12)$$

$$\frac{[Ct^-]}{C_0} = \frac{K_{Ct1} K_h K_t K_i [H^+]}{D} \quad (13)$$

$$\frac{[Ct^{2-}]}{C_0} = \frac{K_h K_t K_i K_{Ct1} K_{Ct2}}{D} \quad (14)$$

$$D = [H^+]^3 + (K_{a1} + K_h K_t K_i) [H^+]^2 + (K_{a1} K_{a2} + K_h K_t K_i K_{Ct1}) [H^+] + K_h K_t K_i K_{Ct1} K_{Ct2} \quad (15)$$

The equilibrium constants that have been calculated are the following:

$$K'_a = 10^{-3.8} \quad K_{a1} = 10^{-4} \quad K_{a2} = 10^{-7.5} \quad K_{Ct1} = 10^{-7.0} \quad K_{Ct2} = 10^{-9.9}$$

The ratio K_{a1}/K'_a should give the percentage of the base at the equilibrium 64%. Moreover the product $K_h K_t K_i$ can be made equal to 5.9×10^{-5} (corresponding to 37 % of **Ct**).

The mole fraction distribution of the several species can now be calculated, and are represented in Figure 1.20, chapter 1, p.29).

II.3.1.1 Confirmation of the A^- amount at the equilibrium

In order to confirm the mole fraction distribution of the ionized base, a pH jump from 1 to 8.8 was carried out, see figure II.6. The calculated percentage of A^- at this pH values, 41% is in agreement with the predicted value.

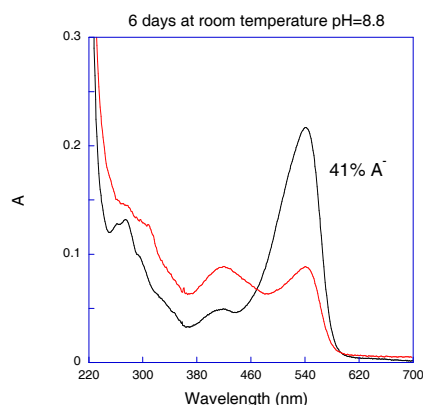


Figure II.6 - pH jump of the compound 7,4'-dihydroxy-5-methoxyflavylum, from 1 to 8.8 at room temperature.

II.3.2 *Dracorhodin and 7,4'-dihydroxyflavylum*

For dracorhodin the same set of equations accounted for dracoflavylum can be considered, however the equilibrium constants and mole fraction distribution of the several species involved in the equilibrium was not calculated as the amount separated by HPLC-DAD was not enough to repeat for a second time the pH jumps preliminary tests. Nevertheless it was possible to calculate the percentage of the base at the equilibrium through the ratio K_{a1}/K_a (~63%).

For the 7,4'-dihydroxyflavylum the network of chemical reaction and respective equations is already published in the literature [5].

II.4 References

- [1] Costantino, L.; Rastelli, G.; Rossi, M. C.; Albasini, A. *Journal Chemical Society, Perkin Transactions 2* **1995**, 227.
- [2] Pina, F.; Lima, J. C.; Parola, A. J.; Afonso, C. A. M. *Angewandte Chemie-International Edition* **2004**, 43, 1525.
- [3] Rustiami, H.; Setyowati, F. M.; Kartawinata, K. *Journal of Tropical Ethnobiology* **2004**, 1-2, 65.
- [4] Govaerts, R.; Dransfield, J. *World Checklist of Palms*. Royal Botanic Gardens: Kew, 2005.
- [5] Pina, F.; Benedito, L.; Melo, M. J.; Parola, A. J.; Lima, J. C.; Maçanita, A. *Anales de Química International Edition* **1997**, 93, 111.

Appendix III – Indigo Data

III.1 I_0 and photodegradation quantum yields

The I_0 obtained for the 335 nm and 610 nm irradiation with the equation 2 (for more details see appendix I, section 1.3.2.1) is presented in table III.1

$$I_0 = \frac{V_{\text{sol}} \cdot (\Delta A / \Delta t)}{1000 \cdot \Phi_R \cdot \Delta t} \quad (2)$$

Table III.1 – I_0 and parameters considered for the 335 nm and 610 nm irradiations.

Actinometry	I_0 (Einstein/min)	m^*	V_{sol} (mL)	Observations
335 nm	1.0×10^{-6}	0.0283	3	Cell near to the monochromator
	1.1×10^{-6}	0.0309		
	1.3×10^{-6}	0.0349		
	7.7×10^{-7}	0.0216		Cell far from the monochromator
	7.3×10^{-7}	0.0203		monochromator
610 nm	1.7×10^{-7}	0.0732	$3^{*(5/2)}$	Cell near to the monochromator
	1.8×10^{-7}	0.0317		monochromator

*The m is the equation slope of ΔA over the irradiation time period, Δt , after the correction of light (when necessary) for the reagent at the irradiation wavelength.

The indigo Φ_R obtained for the 335 nm and 610 nm irradiations with the equation 5 (for more details see appendix I, section 1.3.2.1) are presented in table III.2

$$\Phi_R = \frac{V_{\text{sol}} \cdot (\Delta A / \Delta t)}{1000 \cdot I_{\text{abs}} \cdot \Delta t} \quad (5)$$

Table III.2 – Indigo Φ_R and parameters considered for the 335 nm and 610 nm irradiation.

λ_{irr} (nm)	Indigo/DMF	I_0 (Einstein/min)	Φ_R	M	V_{sol} (mL)
335	O ₂	7.3×10^{-7}	8×10^{-3}	0.0417	3
	O ₂ free	7.3×10^{-7}	3×10^{-4}	0.0015	
610	O ₂	1.8×10^{-7}	2×10^{-3}	0.0017	
	O ₂ free	1.8×10^{-7}	*	*	

* Φ_R not calculated with the available set-up.

The indigo carmine Φ_R in liquid and solid media obtained for the 335 nm and 610 nm irradiations with the equation 5 are presented in table III.3

Table III.3 – Indigo carmine Φ_R and parameters considered for the 335 nm and 610 nm irradiations.

λ_{irr} (nm)	Indigo Carmine/ Medium	I_0 (Einstein/min)	Φ_R	m	V_{sol} (mL)
335	H ₂ O	1.1×10^{-6}	9×10^{-6}	6.8E-05	3
	DMF	1.1×10^{-6}	2×10^{-3}	0.0140	
	CMC	7.7×10^{-7}	5×10^{-4}	0.0053	
	Vahine gelatine	7.7×10^{-7}	4×10^{-4}	0.0040	1.45
	Jerónimos gelatine	7.7×10^{-7}	9×10^{-4}	0.0100	
	Bacteriological gelatine	7.7×10^{-7}	2×10^{-3}	0.0173	
610	H ₂ O	1.1×10^{-6}	*	-	3
	CMC	1.7×10^{-7}	2×10^{-4}	0.0008	1.45
	Vahine gelatine	1.7×10^{-7}	5×10^{-4}	0.0011	
	Jerónimos gelatine	1.7×10^{-7}	4×10^{-4}	0.0010	
	Bacteriological gelatine	1.7×10^{-7}	3×10^{-4}	0.0007	

* Φ_R not calculated with the available set-up.

III.2 Indigo photodegradation HPLC-DAD calibration curves

The expressions obtained with indigo and isatin HPLC-DAD calibration curves, previously to HPLC-DAD analysis of indigo irradiated at 335 and 610 nm, are presented in table III.4

Table III.4 – HPLC-DAD calibration curves of indigo and isatin

Compound	Concentration range (M)	Equation (y=mx+b)	Correlation coefficient
Indigo	1.5×10^{-4} - 1.5×10^{-5}	$6.10^{10}x + 18908$	0.9858
Isatin	10^{-5}	$1.10^{11}x - 185817$	0.9931

III.3 HPLC-DAD characterization

III.3.1 Indigo dye

The HPLC-DAD chromatograms of indigo dye in homogeneous medium (DMF), irradiated at 335 nm and acquired at 275 nm are presented in figure III.1. The irradiations at 610 nm and in heterogeneous media at both wavelengths revealed the same chromatographic pattern. After the indigo photodegradation isatin ($rt=10.5\text{min}$; $\lambda_{\text{max}}=302$) and two unknown compounds were formed (compound 1: $rt=6.3\text{min}$; $\lambda_{\text{max}}=311\text{nm}$; compound 2: $rt=8.2\text{min}$; $\lambda_{\text{max}}=311, 432\text{nm}$), see figure III.1.

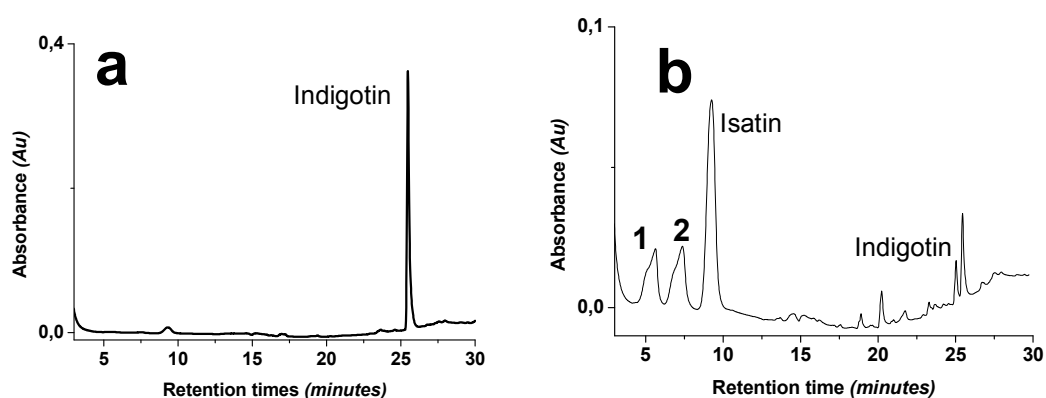


Figure III.1 – HPLC-DAD chromatogram of indigo dye in DMF at 275 nm. a) Before the irradiation; $t_{\text{irr}}=0$ min, Indigotin= 1×10^{-4} M; b) After the irradiation; $t_{\text{irr}}=120$ min, Indigotin= 1×10^{-6} M.

III.3.2 Indigo carmine

The HPLC-DAD chromatograms of indigo carmine in homogeneous medium (water), irradiated at 335 nm and acquired at 275 nm are presented in figure III.2. The irradiations at 610 nm and in heterogeneous media at both wavelengths revealed the same chromatographic pattern.

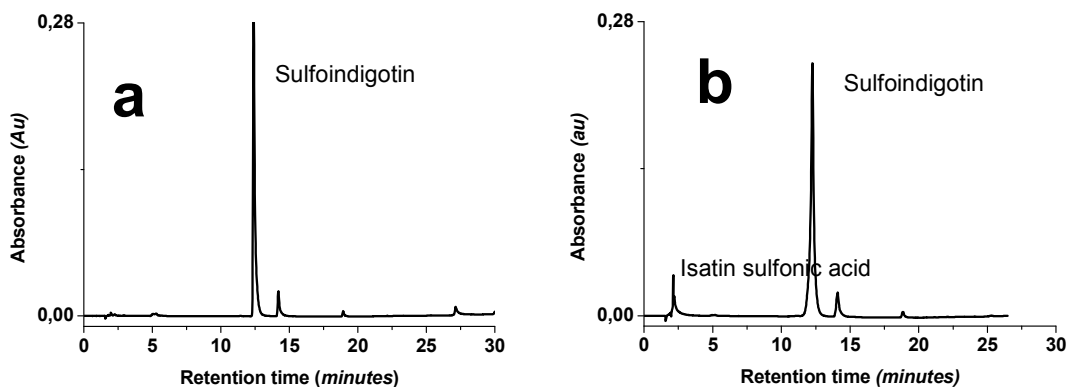


Figure III.2– HPLC-DAD chromatogram of indigo carmine $\approx 1 \times 10^{-5}$ M at 275 nm. a) Before the irradiation; $t_{irr}=0$ min, sulfoindigotin= 1×10^{-4} M; b) After the irradiation; $t_{irr}=9$ h, sulfoindigotin.

III.4 Solar Box exposure

According to Feller [1] the total light annual exposure found in a museum in London is 1.55% of the exterior exposure (900Kwh [2]).

Indigo faded almost with circa of 5950MJ over 2700h of irradiation with a light source simulating the outdoor exposure ($\lambda > 300$ nm). Therefore it is expected that in a museum indigo will fade after circa 120 years of exhibition, which correspond to a compound class A (excellent material for conservation) [1]:

One year of light exposure in London: 900Kwh=3240 MJ.

$$3240 \times 1.55 / 100 = 50.22$$

$$5950 / 50.22 = 118.48 \text{ years in a museum}$$

III.5 Indigo Andean Textiles

The HPLC-DAD chromatogram of an indigo Andean textile sample (*Skirt, 21.2581 (200BC – 200AD)*) acquired at 275 nm is presented in figure III.3. All the samples analysed exhibited a similar chromatographic pattern. Previously to HPLC-DAD analysis of Andean textiles, calibration curves were made with indigo, isatin and indirubin standards dissolved in DMF for the concentration range expected (from 1×10^{-5} M to 1×10^{-6} M). Afterwards, the respective areas of the compounds were calculated at their maximum wavelength with the chromatographic program Chromquest[3] and represented as a function of the concentration. The correlation coefficients for all the calibration curves were good, ≥ 0.98

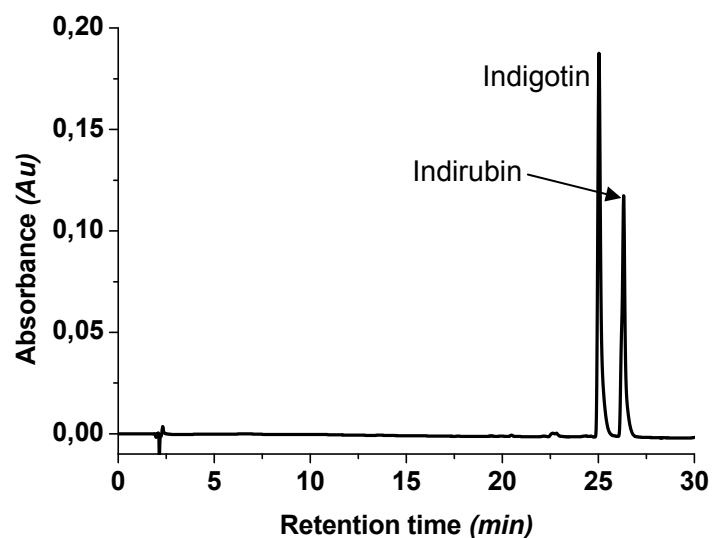


Figure III.3 - HPLC-DAD chromatogram of an indigo Andean textile sample *Skirt, 21.2581 (200BC – 200AD)*, acquired at 610 nm.

III.6 References

- [1] Feller, R. *Accelerated aging – Photochemical and Thermal aspects*. The Getty Conservation Institute: United States of America, 1994.
- [2] In <http://www.geni.org/globalenergy/library/renewable-energy-resources/world/europe/solar-europe/solar-united-kingdom.shtml>, April 2008.
- [3] 4.1 ed., *ChromQuest 4.1*, Thermo Scientific, **2003**.

Appendix IV – Mauve dye data

IV.1 Syntheses – Stoichiometries of the mauveine chromophores

IV.1.1 Formation of Mauveine A

For the formation of Mauveine A, 2 equivalents of aniline; 1 of *o*-toluidine and 1 of *p*-toluidine are required (see figure IV.1).

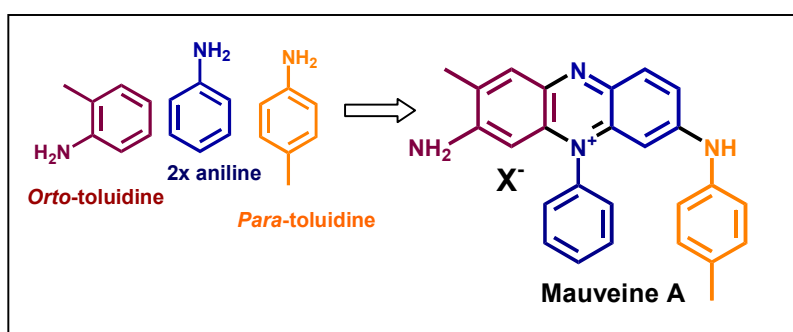
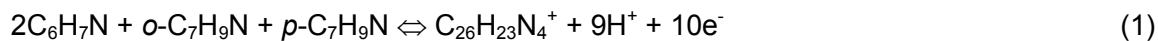
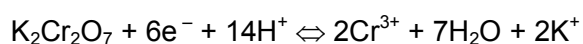


Figure IV.1 – Formation of mauveine A.

The equation of formation of mauveine A can be written as:

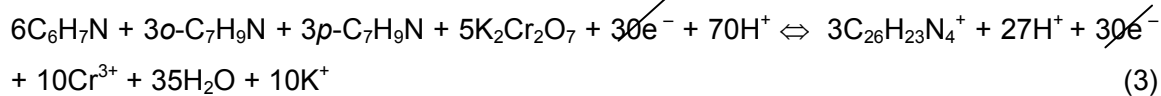


Considering the equation involving the oxidant, potassium dichromate:

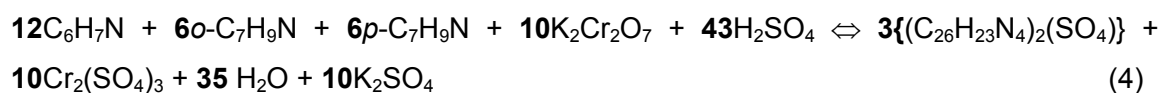


(2)

The global equation of the reaction is:



Replacing H^+ by H_2SO_4 :



IV.1.2 Formation of Mauveine B

For the formation of Mauveine B, 1 equivalent of aniline; 2 of *o*-toluidine and 1 of *p*-toluidine are required (see figure IV.2).

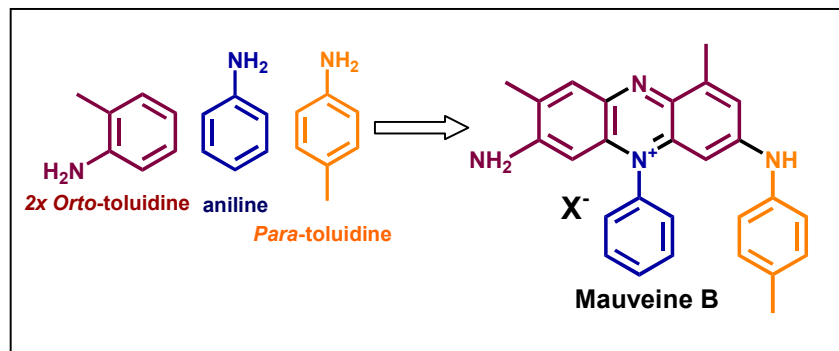
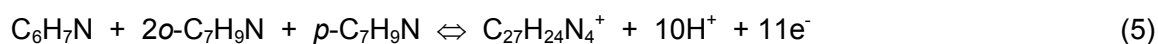


Figure IV.2 –Formation of mauveine B.

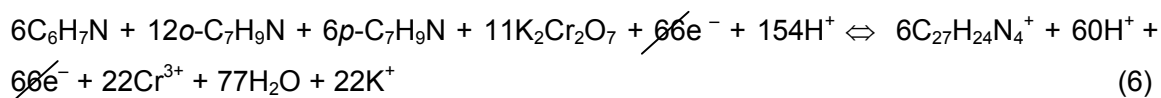
The equation of formation of mauveine B can be written as:



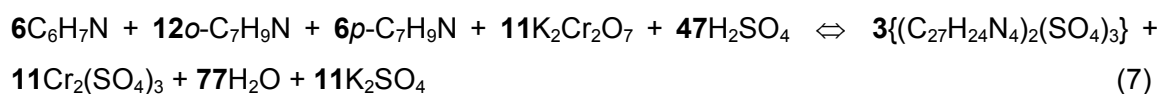
Considering the equation involving the oxidant, potassium dichromate:



The global equation of the reaction is:



Replacing H^+ by H_2SO_4 :



IV.1.3 Formation of Pseudo-mauveine

For the formation of Pseudo-mauveine, 4 equivalents of aniline are required (see figure IV.3).

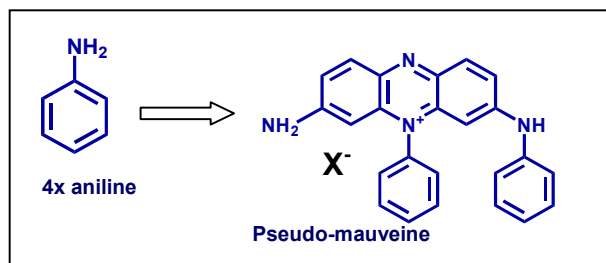


Figure IV.3 –Formation of pseudo-mauveine.

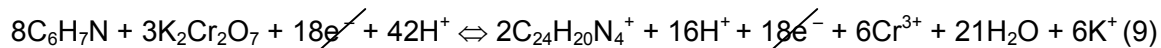
The equation of formation of pseudo-mauveine can be written as:



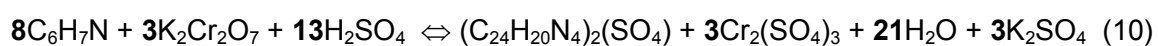
Considering the equation involving the oxidant, potassium dichromate:



The global equation of the reaction is:



Replacing H^+ by H_2SO_4 :



These stoichiometry results for mauveine A, B and pseudo-mauveine reveal that the amount of the reagents for the 4 syntheses performed (table IV.1), specially the amounts of $K_2Cr_2O_7$ and H_2SO_4 , were not enough for the complete reactions to occur (see table IV.2).

Table IV.1 – Concentration of the starting materials used in the 4 mauve dye syntheses.

Synthesis	Starting Material					
	Amount	Aniline	o-Toluidine	p-Toluidine	$K_2Cr_2O_7$	H_2SO_4
1	mol	0.056	0.056	0.114		
<i>JCE 1998</i>	mL/mg	5.2 mL	6 mL	12.2 g		
2	mol	0.056	0.112	0.057		
<i>Mauveine B</i>	mL/mg	5.2 mL	12 mL	6.1 g	0.010 mol	0.060 mol
3	mol	0.112	0.056	0.057	(3 g)	(60 mL of
<i>Mauveine A</i>	mL/mg	10.4 mL	6 mL	6.1 g		H_2SO_4 1 M)
4	mol	0.056	0.0056	0.0057		
<i>Pseudo-mauveine C₂₄</i>	mL/mg	5.2 mL	0.6 mL	0.61 g		

Table IV.2 – Concentrations of $K_2Cr_2O_7$ and H_2SO_4 necessary for the different mauveines chromophores formation in syntheses 2, 3 and 4

Reagent	Synthesis		
	2 (B)	3 (A)	4 (C ₂₄)
$K_2Cr_2O_7$ (mol)	0.103	0.093	0.021
H_2SO_4 (mol)	0.439	0.401	0.091

For the syntheses 2 and 3 almost 10 times more amount H_2SO_4 were needed. In the synthesis 2, also 10 times more $K_2Cr_2O_7$ was necessary to the formation of mauveine B. In the synthesis 4 the limiting reagent was $K_2Cr_2O_7$ being necessary almost 2 times more of this oxidant.

IV.2 Mauve summarized characterization

The MS, NMR and HPLC data are summarized in table IV.3; for more details, see next sections.

Table IV.3 - Structures and summarized spectral data for mauveine compounds isolated from different historical samples.

	mauveine A	mauveine B	Mauveine B2	mauveine C
FDMS <i>m/z</i>	391.2	405.3	405.3	419.3
HRMS <i>m/z</i>	391.19172 (calc. for C ₂₆ H ₂₃ N ₄ ⁺ : 391.19226)	405.20737 (calc. for C ₂₇ H ₂₅ N ₄ ⁺ : 405.20791)	405.20737 (calc. for C ₂₇ H ₂₅ N ₄ ⁺ : 405.20791)	419.22302 (calc. for C ₂₈ H ₂₇ N ₄ ⁺ : 419.22356)
Structure (¹ H NMR)				
HPLC-DAD				
<i>t_r</i> /min	16.57	21.10	16.85	22.88
<i>λ_{max}</i> /nm	549	548	550	549
	pseudo-mauveine	mauveine C₂₅a	mauveine C₂₅b	Mauveine C₂₅c
FDMS <i>m/z</i>	364.17	378.47	378.47	378.47
HRMS <i>m/z</i>	363.16042 (calc. for C ₂₄ H ₁₉ N ₄ ⁺ : 363.16096)	377.17607 (calc. for C ₂₅ H ₂₁ N ₄ ⁺ : 377.17661)	377.17607 (calc. for C ₂₅ H ₂₁ N ₄ ⁺ : 377.17661)	377.17607 (calc. for C ₂₅ H ₂₁ N ₄ ⁺ : 377.17661)
structure (¹ H NMR)				-
HPLC-DAD				
<i>t_r</i> /min	11.83	14.12	14.12	16.08
<i>λ_{max}</i> /nm	547	548	548	548
	Mauveine B3	Mauveine B4	Mauveine C1	Mauveine D
FDMS <i>m/z</i>	405.3	405.3	419.3	433.2
HRMS <i>m/z</i>	405.20737 (calc. for C ₂₇ H ₂₅ N ₄ ⁺ : 405.20791)	405.20737 (calc. for C ₂₇ H ₂₅ N ₄ ⁺ : 405.20791)	419.22302 (calc. for C ₂₈ H ₂₇ N ₄ ⁺ : 419.22356)	433.23867 (calc. for C ₂₉ H ₂₉ N ₄ ⁺ : 433.23921)
HPLC-DAD				
<i>t_r</i> /min	17.70	18.12	22.23	23.67
<i>λ_{max}</i> /nm	544	544	541	545

IV.3 HPLC-DAD/LC-MS characterization of historical samples

IV.3.1 Mauve dyed textile samples

The HPLC-DAD chromatograms of mauve dyed textiles acquired at 550 nm are presented in figure IV.4. The peak areas of the chromophores were obtained with the chromatographic software ChromQuest [1]. These areas were then corrected for the different molar absorptivity of each compound and are shown in chapter 3, section 3.3. The following molar absorptivities were determined: ($\epsilon / M^{-1} \text{ cm}^{-1}$) mauveine A = 22000; mauveine B = 29000; mauveine B2 = 33000; mauveine C = 36500, giving rise to the following correcting factors: mauveine A = 0.6; mauveine B = 0.8; mauveine B2 = 0.9 (value also used for mauveines B3 and B4); mauveine C = 1 (value also used for mauveine C1).

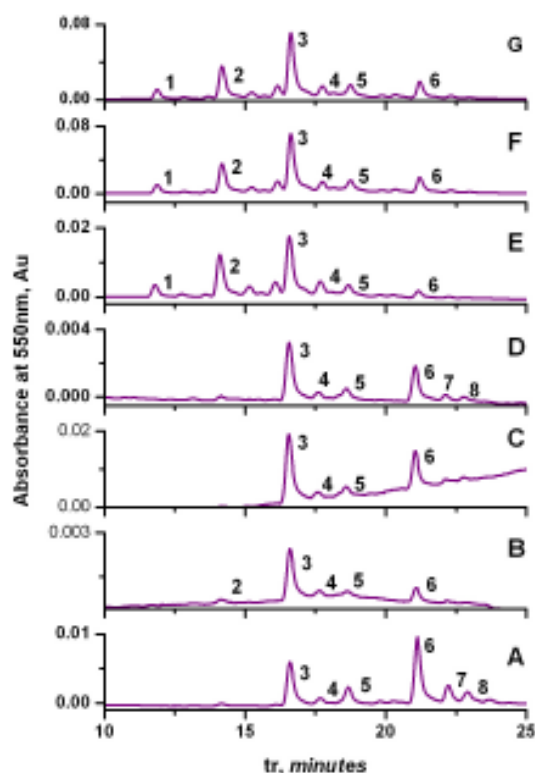


Figure IV.4 – Mauve dyed textiles HPLC-DAD chromatograms obtained at $\lambda = 551 \text{ nm}$ for A: Science Museum F1; B: Science Museum F2; C: Science Museum F3; D: Science Museum F4, E: Science Museum F5; F: Perth Museum; G: Science Museum F6. All the samples were extracted with MeOH + 1 drop of HCl/H₂O (pH=2), for more details see extraction methods Appendix I- Experimental section. The major compounds identified correspond to the numbered peaks: 1- pseudo-mauveine; 2- mauveines C_{25a} + C_{25b}; 3- mauveine A; 4- mauveines B3 + B4; 5- mauveine B2; 6- mauveine B; 7- mauveine C1; 8 - Mauveine C.

The names for the compounds given in table IV.3 are in accordance with those introduced by Meth-Cohn and Smith in 1994 [2]. The logic assisting these names is based on the number of methyl groups around the 7-amino-5-phenyl-3-(phenylamino)phenazin-5-ium core (pseudo-mauveine) common to all mauveine compounds: two methyl groups - mauveines A; three methyl groups - mauveines B; four methyl groups - mauveines C. Peaks **3** and **6** correspond, respectively, to the mauveine A and the mauveine B described by Meth-Cohn and Smith in 1994 [2]; peaks **5** and **8** correspond, respectively, to mauveines B2 and C [3]; peak **1** was identified as pseudo-mauveine; the compounds corresponding to peak **4** were designated as mauveine B3 and mauveine B4 since they are isomers of mauveine B; the compound corresponding to peak **7** was named mauveine C1 since it is an isomer of mauveine C; finally, the compounds corresponding to peak **2** are two C₂₅ isomers containing one methyl group each and were designated as mauveine C_{25a} and mauveine C_{25b}.

The MS determination of some mauveine minor compounds, namely those corresponding to peaks **4** and **8**, was performed by LC-MS for sample *Science Museum 1* and for a mauve-dyed textile sample *Science Museum F6* (see figure IV.5 and figure IV.6, respectively). The *Museum SI Manchester 2* sample was also analysed by LC-MS (see figure IV.7).

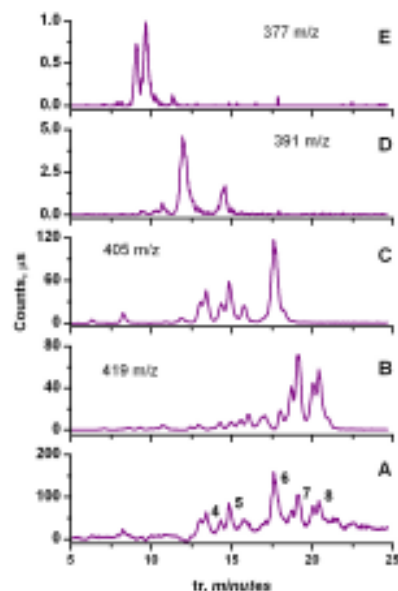


Figure IV.5 - HPLC-MS total ion chromatogram (TIC) of A) *Science Museum 1* salt sample; B) 419 m/z compounds; C) 405 m/z compounds; D) 391 m/z compounds, E) 377 m/z compounds. The compounds identified in TIC correspond to the numbered peaks: 4- mauveines B3 + B4; 5- mauveine B2; 6- mauveine B, 7- mauveine C1, 8- mauveine C.

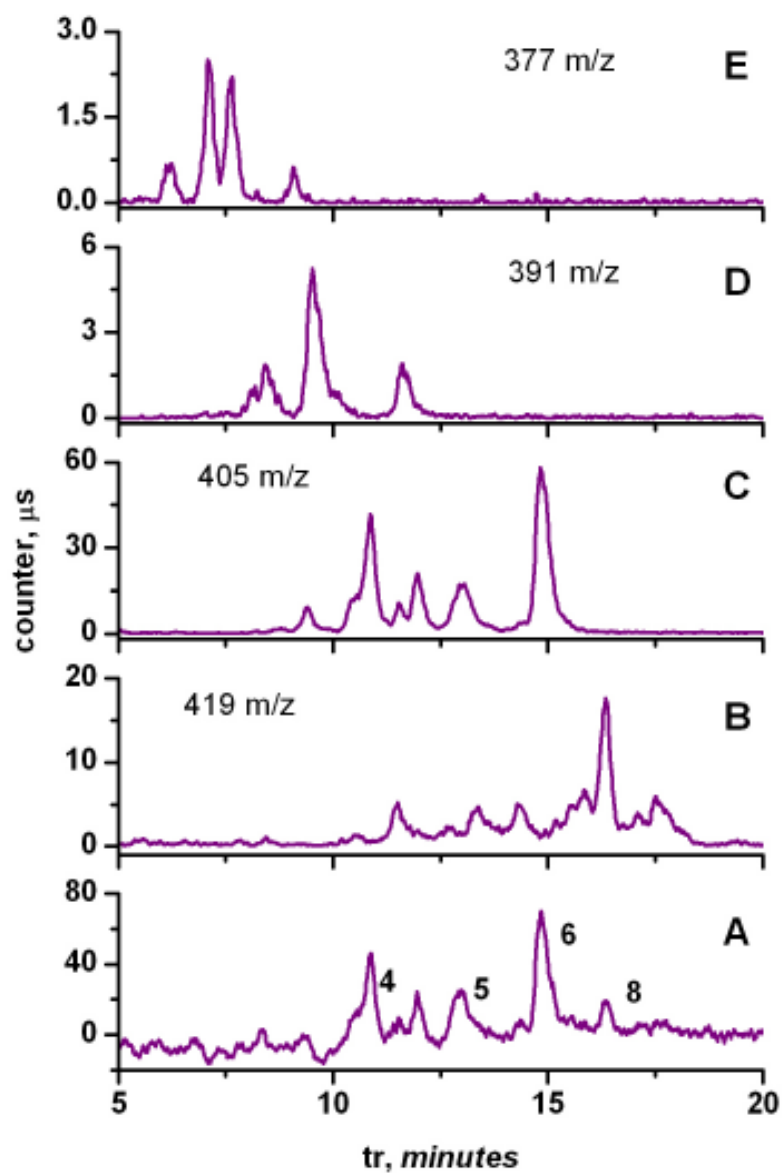


Figure IV.6 - HPLC-MS total ion chromatogram (TIC) of A) Science Museum F6 mauve dyed shawl; B) 419 m/z compounds; C) 405 m/z compounds; D) 391 m/z compounds, E) 377 m/z compounds. The compounds identified in TIC correspond to the numbered peaks: 4- mauveines B3 + B4; 5- mauveine B2; 6- mauveine B, 8- mauveine C.

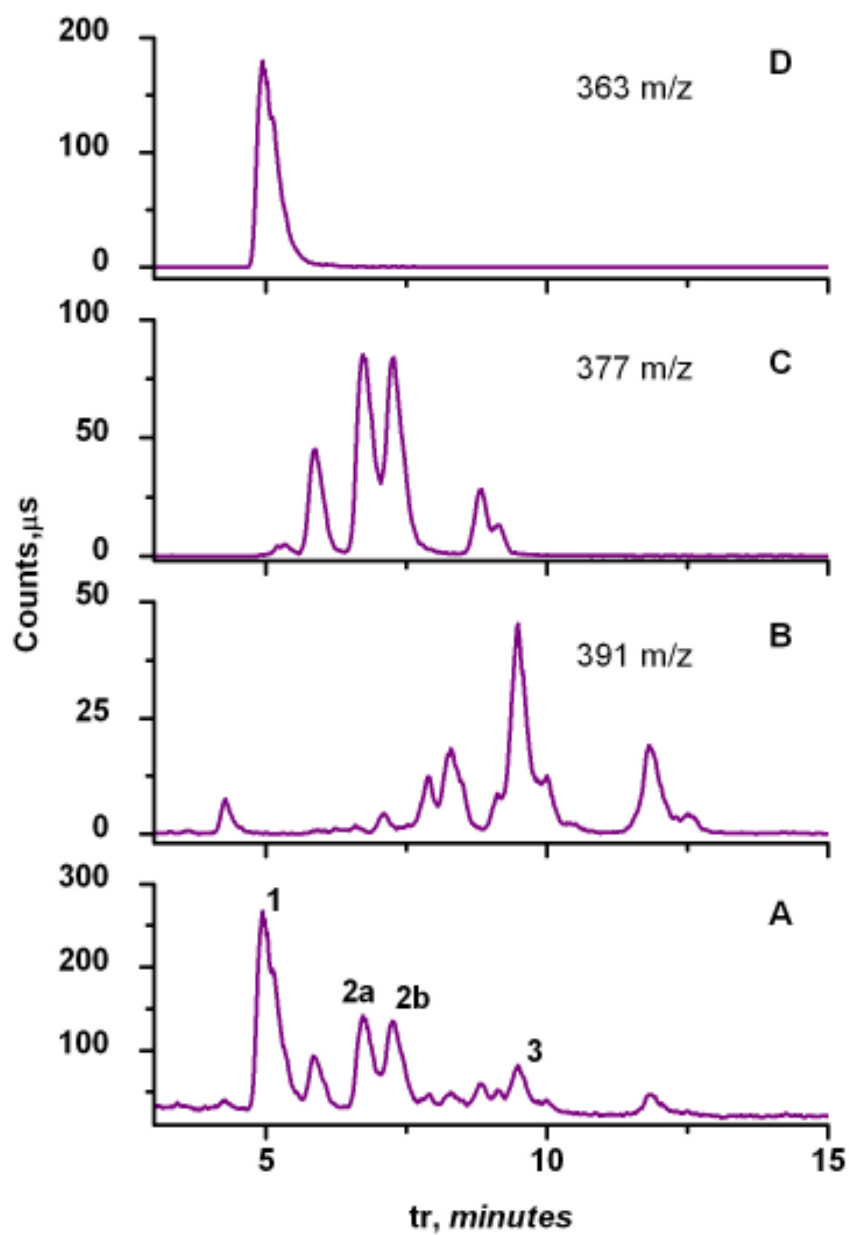


Figure IV.7 - HPLC-MS total ion chromatogram (TIC) of A) Museum SI Manchester 2 salt sample; B) 391 m/z compounds; C) 377 m/z compounds; D) 363 m/z compounds. The compounds identified in TIC correspond to the numbered peaks: 1- pseudo-mauveine; 2- mauveines C_{25a} and C_{25b}; 3- mauveine A.

IV.3.2 Mauve salt samples

The HPLC-DAD chromatograms for mauve salt samples are shown in Figure IV.8. The structures are identical to those found in the mauve dyed textiles samples and can be found in Table IV.3.

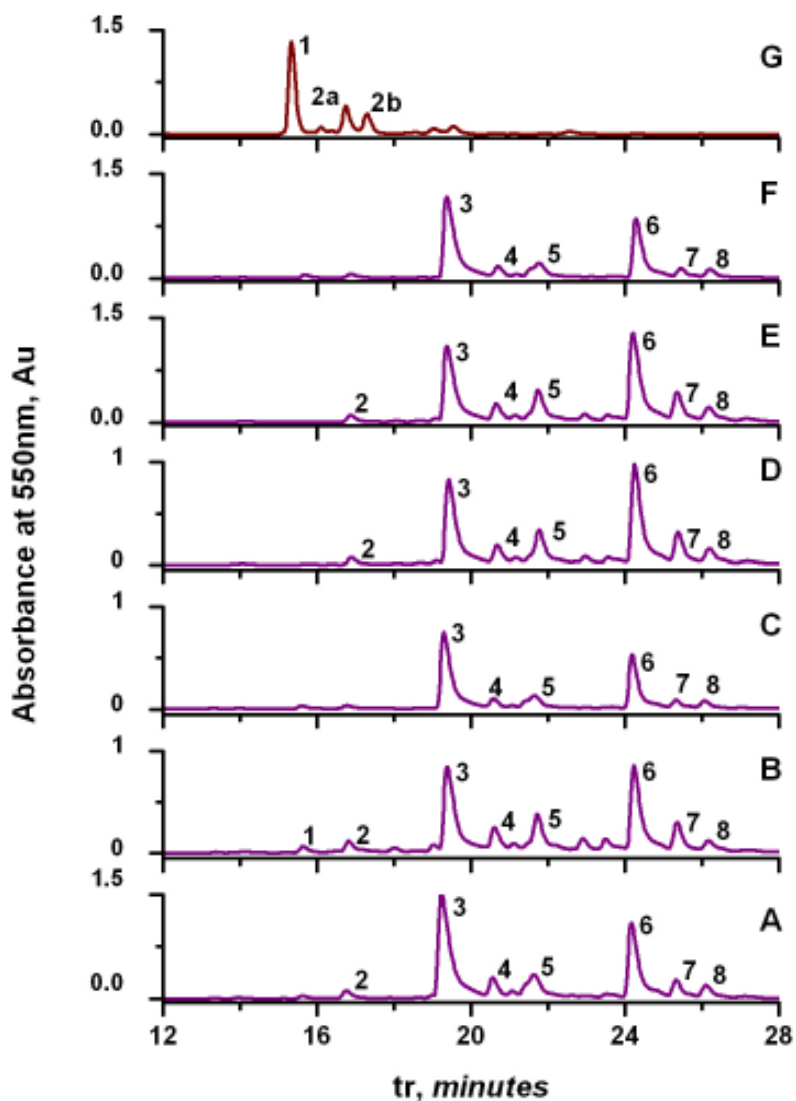


Figure IV.8 - Mauve salts HPLC-DAD chromatograms obtained at $\lambda = 551$ nm for A: Science Museum 1; B: Science Museum 2; C: Science Museum 3; D: Science Museum 4, E: Museum SI Manchester 1; F: Chandler Museum; G: Museum SI Manchester 2 (This sample was analyzed with the Polaris C18-A column (150mm \times 2mm) in order to separate successfully the mauveine C_{25} isomers). All the samples were dissolved in methanol. The major compounds identified correspond to the numbered peaks: 1- pseudo-mauveine; 2- two C_{25} isomers; 3- mauveine A; 4- mauveines B3 + B4; 5- mauveine B2; 6- mauveine B; 7- mauveine C1; 8 - mauveine C. For more details see chapter 3 and table IV.1 for structures.

IV.3.3 Mauve from other sources

The HPLC-DAD chromatograms acquired at 550 nm are presented in Figure IV.9. In the *DHA 2001* sample, the major compound is Mauve A (38%), whereas in the tissue taken from *JCE 1926* volume the major compounds are mauveine C_{25a} + C_{25b} isomers (80%).

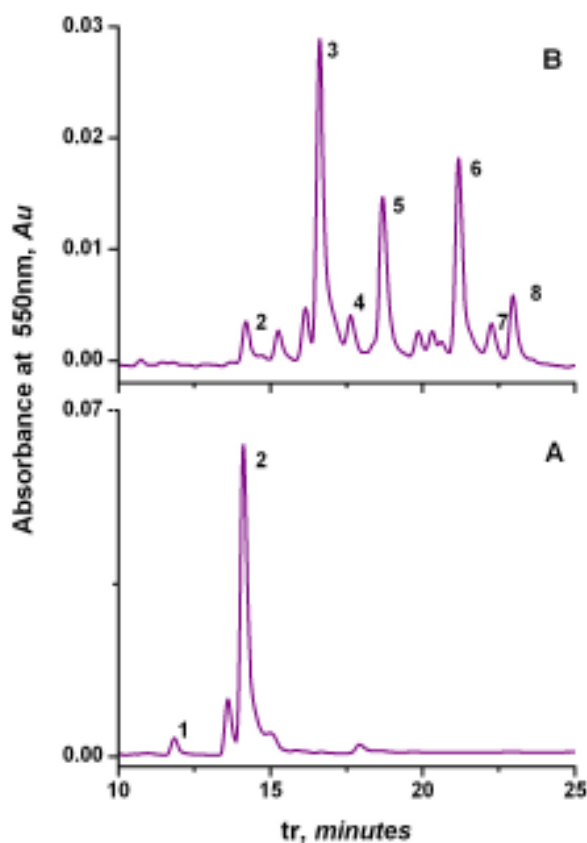


Figure IV.9 - Mauve-dyed textiles HPLC-DAD chromatograms obtained at $\lambda=551$ nm for **A**: *JCE 1926*, [4]; **B**: *DHA 2001*, [5]. All the samples were extracted with methanol with one drop of HCl (for more details see appendix I, section I.3.3.3). The major compounds identified correspond to the numbered peaks: **1**- pseudo-mauveine; **2**- mauveines C_{25a} + C_{25b} ; **3**- mauveine A; **4**- mauveines B3 + B4; **5**- mauveine B2; **6**- mauveine B; **7**- mauveine C1; **8** - mauveine C. For more details see text and table IV.3 for structures.

Together with the mauveine salt from Schunk's collection, the fibre dyed with mauve from the 1926 library volume of the *Journal of Chemical Education* is the only sample where mauveine C_{25} compounds are present as major chromophores. The availability of this volume in numerous libraries makes it a standard for the analysis of mauveine-like compounds.

IV.4 NMR characterization (structure elucidation)

The NMR data (^1H and ^{13}C) of the mauveine chromophores isolated by HPLC-DAD is presented in tables IV.4-IV.8. Spectra were run at 298.0 K, in CD_3OD , at 400.13 Hz (^1H) and 100.00 Hz (^{13}C) for pseudo-mauveine and mauveines B2 and C and at 600.13 Hz (^1H) and 150.91 Hz (^{13}C) for isomeric mauveines $\text{C}_{25\text{a}}$ and $\text{C}_{25\text{b}}$. HMBC data refers to correlations of each hydrogen atom to the indicated carbon atoms.

IV.4.1 Mauveine B2

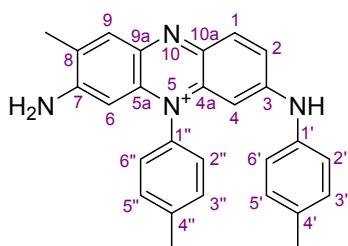


Figure IV.10 - Mauveine B2: 7-amino-8-methyl-5-p-tolyl-3-(p-tolylamino)phenazin-5-ium.

Table IV.4 - ^1H - and ^{13}C -NMR data for the isolated mauveine B2.

Position	^1H δ /ppm (J/Hz)	^{13}C (δ /ppm)	HMBC
1	8.01 (d, 9.3)	134.36	3, 4a
2	7.41 (dd, 9.3, 2.2)	121.57	
3		153.91	
4	6.33 (d, 2.2)	95.12	2, 10a
4a		137.88	
5a		137.60	
6	6.08 (s)	95.27	8, 9a
7		159.10	
8		131.92	
9	7.92 (s)	133.68	5a, 7, 8- CH_3
9a		139.01	
10a		137.70	
1'		137.36	
2',6'	7.03 (d, 8.4)	123.45	2',6', 4'
3',5'	7.12 (d, 8.4)	131.05	1', 3',5', 4'- CH_3
4'		136.77	
1''		135.23	
2'',6''	7.36 (d, 8.1)	128.51	2'',6'', 4''
3'',5''	7.61 (d, 8.1)	133.00	1'', 3'',5'', 4''- CH_3
4''		142.82	
8- CH_3	2.37 (s)	20.96	7, 8, 9
4'- CH_3	2.30 (s)	17.54	2', 3', 4'
4''- CH_3	2.52 (s)	21.31	3'', 4''

IV.4.2 Mauveine C

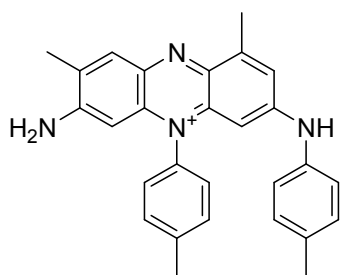


Figure IV.11 - Mauveine C: 7-amino-1,8-dimethyl-5-p-tolyl-3-(p-tolylamino)phenazin-5-ium

Table IV.5 - ^1H - and ^{13}C -NMR data for the isolated mauveine C.

Position	^1H δ /ppm (J/Hz)	^{13}C (δ /ppm)	HMBC
1		138.99	
2	7.25 (br. s)	121.02	
3		153.70	
4	6.17 (d, 2.0)	93.78	2, 10a
4a		143.83	
5a		137.3	
6	6.11 (s)	95.09	8, 9a
7		158.67	
8		131.17	
9	7.89 (s)	133.90	5a, 7, 8-CH ₃
9a		137.3	
10a		137.61	
1'		137.3	
2',6'	7.01 (d, 8.2)	123.58	2',6', 4'
3',5'	7.11 (d, 8.2)	131.01	1', 3',5', 4'-CH ₃
4'		136.73	
1''		135.55	
2'',6''	7.33 (d, 8.1)	128.52	1'', 2'',6'', 4''
3'',5''	7.60 (d, 8.1)	132.95	1'', 3'',5'', 4''-CH ₃
4''		142.70	
1-CH ₃	2.77 (s)	17.88	1, 2, 10a
8-CH ₃	2.37 (s)	17.53	7, 8, 9
4'-CH ₃	2.30 (s)	20.95	3', 4'
4''-CH ₃	2.52 (s)	21.30	3'', 4''

IV.4.3 Pseudo-mauveine

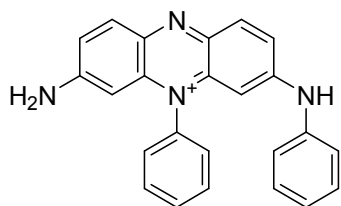


Figure IV.12- Pseudo-mauveine: 7-amino-5-phenyl-3-(phenylamino)phenazin-5-ium

Table IV.6 - ^1H - and ^{13}C -NMR data for the isolated pseudo-mauveine.

Position	^1H δ /ppm (J/Hz)	^{13}C (δ /ppm)	HMBC	Position
1	7.95 (d, 9.2)	134.75	3, 4a	
2	7.43 (m)	121.77	10a	
3		154.11		
4	6.33 (d, 1.3)	95.45	2, 10a	4 \leftrightarrow 2',6', 2'',6''
4a		138.08		
5a		138.89		
6	6.02 (d, 1.4)	94.88	8, 9a	6 \leftrightarrow 2'',6''
7		159.70		
8	7.28 (dd, 8.0, 1.3)	123.36	9a	
9	8.02 (d, 9.2)	135.43	5a, 7	
9a		139.17		
10a		137.66		
1'		139.90		
2',6'	7.14 (m)	123.30	2',6', 4'	
3',5'	7.30 (m)	130.61	1', 3',5'	
4'	7.13 (m)	126.72	2',6'	
1''		137.74		
2'',6''	7.51 (d, 7.4)	128.81	2'',6'', 4''	
3'',5''	7.81 (m)	132.63	1'', 3'',5''	
4''	7.75 (m)	126.72	2'',6''	

IV.4.4 Mauveine C_{25a}

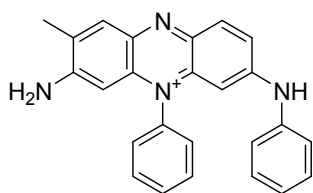


Figure IV.13 – Mauveine C_{25a}: 7-amino-8-methyl-5-phenyl-3-(phenylamino)phenazin-5-ium

Table IV.7 - ¹H- and ¹³C-NMR data for the isolated mauveine C_{25a}.

Position	¹ H δ/ppm (J/Hz)	¹³ C (δ/ppm)	HMBC
1	8.04 (d, 9.4)	134.74	3, 4a
2	7.44 (dd, 9.4, 2.0)	121.63	10a
3		153.52	
4	6.38 (d, 2.0)	95.38	2, 3, 10a
4a		137.53	
5a		137.74	
6	6.11 (s)	94.98	5a, 7, 8, 8-CH ₃ , 9a
7		159.36	
8		132.24	
9	7.87 (d, 1)	133.79	5a, 7, 8-CH ₃
9a		139.38	
10a		137.66	
1'		140.06	
2',6'	7.14 (m)	123.13	1', 2',6', 3',5', 4'
3',5'	7.29 (dd, 8, 8)	130.60	1', 2',6', 3',5'
4'	7.13 (m)	126.50	2',6'
1''		137.77	
2'',6''	7.52 (d, 7)	128.83	1'', 2'',6'', 4''
3'',5''	7.81 (dd, 8, 8)	132.62	1'', 2'',6'', 4''
4''	7.75 (t, 8)	132.19	1'', 2'',6'', 3'',5''
8-CH ₃	2.38	17.58	7, 8, 9, 9a

IV.4.5 Mauveine C_{25b}

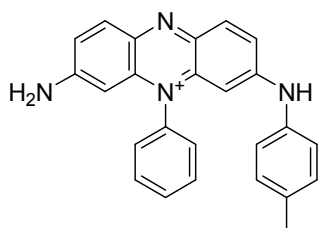


Figure IV.14 – Mauveine C_{25b} 7-amino-5-phenyl-3-(p-tolylamino)phenazin-5-ium.

Table IV.8 - ¹H- and ¹³C-NMR data for the isolated mauveine C_{25b}.

Position	¹ H δ/ppm (J/Hz)	¹³ C (δ/ppm)	HMBC
1	8.01 (d, 9.2)	134.46	3, 4a
2	7.41 (dd, 9.2, 2.0)	121.83	10a
3		154.32	
4	6.29 (d, 2.0)	95.08	2, 3, 10a
4a		138.23	
5a		138.86	
6	6.01 (d, 2.0)	94.87	7, 8, 9a
7		159.56	
8	7.27 (dd, 9.2, 2.0)	123.02	9a
9	7.95 (d, 9.4)	135.37	5a, 7
9a		138.86	
10a		137.80	
1'		137.18	
2',6'	7.02 (d, 8.0)	123.38	2',6', 3',5', 4'
3',5'	7.12 (m)	131.08	1', 2',6', 3',5', 4'- CH ₃
4'		136.92	
1''		137.85	
2'',6''	7.51 (d, 7)	129.08	1'', 2'',6'', 4''
3'',5''	7.81 (dd, 8, 8)	132.65	1'', 2'',6'', 3'',5''
4''	7.75 (t, 8)	132.19	2'',6'', 1''
4'-CH ₃	2.29	20.97	2',6', 3',5', 4'

IV.5 ICP-AES characterization of the mordants from mauve dyed textiles

The results obtained with ICP-AES are summarized in table IV.9.

Table IV.9 - Mordant analysis of three mauve-dyed textile samples.

Sample/textile	Iron (mg) / textile (g)	Tin (mg)/ textile (g)	Aluminium (mg) / textile (g)
Science Museum F4 / cotton	1.20	10.06	-
Science Museum F6 / wool	5.59	-	5.89
Perth Museum / silk	1.06	-	-

IV.6 HPLC anion exchange chromatography of counter ions from mauve salts

The HPLC anion exchange chromatograms of counter ions are presented in figure IV.15 and their relative percentage in table IV.10. The mauve salts chromatograms were compared with ion standards presented in table I.5, appendix I.

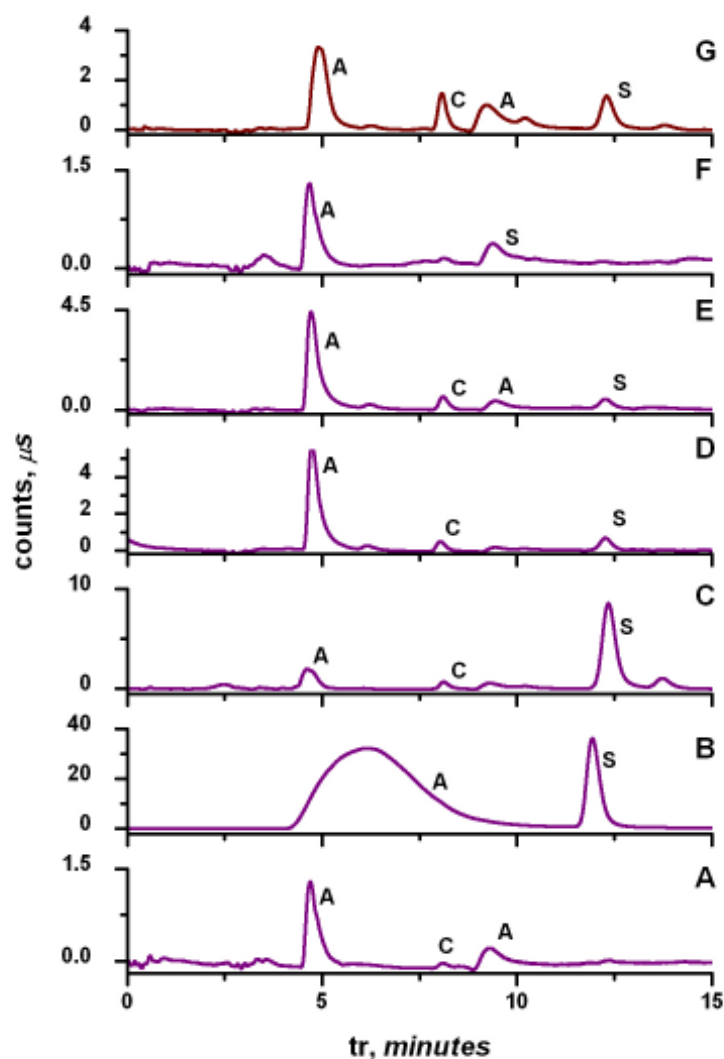


Figure IV.15 - Mauve salts HPLC-AEC chromatograms obtained for A: Science Museum 1; B: Science Museum 2; C: Science Museum 3; D: Science Museum 4, E: Museum SI Manchester 1; F: Chandler Museum; G: Museum SI Manchester 2. All the mauveine salts were dissolved in water, with exception of Science Museum 2 sample which did not dissolve in water and thus methanol had to be added*. The major compounds identified correspond to the signalled peaks: A - acetate; C - chloride; S - sulphate. For more details see chapter 3, section 3.3 and Table IV.9 with relative areas.

* decreasing order of solubility in water: Science Museum 1, Science Museum 4, Chandler Museum, Museum SI Manchester 1 >> Museum SI Manchester 2 > Science Museum 3 >>> Science Museum 2. The sample's solubility is clearly related to the increase in the percentage of the sulphate counter-ion.

Table IV.10 - Counter-ions of the mauve salt samples.

Sample	counter-ions		
	acetate (%)	chloride (%)	sulphate (%)
<i>Science Museum 1</i>	97	3	0
<i>Science Museum 2*</i>	2	0	98
<i>Science Museum 3</i>	19	4	67
<i>Science Museum 4</i>	82	6	9
<i>Museum SI Manchester 1</i>	86	7	6
<i>Museum SI Manchester 2</i>	68	13	17
<i>Chandler Museum 2</i>	100	0	0

*For the *Science Museum 2* sample which did not dissolve in water, the value for the acetate percentage in this sample was obtained by comparison with the acetate standard in methanol.

IV.7 Solar Box exposure

Mauve dye faded almost with circa of 700MJ over 200h of irradiation with a light source simulating the outdoor exposure ($\lambda > 300\text{nm}$). Therefore it is expected that in a museum mauve will fade after circa 14 years of exhibition, which correspond to a compound class C (unstable material) [3]:

One year of light exposure in London: $900\text{Kwt}=3240\text{ MJ}$.

$3240 \times 1.55/100=50.22$

$700/50.22=13.94$ years in a museum

IV.8 References

- [1] 4.1 ed., ChromQuest 4.1, Thermo Scientific, **2003**.
- [2] Meth-Cohn, O.; Smith, M. *Journal of the Chemical Society-Perkin Transactions 1* **1994**, 5.
- [3] Melo, J. S.; Takato, S.; Sousa, M.; Melo, M. J.; Parola, A. J. *Chemical Communications* **2007**, 2624.
- [4] Rose, R. E. *Journal of Chemical Education* **1926**, 8, 973.
- [5] Dronsfield, A.; Edmonds, J. *Dyes History and Archaeology* **2001**, 6, 1.
- [6] Scaccia, R.; Coughlin, D.; Ball, D. *Journal of Chemical Education* **1998**, 75-6, 769.